Holmium radioembolization:

Efficacy and safety

Jip Frederik Prince

Holmium radioembolization: efficacy and safety
PhD thesis, Utrecht University, the Netherlands

jipfprince@gmail.com

Part of the research in this thesis was supported by a grant from the Dutch Cancer Society (KWF Kankerbestrijding)

Publication of this thesis was financially supported by:
Chipsoft,
Elekta Brachytherapy,
Philips,
Sectra,
TD Medical,
Terumo,
Quirem Medical

ISBN: 978-90-393-6489-5

Cover: Marieke Bremer, marieke.s.bremer@gmail.com
Design: Ferdinand van Nispen tot Pannerden,
Citroenvlinder DTP&Vormgeving, my-thesis.nl
Printed by: GVO Drukkers en vormgevers, Ede, The Netherlands

Holmium radioembolization: Efficacy and safety

Radioembolisatie met holmium: werkzaamheid en veiligheid

(met een samenvatting in het Nederlands)

Proefschrift

ter verkrijging van de graad van doctor aan de Universiteit Utrecht
op gezag van de rector magnificus, prof.dr. G.J. van der Zwaan,
ingevolge het besluit van het college voor promoties
in het openbaar te verdedigen op dinsdag 16 februari 2016
des middags te 4.15 uur

door

Jip Frederik Prince
geboren op 24 maart 1989
te 's-Hertogenbosch

Promotor:	Prof. dr. M.A.A.J. van den Bosch
Copromotor:	Dr. M.G.E.H. Lam

Content

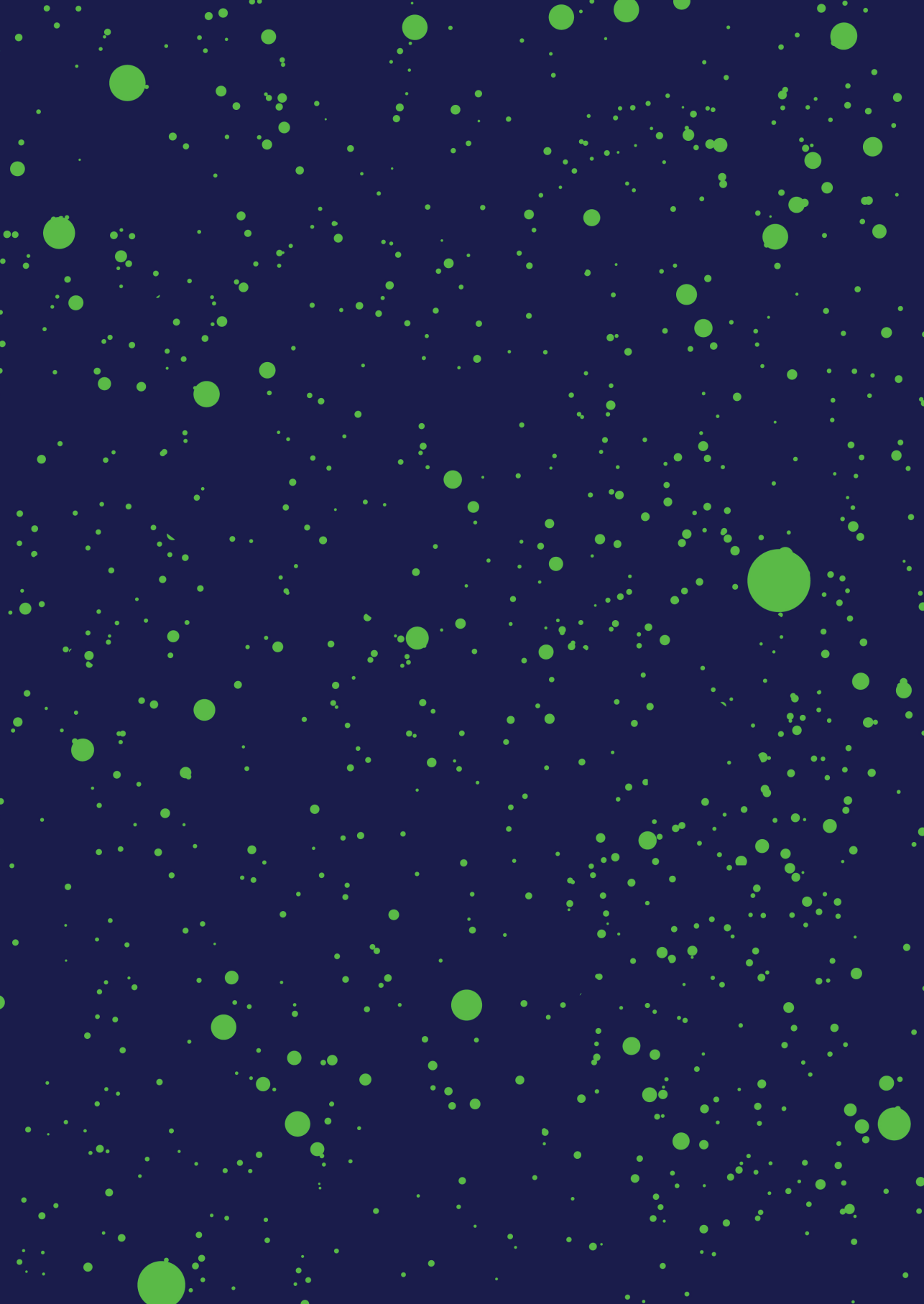

CHAPTER 1

Introduction and outline

Introduction and outline

In the early 1960s, Dr. Irving Ariel noticed that cancer in the liver was resistant to treatment with external beam radiation therapy and chemotherapy. He wanted to try a new treatment using a medical device that he and several colleagues had previously tried in animals: ceramic microspheres loaded with radioactivity. The microspheres contained the radioisotope yttrium-90 (^{90}Y) that releases beta radiation and induces cell death through DNA damage. To administer the microspheres, he placed a catheter at the level of the celiac artery in the aorta via a groin puncture and femoral artery access. He protected the patient's legs from the radioactive microspheres by strapping tourniquets on both of them. After injecting the microspheres, a photoscan was obtained to illustrate the distribution of the radioisotopes (Figure 1). Unfortunately, the complications were sometimes severe. One patient experienced a paresis of the right leg, while another became completely paraplegic. It was hypothesized that these complications arose from microspheres entering the spinal canal because the patients were positioned on their backs and gravity would pull the microspheres towards the arteries in the spinal canal. Still, several of his patients reported a temporary relief of complaints; their sense of wellbeing improved, appetite returned and pain decreased.[1]

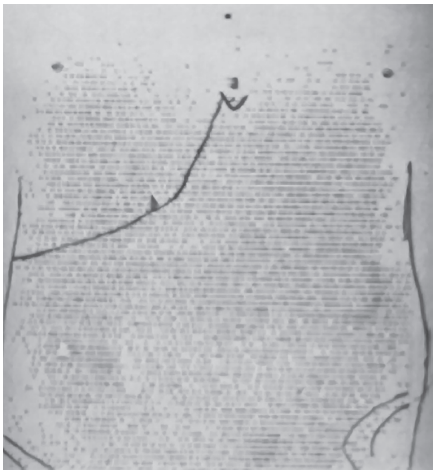

Figure 1 *Photoscan showing abdomen after administration of yttrium-90 microspheres, to which was also attached ytterbium-169 as gamma emitter, (a) xiphoid process, (b) right costal margin. A photoscan was made by moving a radiation probe along multiple horizontal lines and plotting the output as dots (larger dot equals more radiation). Figure reused with permission*[1]

Around 50 years later, the intra-arterial injection of radioactive microspheres evolved into radioembolization and became mainstream clinical practice performed in hospitals worldwide. Microspheres with ^{90}Y gained European CE market approval in two forms, a resin sphere in 2002 (SIR-Spheres, SIRTeX Medical Ltd., Australia) and a glass sphere in 2006 (TheraSphere, BTG, Canada). Three randomized controlled trials have been published and several others are trials recruiting patients or awaiting follow up.[2] Multiple oncology guidelines now include radioembolization as a treatment option and reimbursement is recently established for colorectal cancer patients in the Netherlands.[3,4]

To be eligible, candidates should have primary or metastatic hepatic disease that is liver-dominant (Figure 2), and have a life expectancy of more than 3 months.[5] A contrast enhanced CT is acquired to assess the hepatic vasculature. In a pretreatment procedure, injection positions are determined and optionally, extra-hepatic arteries are embolized.[6] A scout dose consisting of technetium-99m macroaggregated albumin (^{99m}Tc-MAA) is injected as a surrogate particle. It functions as a tracer by only emitting gamma rays that are visualized on SPECT/CT, while keeping radiation exposure to patients low. Extrahepatic deposition in a gastrointestinal organ (e.g., stomach, duodenum or pancreas) is a contraindication for treatment and requires another pretreatment procedure with different injection positions, additional embolization or the use of an anti-reflux catheter.[7] If targeted liver segments are missed, different injection positions can be chosen or intrahepatic embolization can redirect flow to ensure all desired segments (i.e., tumors) are reached.[8] Some of the particles will inadvertently shunt to the lungs, but this is a contraindication only if an absorbed dose of more than 30 Gy is expected in the lungs (often approximated as a shunt percentage of >20%).[9] After an adequate pretreatment procedure, microspheres loaded with ^{90}Y are administered at the injection position(s) and their distribution is confirmed using PET/CT. The microspheres remain in the liver indefinitely; most radiation is deposited in a week.

As an alternative to ^{90}Y microspheres, holmium-166 (^{166}Ho) microspheres were developed to provide superior imaging capabilities.[10] ^{166}Ho also emits an electron that induces cell death and additionally emits gamma rays (81 keV, 6.2%) that can be detected using SPECT/CT.[11] Also, holmium is paramagnetic and can be visualized on MR imaging.[12] After

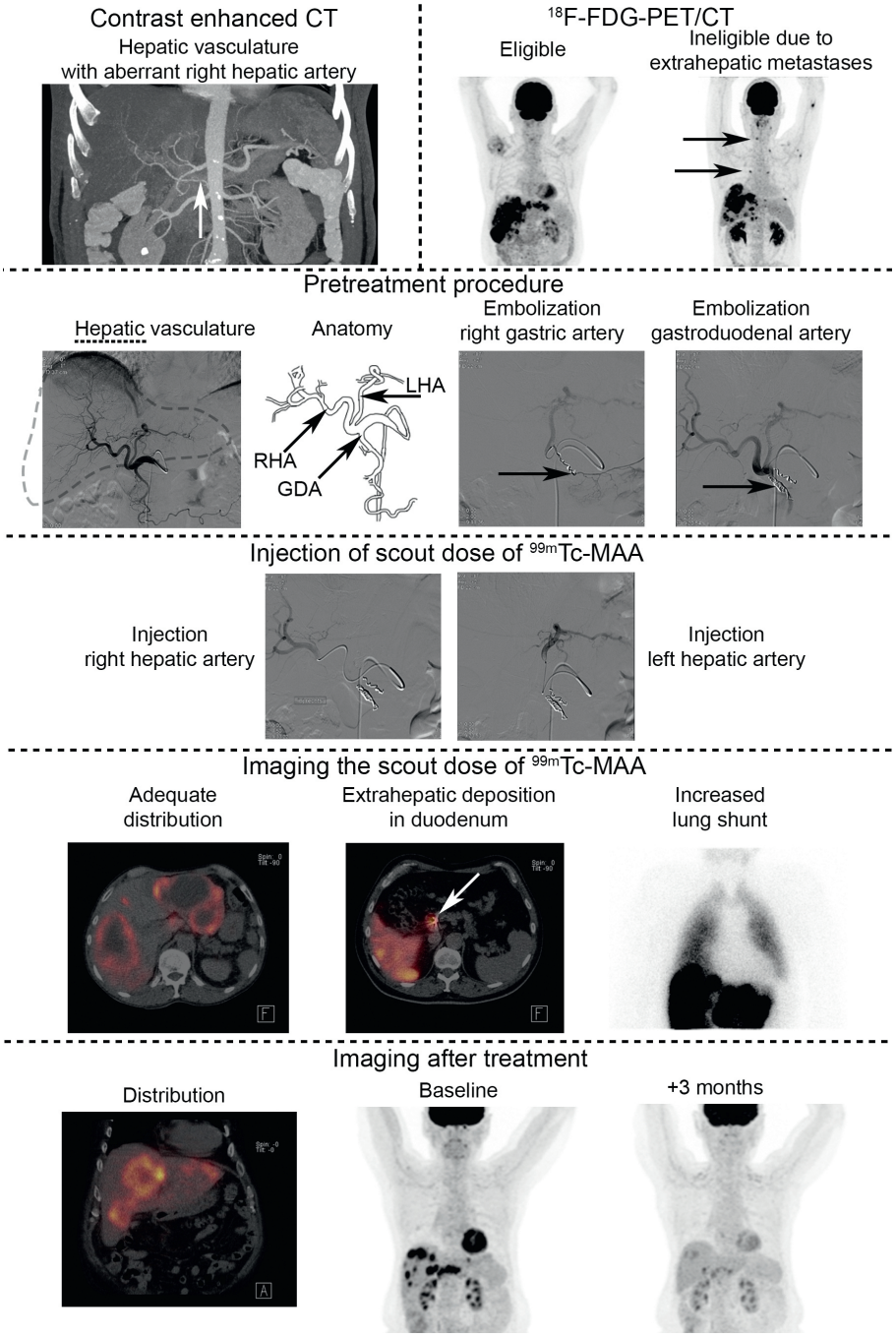

Figure 2 *Imaging of radioembolization during all procedures. RHA = right hepatic artery, LHA = left hepatic artery, GDA = gastroduodenal artery*

laboratory and animal testing, the first human trial in 2011 concluded that radioembolization with ^{166}Ho microspheres was feasible and safe.[13,14] ^{166}Ho can improve radioembolization, because a scout dose of ^{99m}Tc-MAA can be replaced by ^{166}Ho microspheres. The prediction of distribution is better when using the same microspheres for scout and treatment because ^{99m}Tc-MAA does not resemble ^{90}Y or ^{166}Ho microspheres in shape or size distribution. The lung dose is estimated more accurately and the intra-hepatic distribution is expected to be more similar to treatment.[15,16] Better prediction could lead to improved efficacy and reduced toxicity. The prescribed absorbed dose is currently averaged over the whole liver, but the dose per tumor varies per patient (and per tumor) because of heterogeneity in uptake.[17] An accurate scout dose could determine the maximum amount of radioactivity that can safely be administered, maximizing impact. In addition, MR quantification can enable dosimetry during treatment.[18]

However, ^{166}Ho microspheres also differ from ^{90}Y microspheres: half-life is shorter (27 versus 64 hours) and more activity is needed to obtain the same dose. Before large-scale clinical trials can be initiated, efficacy of ^{166}Ho microspheres had to be investigated in the second human trial, the Holmium Embolization Particles for Arterial Radiotherapy (HEPAR) 2 trial. Patients were first given a scout dose of ^{99m}Tc-MAA to check for contraindications. A second scout dose, with ^{166}Ho microspheres, preceded treatment to eventually compare both scout doses with treatment. SPECT/CT and MR imaging were acquired after the scout and treatment dose of ^{166}Ho microspheres to assess quantification accuracy. The primary outcome, efficacy, was evaluated using contrast enhanced CT and ^{18}F-FDG-PET/CT every 3 months up to 1 year after treatment. The primary outcome was rated by three radiologists independently and blinded for time of imaging (baseline or follow up), alike central independent review.[19] Adverse events were recorded in addition to frequent quality of life questionnaires. Because quality of life is important in a salvage setting, the first questionnaire was returned just 1 week after treatment. A sequential trial design with different stopping criteria after every interim analysis ensured timely completion; 30 to 48 patients were to be included with analyses following every 6 patients. Data from the first patients were used to obtain CE marking for ^{166}Ho microspheres in 2015, making it the third commercially available microsphere. The HEPAR 2 trial was completed in August 2015 (Chapter 6).

In future trials, the scout dose of ^{99m}Tc-MAA might be replaced by a scout dose of ^{166}Ho microspheres. In the HEPAR 2, both were performed consecutively because ^{99m}Tc-MAA is only a diagnostic isotope, while ^{166}Ho can induce radiation damage in case an extrahepatic deposition occurred. The infused radioactivity of a scout dose of ^{166}Ho microspheres (250 MBq) was considerably lower than during treatment (≈7.000 MBq), but a high concentration could hypothetically deposit enough energy to induce gastrointestinal ulceration or pancreatitis. Because a scout dose with ^{99m}Tc-MAA always preceded it in trials, few cases of extrahepatic depositions of ^{166}Ho microspheres were available. The radioactivity concentrations of all available cases of extrahepatic deposition of ^{99m}Tc-MAA were measured and translated to a theoretical infusion of 250 MBq of ^{166}Ho microspheres. For example, if 10% of the infused amount of ^{99m}Tc-MAA was found in an extrahepatic deposition, 10% of a scout dose of ^{166}Ho microspheres was assumed to have been deposited if it was used instead. The volumes of the extrahepatic depositions of ^{99m}Tc-MAA were measured to complete the calculation of the radiation damage. Because the volumes were near the detection limit for SPECT, a novel method for volume estimation was also developed and tested in a phantom study (Chapter 5).

During the HEPAR 2 trial, an example of an inadvertent deposition was seen in our practice. A patient had a high predicted dose to the gallbladder, which increased the risk for cholecystitis. It was decided to adjust the catheter position to change the preferential blood flow and alter microsphere deposition. The resulting absorbed dose reduction was measured and existing literature was summarized to inform colleagues about other possible treatment strategies (Chapter 4).

One of the unique properties of ^{166}Ho microspheres is the ability to measure the deposition of microspheres in the lungs via the emitted gamma rays. Measurements by Elschot et al. revealed that, although a scout dose with ^{99m}Tc-MAA was supposed to accurately predict the lung shunt, it did not.[15] In contrast to this observation, in 2012, Jha et al. found a near-perfect association between the lung shunt of a scout dose of ^{99m}Tc-MAA and the lung shunt of the treatment with ^{90}Y microspheres.[20] However, ^{90}Y releases gamma photons only by bremsstrahlung (produced by beta radiation), which is difficult to image due to its wide range in low-energy emissions.[21] To explain this discrepancy, we replicated their study (Chapter 2).

For a high lung shunt, the boundary above which the risk of radiation damage becomes too high (30 Gy) was estimated using planar scintigraphy after administration of a ^{99m}Tc-MAA scout dose.[22] Theoretically, this boundary could be more accurately estimated using SPECT/CT, which is used increasingly after scout procedures and includes scatter and attenuation correction. We suggested a more accurate boundary, discussed resulting differences in patient selection and assessed known risk factors for a high lung shunt on both planar scintigraphy and SPECT/CT (Chapter 3).

Especially for salvage patients, contact restrictions after treatment are burdensome (e.g., sleeping separate from their partner). After ^{166}Ho radioembolization, patients are released within 24 hours, at which time they still emit some radiation and have to abide to contact restricts for 2 additional days. We calculated and measured the potential radiation exposure to bystanders to see if this was necessary (Chapter 7).

In summary, Dr. Ariel and his colleagues pioneered a new treatment of liver cancers (radioembolization) that has become a mainstream therapy for hepatic malignancies. The most recent innovation, ^{166}Ho microspheres, has the potential to further improve two important aspects of treatment: efficacy and safety.

References

1. Ariel IM. Treatment of inoperable primary pancreatic and liver cancer by the intra-arterial administration of radioactive isotopes (Y90 radiating microspheres). Ann Surg. 1965;162:267–78.
2. Braat AJAT, Huijbregts JE, Molenaar IQ, Borel Rinkes IHM, van den Bosch MAAJ, Lam MGEH. Hepatic radioembolization as a bridge to liver surgery. Front Oncol. 2014;4:199.
3. Van Cutsem E, Cervantes A, Nordlinger B, Arnold D, ESMO Guidelines Working Group. Metastatic colorectal cancer: ESMO Clinical Practice Guidelines for diagnosis, treatment and follow-up. Ann Oncol Off J Eur Soc Med Oncol ESMO. 2014;25 Suppl 3:iii1–9.
4. Frilling A, Modlin IM, Kidd M, Russell C, Breitenstein S, Salem R, et al. Recommendations for management of patients with neuroendocrine liver metastases. Lancet Oncol. 2014;15(1):e8–21.
5. Kennedy A, Nag S, Salem R, Murthy R, McEwan AJ, Nutting C, et al. Recommendations for radioembolization of hepatic malignancies using yttrium-90 microsphere brachytherapy: a consensus panel report from the radioembolization brachytherapy oncology consortium. Int J Radiat Oncol Biol Phys. 2007;68(1):13–23.
6. Salem R, Thurston KG. Radioembolization with 90Yttrium microspheres: a state-of-the-art brachytherapy treatment for primary and secondary liver malignancies. Part 1: Technical and methodologic considerations. J Vasc Interv Radiol JVIR. 2006;17(8):1251–78.
7. Fischman AM, Ward TJ, Patel RS, Arepally A, Kim E, Nowakowski FS, et al. Prospective, Randomized Study of Coil Embolization versus Surefire Infusion System during Yttrium-90 Radioembolization with Resin Microspheres. J Vasc Interv Radiol JVIR. 2014;25(11):1709–16.
8. Bilbao JI, Garrastachu P, Herraiz MJ, Rodriguez M, Inarrairaegui M, Rodriguez J, et al. Safety and efficacy assessment of flow redistribution by occlusion of intrahepatic vessels prior to radioembolization in the treatment of liver tumors. Cardiovasc Intervent Radiol. 2010;33(3):523–31.
9. Ho S, Lau WY, Leung TW, Chan M, Johnson PJ, Li AK. Clinical evaluation of the partition model for estimating radiation doses from yttrium-90 microspheres in the treatment of hepatic cancer. Eur J Nucl Med. 1997;24(3):293–8.
10. Mumper RJ, Ryo UY, Jay M. Neutron-activated holmium-166-poly (L-lactic acid) microspheres: a potential agent for the internal radiation therapy of hepatic tumors. J Nucl Med. 1991;32(11):2139–43.
11. Nijsen JF, Zonnenberg BA, Woittiez JR, Rook DW, Swildens-van Woudenberg IA, van Rijk PP, et al. Holmium-166 poly lactic acid microspheres applicable for intra-arterial radionuclide therapy of hepatic malignancies: effects of preparation and neutron activation techniques. Eur J Nucl Med. 1999;26(7):699–704.
12. Seevinck PR, Seppenwoolde J-H, de Wit TC, Nijsen JFW, Beekman FJ, van Het Schip AD, et al. Factors affecting the sensitivity and detection limits of MRI, CT, and SPECT for multimodal diagnostic and therapeutic agents. Anticancer Agents Med Chem. 2007;7(3):317–34.
13. Vente M a D, Nijsen JFW, de Wit TC, Seppenwoolde JH, Krijger GC, Seevinck PR, et al. Clinical effects of transcatheter hepatic arterial embolization with holmium-166 poly(L-lactic acid) microspheres in healthy pigs. Eur J Nucl Med Mol Imaging. 2008;35(7):1259–71.
14. Smits ML, Nijsen JF, van den Bosch MA, Lam MG, Vente MA, Mali WP, et al. Holmium-166 radioembolisation in patients with unresectable, chemorefractory liver metastases (HEPAR trial): a phase 1, dose-escalation study. Lancet Oncol. 2012;13(10):1025–34.
15. Elschot M, Nijsen JFW, Lam MGEH, Smits MLJ, Prince JF, Viergever M a, et al. (99m)Tc-MAA overestimates the absorbed dose to the lungs in radioembolization: a quantitative evaluation in patients treated with (166)Ho-microspheres. Eur J Nucl Med Mol Imaging. 2014;41(10):1965–75.
16. Wondergem M, Smits MLJ, Elschot M, de Jong HWAM, Verkooijen HM, van den Bosch MAAJ, et al. 99mTc-macroaggregated albumin poorly predicts the intrahepatic distribution of 90Y resin microspheres in hepatic radioembolization. J Nucl Med. 2013;54(8):1294–301.
17. Smits MLJ, Elschot M, van den Bosch M a a J, van de Maat GH, van het Schip AD, Zonnenberg B a, et al. In vivo dosimetry based on SPECT and MR imaging of 166Ho-microspheres for treatment of liver malignancies. J Nucl Med. 2013;54(12):2093–100.
18. Nijsen JFW, Seppenwoolde J-H, Havenith T, Bos C, Bakker CJG, van het Schip AD. Liver tumors: MR imaging of radioactive holmium microspheres–phantom and rabbit study. Radiology. 2004;231(2):491–9.

19. Ford R, Schwartz L, Dancey J, Dodd LE, Eisenhauer E a, Gwyther S, et al. Lessons learned from independent central review. Eur J Cancer 1990. 2009;45(2):268–74.

20. Jha AK a, Zade A a, Rangarajan V, Purandare N, Shah S a, Agrawal A, et al. Comparative analysis of hepatopulmonary shunt obtained from pretherapy 99mTc MAA scintigraphy and post-therapy 90Y Bremsstrahlung imaging in 90Y microsphere therapy. Nucl Med Commun. 2012;33(5):486–90.

21. Elschot M, Lam MGEH, van den Bosch MAAJ, Viergever MA, de Jong HWAM. Quantitative Monte Carlo-based 90Y SPECT reconstruction. J Nucl Med. 2013;54(9):1557–63.

22. Leung WT, Lau WY, Ho SK, Chan M, Leung NW, Lin J, et al. Measuring lung shunting in hepatocellular carcinoma with intrahepatic-arterial technetium-99m macroaggregated albumin. J Nucl Med. 1994;35(1):70–3.

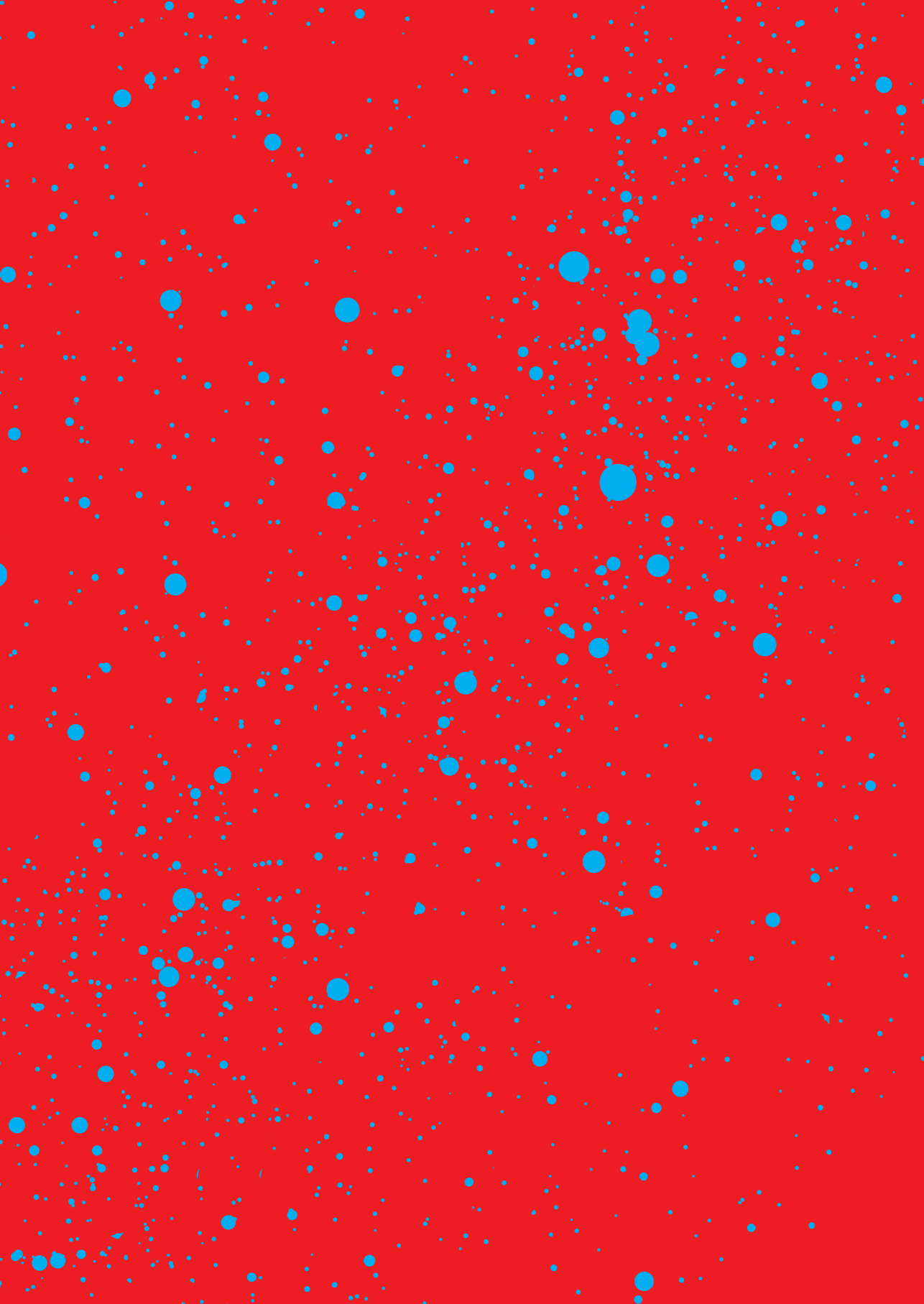

CHAPTER 2

Is there a correlation between planar scintigraphy after ^{99m}Tc-MAA and ^{90}Y administration?

J.F. Prince
R. van Diepen
R. van Rooij
M.G.E.H. Lam

Nuclear Medicine Communications 2015

Comparative analysis of hepatopulmonary shunt obtained from pretherapy ^{99m}Tc MAA scintigraphy and post-therapy ^{90}Y Bremsstrahlung imaging in ^{90}Y microsphere therapy*

Jha AK, Zade AA, Rangarajan V, Purandare N, Shah SA, Agrawal A, Kulkarni SS, Shetty N

Introduction

^{99m}Tc macroaggregate albumin (MAA) scintigraphy is routinely used to estimate the hepatopulmonary shunt (HPS) of ^{90}Y microspheres because of their comparable average particle sizes (20-30 μm). However, the MAA particle size can vary from 10 to 90 μm. Therefore, HPS computed from ^{99m}Tc MAA scintigraphy may not accurately represent the HPS of ^{90}Y microspheres. In view of this, the present study was undertaken to investigate the accuracy of ^{99m}Tc MAA scintigraphy in estimating the HPS of ^{90}Y microspheres.

Materials and methods

Nineteen sessions of transarterial radioembolization using ^{90}Y therasphere were carried out in 17 patients for hepatic malignancies (both primary and secondary). For each session of therapy, a pretherapeutic ^{99m}Tc MAA scintigraphy and post-therapeutic ^{90}Y Bremsstrahlung scintigraphy were performed. The HPSs obtained from these images were compared.

Results

The mean HPS fractions calculated from the pretherapeutic ^{99m}Tc MAA study and the post-therapeutic ^{90}Y Bremsstrahlung images were 4.77 ± 2.81 and 4.52 ± 2.5%, respectively. The coefficient of correlation (r) was 0.96.

Conclusion

^{99m}Tc MAA scintigraphy accurately predicts the HPS of ^{90}Y microspheres.

* *Published as Jha AKA, Zade AA, Rangarajan V, Purandare N, Shah SA, Agrawal A, et al. Comparative analysis of hepatopulmonary shunt obtained from pretherapy 99mTc MAA scintigraphy and post-therapy 90Y Bremsstrahlung imaging in 90Y microsphere therapy. Nucl Med Commun. 2012;33(5):486–90*

Letter to the Editor: Is there a correlation between planar scintigraphy after ^{99m}Tc-MAA and ^{90}Y administration?

Recently, Jha et al. presented an excellent correlation between planar scintigraphy of technetium-99m macroaggregated albumin (^{99m}Tc-MAA) and yttrium-90 (^{90}Y) microspheres.[1] This finding seems to validate the use of ^{99m}Tc-MAA for the prediction of lung shunt after radioembolization with ^{90}Y microspheres, but in our experience, lung shunting is rarely seen on planar scintigraphy after ^{90}Y radioembolization.

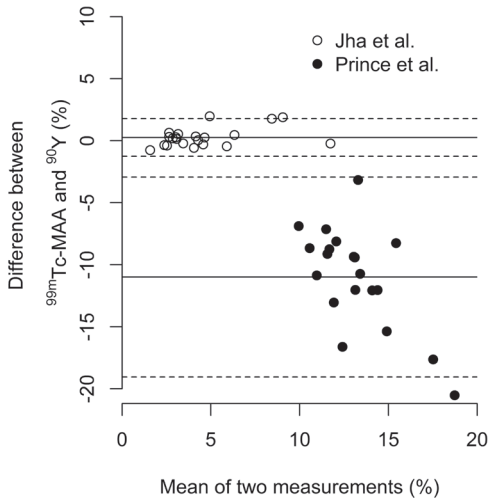

Figure 1 *Agreement of the lung shunt (in %) of ^{99m}Tc-MAA and ^{90}Y differs between the two studies as shown by this Bland Altman plot.*

^{99m}Tc-MAA is used in combination with planar scintigraphy to predict the lung shunt after treatment with ^{90}Y hepatic radioembolization. When sufficient ^{90}Y microspheres shunt to the lungs, their release of beta radiation can result in radiation pneumonitis. Patients are precluded from treatment if the lung shunt of ^{99m}Tc-MAA is too high. The predictive value of ^{99m}Tc-MAA is important for clinical practice, because around 40% of patients have their administered activity reduced or denied because of a high lung shunt.[2] After treatment, ^{90}Y microspheres can be detected using bremsstrahlung radiation, for which some centers, including ours, perform planar scintigraphy after treatment.

Jha et al. selected 17 patients with 19 treatment sessions for whom they measured the lung shunt fraction on planar scintigraphy after injection of ^{99m}Tc-MAA and after treatment with ^{90}Y microspheres. They reported an excellent correlation coefficient between the two of 0.96. To replicate the findings of Jha et al., we analyzed our own data of 20 consecutive patients treated with ^{90}Y (20 treatment sessions) between May 2011 and January 2012 (after which we started using PET), using the same methodology. The research ethics committee waived the need for informed consent. No correlation could be found in our data, Pearson's *r* was 0.10 (95% CI -0.36 – 0.52). Using the data provided by Jha et al., we compared the agreement and reliability. The agreement of our data, as shown by a Bland Altman plot, is much worse. The 95% limits of agreement between the two studies do not even overlap (Figure 1). Our intraclass correlation coefficient is also considerably less: 0.08 (95% CI -0.37 – 0.49) vs 0.95 (95% CI 0.89 – 0.98).

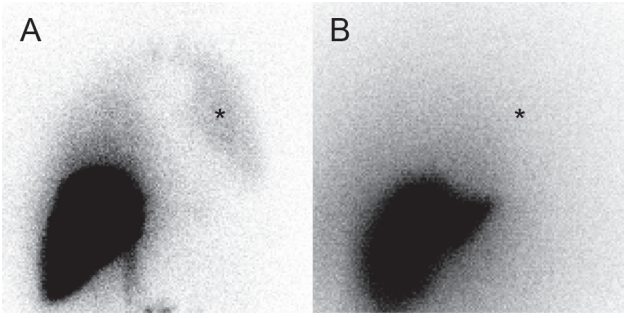

Figure 2 *A lung shunt is visible after 99mTc-MAA (a, 11.6%), while no lung shunt, only scatter, is visible after administration of 90Y (b, 19.6%). Note the falciform artery after 99mTc-MAA injection (a) *Left lung. 99mTc-MAA, technetium-99m macroaggregated albumin; 90Y, yttrium-90.*

This comparison may be limited by technical differences. However, the same methodology for background correction as Jha et al. was used for the bremsstrahlung images. Also, our images are in correspondence with the data and do not suggest any correlation (Figure 2). No visual resemblance between ^{99m}Tc-MAA and ^{90}Y was seen.

The distributions of ^{99m}Tc-MAA and ^{90}Y are probably not comparable. The particle size distribution is different because the aggregated albumin particles are asymmetrical and include several small particles. ^{99m}Tc can also release from the aggregates which is regularly seen as stomach or thyroid uptake. In contrast, the microspheres lodge in the lung parenchyma and are not found anywhere else in

the body. This hypothesis is confirmed by a study in 14 patients performed by Elschot et al., who found a significant difference in lung shunt estimation between ^{99m}Tc-MAA and holmium-166 (^{166}Ho) microspheres (median overestimation 5.4 Gy, range 1.5 – 18.2 Gy, $p < 0.001$).[3] These microspheres are expected to have a similar distribution pattern during radioembolization as ^{90}Y, because of their same morphology (microspheres instead of aggregates) and size (around 30 μm). The used isotope ^{166}Ho emits gamma photons which enables detection and quantification.

In conclusion, we were unable to replicate the results of Jha et al. Other centers using bremsstrahlung imaging may perhaps be able to contradict either our findings or the findings by Jha et al. The results of ^{99m}Tc-MAA imaging changes the treatment plan in many patients, so validation is sorely needed.

References

1. Jha AKA, Zade AA, Rangarajan V, Purandare N, Shah SA, Agrawal A, et al. Comparative analysis of hepatopulmonary shunt obtained from pretherapy 99mTc MAA scintigraphy and post-therapy 90Y Bremsstrahlung imaging in 90Y microsphere therapy. Nucl Med Commun. 2012;33(5):486–90.
2. Gaba RC, Zivin SP, Dikopf MS, Parvinian A, Casadaban LC, Lu Y, et al. Characteristics of primary and secondary hepatic malignancies associated with hepatopulmonary shunting. Radiology. 2014;271(2):602–12.
3. Elschot M, Nijsen JFW, Lam MGEH, Smits MLJ, Prince JF, Viergever M a, et al. (99m)Tc-MAA overestimates the absorbed dose to the lungs in radioembolization: a quantitative evaluation in patients treated with (166)Ho-microspheres. Eur J Nucl Med Mol Imaging. 2014;41(10):1965–75.

Response to Letter to the Editor*

Jha AK, Purandare N, Shah SA, Agrawal A, Rangarajan V, Kulkarni SS

Transarterial radioembolization (TARE) is a choice of treatment for nonresectable primary and secondary hepatic malignancy. Various β-emitting radioisotopes are used in various forms for TARE. For several years, yttrium-90 (^{90}Y)-microspheres have been used clinically to treat this disease. There are two commercially available ^{90}Y-microsphere products that are approved by the US Food and Drug Authority (FDA, Silver Spring, Maryland, USA) for TARE. ^{90}Y-TheraSphere, MDS Nordion, Ottawa, Ontario, Canada (Biocompatibles UK Ltd, Surrey, UK), was approved by the FDA in December 1999. ^{90}Y-SIRSpheres, Sirtex Medical Inc., Sydney, Australia, was approved in March 2002. Both products are utilized for primary and secondary liver malignant tumours. ^{90}Y-SIRSphere is a ^{90}Y resin microsphere that is a polymer bead of 20–40 μm diameter. The specific activity of ^{90}Y-SIRSphere is 40–70 q/Sphere. ^{90}Y-TheraSphere is a ^{90}Y-Glass-Sphere that measures between 20 and 30 μm in diameter and is tagged with ^{90}Y at a specific activity of 2400–2700 Bq/Sphere.[1,2] TARE is known to cause radiation pneumonitis if the hepatopulmonary shunt (HPS) is high. Preclinical and clinical studies with ^{90}Y-microspheres have demonstrated that up to 30 Gy radiation dose to the lungs could be tolerated with a single injection, and up to 50 Gy for multiple injections.[3] Hence, proper therapy planning before TARE is essential to ensure the efficacy of the treatment with minimal side effects. Planning of therapy is performed on the basis of a baseline catheter angiography, contrast enhanced computed tomography of the liver, and a technetium-99m microaggregated albumin (^{99m}Tc-MAA) (median size 20–40 μm ranging from 10 to 70 μm)[4] planar and single-photon emission computed tomographic (SPECT) study. Baseline angiography is performed to evaluate the vascular anatomy of the tumour and its surrounding normal liver. Contrast enhanced computed tomography is performed to estimate the total liver, total tumour volume and volume to be treated. ^{99m}Tc-MAA is used as a surrogate to map the post-therapeutic microsphere distribution in the hepatic tumour, normal liver, shunt in the lung and any other abnormal distribution like in the stomach, duodenum and gallbladder.[1-3] Various studies have been published on ^{90}Y-microsphere therapy, and the use of ^{99m}Tc-MAA has been advocated to estimate

* *Published as Jha AK, Purandare N, Shah SA, Agrawal A, Rangarajan V, Kulkarni SS. Is there a correlation between planar scintigraphy after ^{99m}Tc-MAA and ^{90}Y administration? Nucl Med Commun. 2016;37(2):107-9.*

the HPS and the tumour to normal ratio and to detect the abnormal extrahepatic uptake of tracer. However, the predictive value of a pretherapeutic ^{99m}Tc-MAA scan to depict the therapeutic distribution of ^{90}Y-microspheres is subject to various factors such as (a) pretherapeutic and therapeutic interventional procedure, (b) radiopharmaceutical quality, (c) scan parameters and (d) postprocessing for HPS calculation.

(a) Pretherapeutic and therapeutic intervention procedure: Transarterial administration of ^{99m}Tc-MAA may not always be performed similar to the TARE procedure. Occasionally ^{99m}Tc-MAA is administered from the common hepatic artery or the left or the right hepatic artery, but administration of ^{90}Y-microspheres is super-selective and delivered through the tumour-feeding artery. HPS is a phenomenon that occurs because of arteriovenous shunting in the tumour; therefore, only the super- selective delivery of ^{99m}Tc-MAA will truly depict the therapeutic distribution of the ^{90}Y-microsphere. (b) Radiopharmaceutical quality: ^{99m}Tc-MAA preparation is not stable at room temperature and has to be stored at 2–8°C just after formulation; at the same time, the in-vivo half-life of the ^{99m}Tc-MAA conjugate is only 2h.[4] Hence, the immediate administration of ^{99m}Tc-MAA after the formulation and scanning within a short duration after administration improves the quality of the image. The quality of the image may also be degraded because of free pertechnatate; hence, oral administration of perchlorate 15 min before transarterial administration of ^{99m}Tc-MAA blocks the free pertechnatate uptake in organs like the thyroid and stomach and improves the quality of the image. Although the particle size of TheraSphere and SIRSphere is almost the same, the biological behaviour of both microspheres is different because of the difference in embolic effect. Hence, HPS with the SIRSphere may not be comparable to that of the TheraSphere. (c) Scan parameters: Selection of scan parameters is very important, particularly for ^{90}Y-microsphere bremsstrahlung imaging.[5] The judicious selection of energy window and collimator for scanning is of utmost importance. The scan parameters used in our department for the ^{99m}Tc-MAA scan and ^{90}Y-microsphere bremsstrahlung imaging have been discussed in our earlier publication.[6] (d) Postprocessing for HPS calculation: Drawing a region of interest (ROI) around the liver and the lung is important for appropriate calculation of HPS. However, drawing an ROI around the lung is particularly difficult in the HPS study either with ^{99m}Tc-MAA or with ^{90}Y-microsphere bremsstrahlung images; hence, we use a phantom image to draw a proper ROI around the lung and the

liver. Drawing a background ROI particularly on ^{90}Y-microsphere bremsstrahlung images is more difficult because of cross-contamination of pixels in basal lung ROI produced by the scatter counts for the liver. Background ROI should therefore be drawn judiciously to subtract the scatter count from the lung ROI and the person doing it should have sound knowledge of bremsstrahlung imaging on a gamma camera.

Many authors have questioned the HPS finding of pre-therapeutic ^{99m}Tc-MAA imaging in conjunction with the findings of Prince et al.[7] Elschot et al.[8] have reported overestimation of HPS by ^{99m}Tc-MAA in comparison with post-therapeutic bremsstrahlung imaging. Smits et al.[9] have also disputed the use of ^{99m}Tc-MAA as a predictor of HPS in the range of 10–19% of HPS. The authors in both studies have advocated the use of a small amount of holmium-166 (^{166}Ho)-microspheres as a surrogate of ^{166}Ho-microspheres, which is a reasonable argument. However, none of the studies have even described the bremsstrahlung imaging protocol in detail, and in my view technical and manual error can lead to an erroneous result as these two errors are a part and parcel of nuclear medicine imaging. Prince et al.[7] have claimed to have adopted the same method as ours, but they have not described the procedure in their paper. They have also not described any of the above five steps, which is necessary to produce a reasonable result out of the study. Hence, it would be difficult to pinpoint the exact reason for the difference in results between the two studies. Moreover, we feel that there are a few issues in the study by Prince et al.[7] that need to be addressed: (i) the left lung is marked as the right lung; (ii) the right hepatic artery is seen in the ^{99m}Tc-MAA scan but not seen in the ^{90}Y-SIRSphere bremsstrahlung scan (shows that the delivery of MAA and microsphere might not have been performed identically); and (iii) although authors claim that there was no uptake in the lung on ^{90}Y-SIRSphere bremsstrahlung imaging, the calculated HPS is more than that of the calculated HPS of ^{99m}Tc-MAA. These could be the possible reasons for the discordant results between the two studies.

We would like to cite our earlier study of 19 patients who underwent TARE at our institution, in which we found excellent correlation between HPS (range of HPS<10%) calculated on the pretherapeutic ^{99m}Tc-MAA scan and the ^{90}Y-TheraSphere bremsstrahlung scan.[6] We followed strict criteria to achieve reliable and consistent results and meticulously followed all of the above five described steps. In a recently published study Kao and colleagues have demonstrated the

utility of planar ^{99m}Tc-MAA scan for lung dosimetry in TARE. They have used a methodology similar to the one in our study to calculate HPS on planar scans and compare it with SPECT/computed tomography (CT). The study demonstrated that lung dosimetry by both planar and SPECT/CT was accurate, but SPECT/CT offers better precision. They performed Bland–Altman analysis for planar and SPECT/CT methodology and their result showed the planar methodology to have a small bias of −0.41 Gy compared with SPECT/CT, which is dosimetrically insignificant.[10] Another recently published work by Song et al.[11] on dosimetric comparison between pretherapeutic ^{99m}Tc-MAA SPECT/CT and post-therapeutic ^{90}Y-microsphere PET/CT has also demonstrated a good correlation between pretherapeutic and post-therapeutic dosimetery, and the authors have recommended the use of ^{99m}Tc-MAA for dosimetric planning of TARE. Ahmadzadehfar et al.[12] have also stressed the use of ^{99m}Tc-MAA for pretherapeutic dosimetric planning.

Considering the existing literature, ^{99m}Tc-MAA can be used as a surrogate for the ^{90}Y-microsphere. Correlation between ^{99m}Tc-MAA planar imaging with ^{90}Y-microsphere therapy may be established by performing the procedure meticulously. The use of ^{166}Ho-microsphere in small amounts can be considered for SPECT/CT quantification. The ^{166}Ho-microsphere is also emerging as an alternative TARE agent.[8,13] Considering the complexity of bremsstrahlung imaging we have shifted to ^{90}Y-microsphere PET/CT imaging for better post-therapeutic scan visualization.[14] Recently we have also tested and established the formulation technique of gallium-68 (^{68}Ga)-MAA as a PET agent at our centre, which can be utilized for pretherapeutic TARE planning and dosimetry. Recent literature also favours the use of ^{90}Y-microsphere PET/CT imaging for post-therapeutic quantification.[14-18] The widespread availability of the ^{68}Ga isotope through a ^{68}Ga/^{68}Ge generator and ease of ^{68}Ga-MAA formulation may open new horizons in PET/CT-based TARE therapy planning and dosimetry. PET/CT with ^{68}Ga-MAA is likely to provide better quantitation than SPECT/CT and is more likely to resolve existing issues.

References

1 TheraSphere™ yttrium-90 glass microspheres instructions for use, Biocompatibles UK Ltd, Surrey, UK; 2005. Available at: http://www.therasphere.com/physicians-package-insert/TS_PackageInsert_USA_v12.pdf. [Accessed 5 September 2015].

2 Sirtex Medical Limited. Sirtex medical training manual, training program physicians and institutions; Australia. Available at: http://foxfireglobal.sirtex.com/sites/foxfireglobal.sirtex.com/files/user/trn-rw-04_for_eu_au_nz_and_asia.pdf. [Accessed 5 September 2015].

3 Leung TWT, Lau WY, Ho SKW, Ward SC, Chow JH, Chan MS, et al. Radiation pneumonitis after selective internal radiation treatment with intra-arterial 90-yttrium-microspheres for inoperable hepatic tumors. Int J Radiat Biol Phys 1995;33:919–924.

4 MAA kit for the preparation of 99m Tc-MAA, package insert DRAXIMAGE®. Available at: http://www.accessdata.fda.gov/drugsatfda_docs/label/2009/017881s010lbl.pdf. [Accessed 5 September 2015].

5 Shen S, DeNardo GL, Yuan A, DeNardo DA, DeNardo SJ. Planar gamma camera imaging and quantitation of yttrium-90 bremsstrahlung. J Nucl Med 1994;35:1381–1389.

6 Jha AK, Zade AA, Rangarajan V, Purandare N, Shah SA, Agrawal A, et al. Comparative analysis of hepatopulmonary shunt obtained from pretherapy 99m Tc MAA scintigraphy and post-therapy 90 Y bremsstrahlung imaging in 90 Y microsphere therapy. Nucl Med Commun 2012;33:486–490.

7 Prince JF, van Diepen R, van Rooij R, Lam MGEH. Is there a correlation between planar scintigraphy after 99m Tc-MAA and 90 Y administration? Nucl Med Commun 2015; (in press).

8 Elschot M, Nijsen JFW, Lam MGEH, Smits MLJ, Prince JF, Viergever MA, et al. (99m)Tc-MAA overestimates the absorbed dose to the lungs in radioembolization: a quantitative evaluation in patients treated with (166)Ho-microspheres. Eur J Nucl Med Mol Imaging 2014;41:1965–1975.

9 Smits ML, Nijsen JF, van den Bosch MA, Lam MG, Vente MA, Huijbregts JE, et al. Holmium-166 radioembolization for the treatment of patients with liver metastases: design of the phase I HEPAR trial. J Exp Clin Cancer Res 2010;29:70.

10 Kao YH, Magsombol BM, Toh Y, Tay KH, Chow PKH, Goh ASW, Ng DCE. Personalized predictive lung dosimetry by technetium-99m macroaggregated albumin SPECT/CT for yttrium-90 radioembolization. EJNMMI Res 2014;4:33.

11 Song YS, Paeng JC, Kim HC, Chung JW, Cheon GJ, Chung JK, et al. PET/CT-based dosimetry in 90 Y-microsphere selective internal radiation therapy: single cohort comparison with pretreatment planning on (99m)Tc-MAA imaging and correlation with treatment efficacy. Medicine (Baltimore) 2015;94:e945.

12 Ahmadzadehfar H, Duan H, Haug AR, Walrand S, Hoffmann M. The role of SPECT/CT in radioembolization of liver tumours. Eur J Nucl Med Mol Imaging 2014;41(Suppl 1):115–124.

13 Da Costa Guimarães C, Moralles M, Martinelli JR. Monte Carlo simulation of liver cancer treatment with 166 Ho-loaded glass microspheres. Radiat Phys Chem 2014;95:185–187.

14 Zade AA, Rangarajan V, Purandare NC, Shah SA, Agrawal AR, Kulkarni SS, Shetty N. 90 Y microsphere therapy: does 90 Y PET/CT imaging obviate the need for 90 Y bremsstrahlung SPECT/CT imaging? Nucl Med Commun 2013;34:1090–1096.

15 Attarwala AA, Molina-Duran F, Busing KA, Schonberg SO, Bailey DL, Willowson K, et al. Quantitative and qualitative assessment of yttrium-90 PET/CT imaging. PLoS One 2014;9:e110401.

16 Werner MK, Brechtel K, Beyer T, Dittmann H, Pfannenberg C, Kupferschlager J. PET/CT for the assessment and quantification of (90)Y biodistribution after selective internal radiotherapy (SIRT) of liver metastases. Eur J Nucl Med Mol Imaging 2010;37:407–408.

17 D'Arienzo M, Filippi L, Chiaramida P, Chiacchiararelli L, Cianni R, Salvatori R, et al. Absorbed dose to lesion and clinical outcome after liver radioembolization with 90 Y microspheres: a case report of PET-based dosimetry. Ann Nucl Med 2013;27:676–680.

18 Siva S, Devereux T, Ball DL, MacManus MP, Hardcastle N, Kron T, et al. Ga-68 MAA perfusion 4D-PET/CT scanning allows for functional lung avoidance using conformal radiation therapy planning. Technol Cancer Res Treat 2015. [Epub ahead of print]

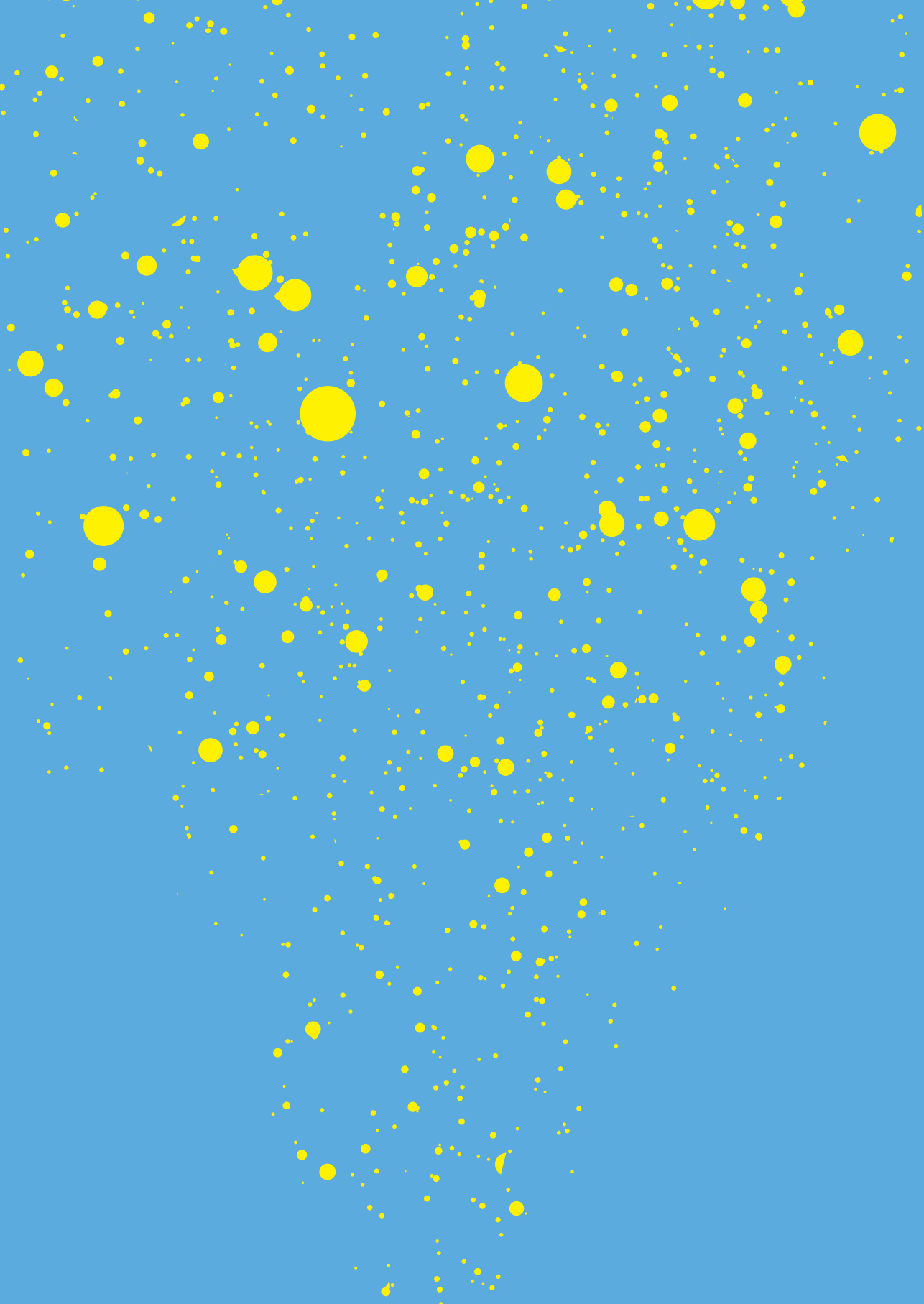

CHAPTER 3

SPECT/CT analysis of ^{99m}Tc-MAA lung shunt: implications for hepatic radioembolization

J.F. Prince
A.F. van den Hoven
G.C. Krijger
B.J. van Nierop
M.N.G.J.A. Braat
M.A.A.J. van den Bosch
H.M. Verkooijen
M.G.E.H. Lam

Submitted

Abstract

Objectives

To investigate if SPECT/CT after injection of ^{99m}Tc-MAA can be used to estimate the lung absorbed dose after radioembolization in order to: define the dose limit on SPECT/CT, investigate if SPECT/CT and planar scintigraphy differ in selecting patients for treatment, and validate risk factors for a high lung shunt.

Methods

All patients eligible for radioembolization between 2011 and 2013 were included in this retrospective, cross-sectional study. The lung shunt after ^{99m}Tc-MAA injection was measured on planar scintigraphy and SPECT/CT and expressed as the lung absorbed dose per GBq yttrium-90. Univariable associations between lung shunting and recognized risk factors were analyzed.

Results

In total, 138 ^{99m}Tc-MAA injections in 111 patients were included. A dose limit of 30 Gy on planar scintigraphy corresponds to only 15 Gy calculated on SPECT/CT. Of patients with a high lung shunt on SPECT/CT, 44% were not identified on planar scintigraphy. The agreement between both modalities was low and the reliability was moderate. Risk factors identified on both modalities were: angioinvasion, tumor burden, time between ^{99m}Tc-MAA injection and imaging, and thyroid uptake.

Conclusions

SPECT/CT and planar scintigraphy differ in estimation of the lung absorbed dose limit. SPECT/CT can be used for more accurate patient selection.

Introduction

Radioembolization is a treatment for liver tumors of various primary origins.[1,2] Microspheres loaded with the radioisotope yttrium-90 (^{90}Y) and a mean diameter of 30 μm are injected in the hepatic artery to radiate and embolize liver tumors. Some of these microspheres will inadvertently shunt to the lung parenchyma, where they can induce radiation pneumonitis.[3,4] The lung shunt is calculated by planar scintigraphy after the administration of a scout dose consisting of technetium-99m macroaggregated albumin (^{99m}Tc-MAA).

If the lung shunt fraction is found to be too high, the risk of radiation pneumonitis is considered too high and the treatment activity has to be reduced or has to not be given at all. For resin microspheres, the prescribed activity is reduced by 20% for patients with a lung shunt fraction of 10-15%, and by 40% for lung shunt fractions ranging from 15-20%.[5] Treatment is contraindicated for a lung shunt fraction larger than 20%.[5] For glass microspheres, treatment is contraindicated if more than 30 Gy (or 610 MBq) is deposited in the lungs.[6] In around 40% of the radioembolization patients, the prescribed activity is reduced or treatment is contraindicated because of a high lung shunt fraction.[7]

The evidence for setting the threshold at 30 Gy is marginal, since it is based on data from only three case series.[4,8,9] In 2008, Salem et al. reported on 58 patients (from a series of 403 patients) with a lung dose higher than 30 Gy: none developed radiation pneumonitis.[10] In addition, Gaba et al. reported that 8 of their patients (of 140) had received a lung dose >30 Gy and 5 a cumulative lung dose >50 Gy: only two developed a cough.[7] So, although early reports indicate a boundary defined by planar scintigraphy around 30 Gy, cases of radiation pneumonitis are rare and a clear relationship to the lung dose has not been established.[11,12] Most likely, the current lung dose limit is too conservative, leading to an unnecessary reduction of treatment activity, which is associated with a decrease in efficacy.[13]

Several authors have suggested that SPECT/CT, rather than planar scintigraphy, could improve dosimetry and thus the accurate identification of risk factors for radiation pneumonitis.[14,15] Quantification on SPECT/CT is more accurate, because it corrects for scatter and attenuation. However, because the estimated lung dose for a particular patient is most likely not the same for planar

scintigraphy and SPECT/CT, the maximum dose limit needs to be redefined. Furthermore, it might be possible to predict which patients have a high lung shunt prior to administration of ^{99m}Tc-MAA. Several authors have identified risk factors for a high lung shunt fraction on either planar scintigraphy or SPECT/CT.[7,16] These risk factors require validation in another cohort and/or adjustment in a multivariable model.

The purpose of this study was to investigate the feasibility of a lung dose estimation based on SPECT/CT instead of planar scintigraphy after injection of ^{99m}Tc-MAA. The objectives of this study were: to define current limits for lung shunting on SPECT/CT, to investigate potential differences in patient selection between SPECT/CT and planar scintigraphy, and to validate risk factors for a high lung shunt.

Materials and Methods

Study design

A single center, retrospective, cross-sectional study was performed. The lung shunt fraction was calculated using SPECT/CT in addition to the clinically used value based on planar scintigraphy. The clinical impact on patient selection of using SPECT/CT instead of planar scintigraphy was determined. To this end, the lung dose after a hypothetical administration of resin (2 GBq) and glass (5 GBq) ^{90}Y microspheres was calculated for both methods, and the number of patients with a high lung shunt according to both methods was compared. Associations between risk factors and shunt fractions were analyzed. The research ethics committee waived the need for informed consent to retrospectively analyze these image data.

Patient selection and treatment

All patients eligible for radioembolization in our center between March 2011 and November 2013 were included in this study. Patients had liver-dominant disease with a life expectancy of more than 3 months, acceptable liver and kidney function, and a moderate performance status (WHO 0-1). During pretreatment angiography, digital subtraction angiography with additional C-arm CT was used to obtain a safe injection position, after which 150 MBq of ^{99m}Tc-MAA (0.8 mg, Technescan

LyoMAA; Mallinckrodt Medical B.V., Petten, The Netherlands) was injected. If more than 1 injection position was used, ^{99m}Tc-MAA was fractionated according to the target liver volume. Nuclear imaging was performed as soon as possible after administration. No perchlorate was administered to inhibit uptake of free pertechnetate in the stomach.

Scan settings

In all patients, both planar and SPECT/CT images were acquired with a Siemens Symbia T16 SPECT/CT system (Siemens Healthcare, Erlangen, Germany).[17] Briefly, low-energy high-resolution collimators (hole length 24.05 mm, septal thickness 0.16 mm, hole diameter 1.11 mm) were mounted. ^{99m}Tc-MAA planar images of the abdomen and the thorax were acquired on a 256 × 256 matrix (zoom 1.0, pixel size 2.4 × 2.4 mm^2) over 300 s with the camera heads in the anterior and posterior position. The photopeak window was set to 140 keV ±7.5%. Abdominal and thoracic geometric mean (GM) images were calculated from the anterior and posterior projections. An anterior thorax projection of a ^{57}Co flood-source placed behind the patient was acquired to aid delineation of the lung regions.

^{99m}Tc-MAA SPECT data of the abdomen (including the basal part of the lungs) were acquired on a 128 × 128 matrix (zoom 1.23, pixel size 3.9 × 3.9 mm^2) using 120 angles (20 s per projection) over a noncircular 360° orbit and a 140 keV ±7.5 % photopeak energy window. Low-dose CT data (130 kVp, 30 mAs, adaptive dose modulation) were acquired and reconstructed to a voxel size of 0.78 × 0.78 × 5 mm^3 using a smoothing kernel (B08s; Siemens Healthcare). SPECT images were reconstructed to a voxel size of 0.85 x 0.85 x 4 mm^3 using a standard, clinical 3D iterative reconstruction algorithm (FLASH 3D, Siemens Healthcare) with CT-based attenuation correction, scatter correction and resolution recovery using 6 iterations, 8 subsets and a 5 mm Gaussian post-reconstruction filter.[18,19]

Lung shunt calculations

To estimate how a 30 Gy dose limit based on planar imaging translates to an appropriate dose limit for SPECT/CT, a linear model was made with the lung dose based on SPECT/CT as dependent variable and the lung dose based on planar scintigraphy as the independent variable. A SPECT/CT-based lung dose with 95% confidence intervals was predicted for a planar lung dose of 30 Gy. The number of misclassifications relative to the planar lung dose was determined for the prediction

of a typical case of radioembolization using resin microspheres (2 GBq) and glass microspheres (5 GBq).

The association between patient characteristics and lung shunt was investigated in terms of lung shunt fractions (instead of lung dose). The lung shunt fraction is defined as the fraction of ^{99m}Tc-MAA particles that end up in the lung after injection in the hepatic artery, which is used as a surrogate for the lung shunt after injection of ^{90}Y. Using planar scintigraphy, counts in the lungs are divided by counts in the lungs plus the liver, and a fraction (expressed as %) is calculated. Using SPECT/CT, the lungs are not always fully imaged so a lung dose (Gy) per infused amount (GBq) is calculated instead. The fraction (expressed as %) is interchangeable with this Gy/GBq if one assumes the amount of lung tissue to be equal across all patients, e.g. 1 GBq of infused ^{90}Y with 10% shunt fraction would result in 100 MBq lung deposition over 1 kg of lung tissue. A SPECT/CT would, in theory, show the same result, but would only measure part of the lungs, e.g. measure 90 MBq in 900g of lung tissue and find the same MBq/kg (and thus Gy/GBq).

After planar scintigraphy, the lungs were delineated using the ^{57}Co flood projection images. The treated part of the liver was delineated based on the count intensity. For both, the geometric mean of the counts was calculated and the lung shunt fraction (expressed as %) was calculated by dividing the number of counts in the lungs by the number of counts in the lungs plus liver, multiplied by 100. The lung dose (Gy) was then estimated from the lung shunt fraction by multiplication with the injected activity (GBq) and the amount of energy deposited per GBq ^{90}Y (49.67 J GBq^{-1}), and assuming a lung mass of 1 kg.[20,21] In contrast to planar scintigraphy, the dose on SPECT/CT was calculated directly from the part of the lungs that was imaged (both activity and tissue mass were known).

For the SPECT-based lung shunt, the lungs and liver were delineated based on the low-dose CT and co-registered to the SPECT. A margin of 2 cm was then added to the liver delineation, to encompass all scatter originating from the liver. Next, the liver delineation was subtracted from the lung delineation to avoid scatter in the lung delineation.[17] The counts in the lung were standardized to a mass of 1 kg lung tissue, analogous to planar scintigraphy, using the volume of lung in the field-of-view and assuming a lung density of 0.3 kg L^{-1} (*counts over imaged lungs*).

Standardization ensured the shunt was not underestimated for patients with a high lung shunt fraction while still using only the imaged part of the SPECT for the dose calculation (for the lung mass). Finally, the SPECT-based lung dose (expressed as Gy/GBq) was calculated by multiplication of the estimated lung shunt by the amount of energy deposited per GBq (49.67 J GBq^{-1}), and by dividing by the lung mass (1 kg):

Counts over total lungs

$$= Counts\ over\ imaged\ lungs * \frac{1\ kg\ lung\ tissue}{Volume\ of\ lung\ delineation\ (in\ L) \times 0.3\ kg\ L^{-1}}$$

$$Lung\ shunt\ \left(in \frac{Gy}{GBq}\right) = \frac{\frac{Counts\ over\ total\ lungs}{Counts\ over\ total\ lungs + liver\ (+2cm)} \times 49.67\ J\ GBq^{-1}}{1\ kg}$$

The actual absorbed lung dose after treatment was estimated by multiplying the net injected activity (in GBq) by the lung shunt (in Gy/GBq). Analysis of the actual lung dose was performed on patients treated with ^{90}Y resin microspheres. ^{90}Y glass microspheres were used only once during the inclusion period while other patients received ^{166}Ho, their results are published elsewhere.[17] Additionally, all suitable CT scans after treatment (thoracic CT or low dose CT accompanying PET) were reviewed for signs of radiation pneumonitis.

Risk factors

The following determinants were analyzed as possible risk factors: tumor type, lung metastasis, hypervascularity, angioinvasion, tumor burden, time since last chemotherapy, time after preparation and injection of MAA, and thyroid uptake of free pertechnetate ($^{99m}TcO_4^-$). Patients were categorized in the following groups of tumor types: colorectal carcinoma, hepatocellular carcinoma, cholangiocarcinoma, uveal melanoma, or other. For colorectal patients, the presence of extrahepatic metastasis was scored on ^{18}F-FDG-PET/CT. A radiologist (MB) evaluated both the hypervascularity and angioinvasion on contrast-enhanced CT or MRI unaware of the lung shunt fraction. Hypervascularity was defined as arterial contrast enhancement. Angioinvasion was defined as tumor growth, compression, or thrombus in the hepatic or portal vein (main or 1st order branch). It was dichotomized as present or absent. The size of the tumor relative to the target volume was estimated on contrast enhanced CT or MRI by one of the investigators (JP) and categorized as <10%, 10-50%, or >50%. The

time since receiving the last chemotherapy was retrieved from the electronic medical records. Preparation times of ^{99m}Tc-MAA were collected from the radiopharmacy quality assurance system. Injection times were based on the dispatch and return of the ^{99m}Tc-MAA syringes. SPECT acquisition times were acquired from the DICOM information. The uptake of $^{99m}TcO_4^-$ in the thyroid was expressed as percentage relative to the liver uptake on planar scintigraphy (analogous to the lung shunt).

Statistics

Values were displayed as median (range). Intraclass correlation coefficients (ICCs) were calculated while taking systematic differences into account ($ICC_{agreement}$) and ignoring them ($ICC_{consistency}$).[22] A Bland-Altman plot was used to display the differences between planar and SPECT-based lung shunt calculation.[23] Because differences between the two measurements were dependent on the mean (differences are higher for higher values), both variables were log-transformed and the limits of agreement were calculated as described previously.[24] Associations between continuous variables were calculated using Pearson's product moment correlation after log-transformation of the outcome variable (planar scintigraphy: lung shunt fraction; SPECT/CT: lung dose per GBq ^{90}Y). Differences between two groups were tested for using the Wilcoxon rank sum test. For more than two groups, the Kruskal-Wallis rank sum test was used. Statistical analyses were performed in R (version 3.1.1 for Windows), with a two-sided significance level (alpha) of 0.05.[25]

Results

Study population

Between March 2011 and November 2013, a total of 138 ^{99m}Tc-MAA injections were performed with subsequent SPECT/CT in 111 patients (Table 1).

Table 1. *Baseline characteristics*

Characteristic	N (%) or median (range)
Patients	111
Male sex	69 (62%)
Age (years)	65 (35-84)
Primary tumor type	
Colorectal	63 (57%)
Cholangiocarcinoma	13 (12%)
Hepatocellular carcinoma	11 (10%)
Uveal melanoma	9 (8%)
Other[a]	15 (14%)
Multifocal disease	98 (88%)
Bilobar disease	89 (80%)
Hypervascular tumors	24 (22%)[b]
Presence of portal or hepatic vein obstruction or thrombus	35 (32%)
Extrahepatic metastasis on PET/CT	21 (25%)[c]
^{99m}Tc-MAA SPECT/CTs	138
Lung shunt (planar scintigraphy)	5.5% (0.3 – 39%)
Time since last chemotherapy (months)	2.7 (0.6 - 30.4)[d]
Target volume	
Whole liver	109 (79%)
Right lobe	18 (13%)
Left lobe	8 (6%)
Other (selective)	3 (2%)
Burden of disease in target volume	
<10%	61 (44%)
10-50%	58 (42%)
>50%	19 (14%)
Injected ^{99m}Tc-MAA (MBq)	126 (58 - 216)[e]
Time between injection and SPECT/CT (min)	65 (27 - 146)[f]
Uptake in thyroid	0.30% (0.02 - 2.06%)

[a] Other includes, ampullary, breast, gastric, GIST, lung, nasopharyngeal, oesophegeal, pancreatic, , and urothelial carcinoma as well as adenocarcinoma of unknown primary, [b] 1 patient not available, [c] 28 patients not available, [d] 39 cases not available, [e] 10 cases not available, [f] 10 cases not available

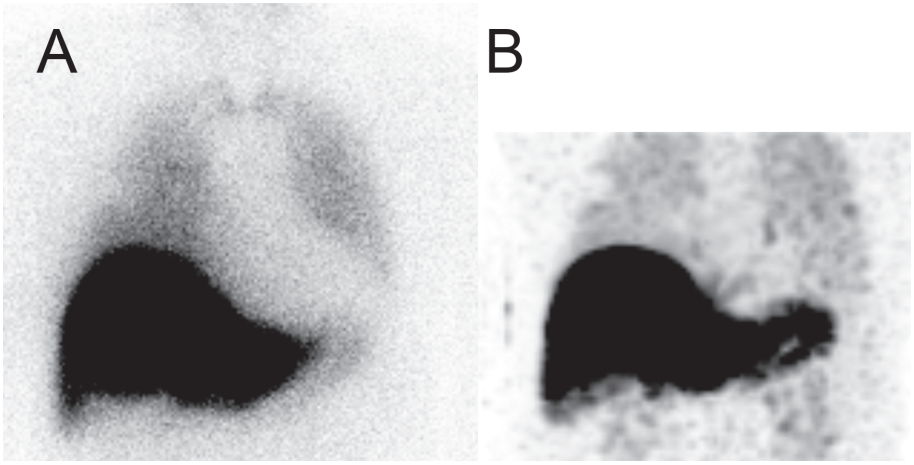

Figure 1 *Typical case of a patient with cholangiocarcinoma (A, planar scintigraphy, front view; B, maximum intensity projection, front view). Planar scintigraphy showed a diffuse uptake of ^{99m}Tc-MAA in the lungs. The estimated lung shunt fraction was 14%. Planar scintigraphy predicted a lung absorbed dose of 7 Gy/GBq ^{90}Y, SPECT/CT estimated 3.9 Gy/GBq ^{90}Y. The treatment dose was reduced to 1.5 GBq because of the lung shunt.*

A typical case is shown in Figure 1. Of all patients treated with ^{90}Y resin microspheres, 11% (10/88) had their treatment activity reduced because of a high lung shunt: 9% (8/88) by 20% and 2% (2/88) by 40%. Of 57 patients, both the amount of injected activity and CT imaging of the lung parenchyma was available. Their median absorbed lung dose was 3.5 Gy (range, 0.2 – 16 Gy) on planar scintigraphy and 1.6 Gy (range, 0.2 – 8.4 Gy) on SPECT/CT. None had developed radiation pneumonitis.

Patient selection

The limit of the lung dose on planar scintigraphy (30 Gy) corresponded to 15 Gy (95% CI 13 – 16 Gy), as calculated on SPECT/CT. When using the different limits for planar scintigraphy (30 Gy) and SPECT/CT (15 Gy), patient selection differed when large activities were administered: 44% of patients with a high lung shunt on SPECT/CT were not identified on planar scintigraphy (Table 2).

Table 2. *Cross tabulation of patient selection*

Typical resin case (2 GBq)			Typical glass case (5 GBq)		
	SPECT/CT > 15 Gy	SPECT/CT < 15 Gy		SPECT/CT > 15 Gy	SPECT/CT < 15 Gy
Planar scintigraphy > 30 Gy	1	1	Planar scintigraphy > 30 Gy	10	0
Planar scintigraphy < 30 Gy	0	136	Planar scintigraphy < 30 Gy	8	120

Values represent number of patients

Comparison of lung shunt

In a direct comparison, planar scintigraphy overestimated the lung dose by a median of 1.5 Gy (range -1.6 – 15 Gy) per GBq of infused ^{90}Y compared to SPECT/CT ($p < 0.01$, Figure 2A). For a lung dose of 30 Gy, the 95% limits of agreement of the difference were -15 - 44 Gy (Figure 2B). The ability of the two measurements to differentiate between patients (the reliability) was moderate, with an $ICC_{consistency}$ (ignoring systematic error) of 0.69 (95%, CI 0.60 – 0.77).

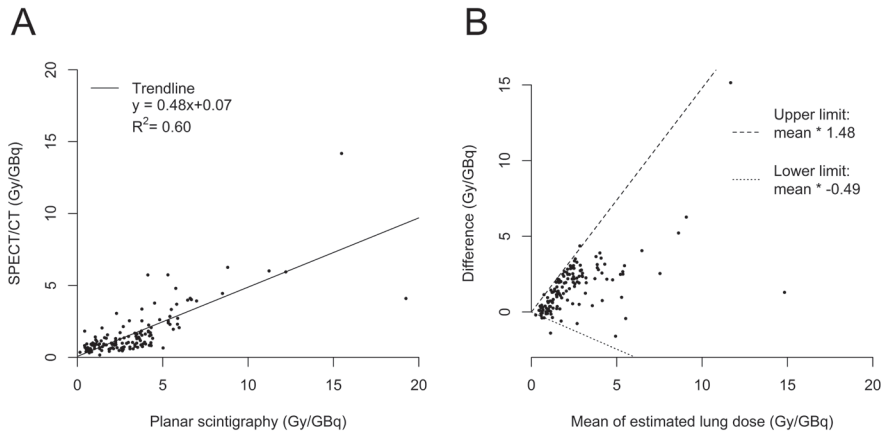

Figure 2 *Scatterplot of the lung dose in Gy per GBq ^{90}Y estimated by planar scintigraphy and SPECT/CT (A). Bland-Altman plot of the lung dose estimated by planar scintigraphy and SPECT/CT in Gy per GBq ^{90}Y (B). Data were plotted on a linear scale, but the limits of agreement were calculated on a log scale, leading to divergent limits. The error increased as the estimated lung dose increased; the limits of agreement were dependent on the mean.*

The importance of imaging a large part of the lungs when using SPECT/CT and assuming a homogeneous ^{99m}Tc-MAA distribution is shown by the case in which planar scintigraphy and SPECT/CT showed the largest difference: 15 Gy per GBq ^{90}Y (Figure 3). This patient with cholangiocarcinoma had COPD, which influenced the lung perfusion. The patient with the next largest difference (6 Gy per GBq) had both a large part of the lungs imaged and a homogeneous distribution (Figure 4).

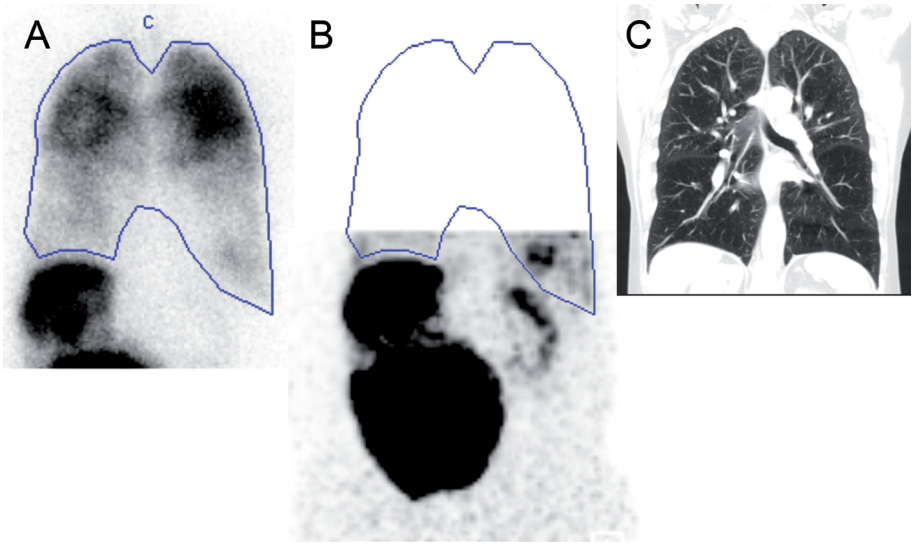

Figure 3 *Unique case of small field of view and perfusion inhomogeneity. Planar scintigraphy showed a lung shunt fraction of 39% with inhomogeneous distribution (A). The patient had COPD, which could explain the differences in perfusion. The blue line shows the lung delineation. Anterior Maximum Intensity Projection from the SPECT had a limited field of view with only 1L of lung tissue (B). The blue line indicates the lung delineation from the planar scintigraphy. The estimated lung dose after 2 GBq of ^{90}Y was 30 Gy higher for planar scintigraphy than for SPECT/CT. Extensive centrilobular emphysema was seen in both the upper and lower lobes (C)*

Repeated procedures

The repeatability of the lung shunt estimation was estimated using the lung shunts of 16 repeated procedures in which ^{99m}Tc-MAA was injected in the same target volume. The accuracy of SPECT/CT was higher than that of planar scintigraphy (Figure 5), indicated by smaller differences and limits of agreement per Bland-Altman analysis. The $ICC_{agreement}$ was moderate for both modalities and did not significantly differ: 0.64 (95%, CI 0.22 – 0.86) for planar scintigraphy and 0.69 (95% CI, 0.32 – 0.88) for SPECT/CT.

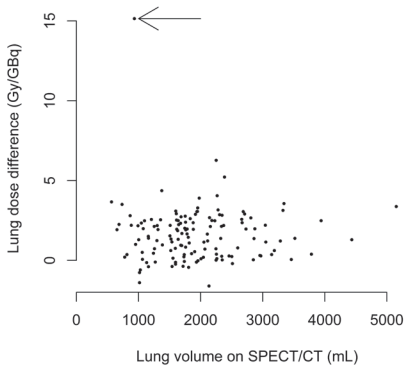

Figure 4 *Lung volumes as used for calculating the lung dose on SPECT/CT plotted versus the difference in lung dose estimation (planar scintigraphy - SPECT/CT). Only one outlier is present (arrow, see also Figure 3).*

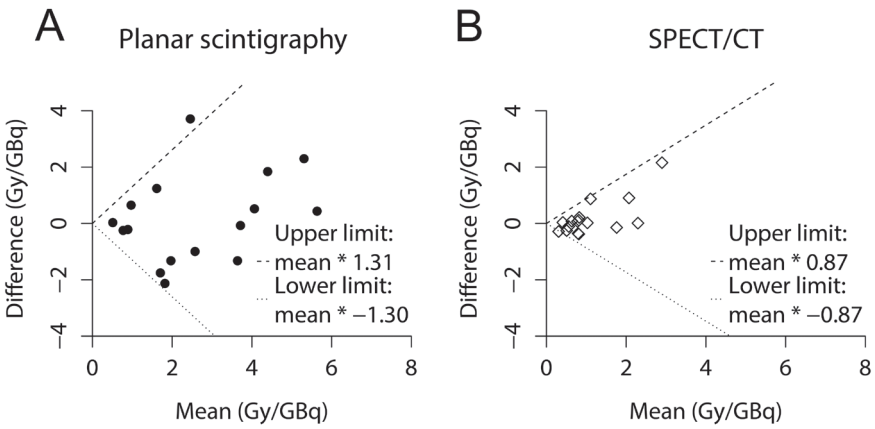

Figure 5 *Bland-Altman plot of estimated lung shunts in the same patients when the ^{99m}Tc-MAA was repeated based on planar scintigraphy (A) and SPECT/CT (B) per GBq ^{90}Y. Data were plotted on a linear scale, but the limits of agreement were calculated on a log scale, leading to divergent limits of agreement*

Univariable analyses

More univariable associations were identified using the lung shunt based on planar scintigraphy than based on SPECT/CT (see Table 3). Four risk factors were significantly associated with a high lung shunt on both modalities: hypervascular tumors, presence of portal or hepatic vein obstruction or thrombus, time between injection and SPECT/CT, and free pertechnetate uptake in the thyroid. Some risk factors showed collinearity. The burden of disease in the target volume was associated with an increase in angioinvasion: 10% of patients with <10% tumor burden had

angioinvasion; 43% of 10-50%; 53% of >50%. The time between injection and SPECT/CT was significantly correlated with the uptake of free pertechnetate in the thyroid ($\rho = 0.2$, $p = 0.02$). No relationship was found between time between injection and SPECT/CT and either the tumor burden or angioinvasion. Tumor type was not significantly associated with a high lung shunt on either modality, even though angioinvasion was, and most patients with cholangiocarcinoma had angioinvasion (56% vs. 25% of colorectal patients). Multivariable analysis was precluded by the risk of model overfitting.

Table 3. *Univariable analysis of determinants with planar and SPECT/CT lung shunt dose*

Characteristic	Planar	p-value	SPECT	p-value
	Lung shunt fraction (%)		Lung dose (Gy / GBq ^{90}Y)	
Primary tumor type[a]		0.43		0.46
Colorectal	5.5 (2.9 – 7.9)		1.0 (0.7– 1.7)	
Cholangiocarcinoma	5.1 (2.8 – 11.8)		1.7 (0.8 – 3.1)	
Hepatocellular carcinoma	6.6 (4.8 – 10.2)		1.0 (0.6 – 3.0)	
Uveal melanoma	5.4 (4.1 – 8.6)		0.9 (0.7 – 1.2)	
Other	4.5 (2.0 – 7.7)		0.9 (0.7 – 1.4)	
Hypervascular tumors [b]		0.03*		0.70
Yes	7.4 (4.3 – 11.0)		0.9 (0.6 – 3.2)	
No	5.3 (2.7 – 7.7)		1.0 (0.7 – 1.7)	
Burden of disease in target volume[a]		0.03*		0.02*
0-10%	5.0 (2.1 – 7.9)		0.9 (0.7 – 1.4)	
10-50%	5.3 (3.4 – 8.3)		1.2 (0.9 – 2.2)	
>50%	7.0 (5.4 – 12.7)		1.5 (0.7 – 4.1)	
Presence of portal or hepatic vein obstruction or thrombus [b]		0.04*		<0.01*
Yes	7.0 (4.4 – 11.1)		1.5 (0.9 – 3.3)	
No	5.0 (2.8 – 7.9)		0.9 (0.7 – 1.5)	
Extrahepatic metastasis on PET/CT (mCRC) [b]		0.02*		0.30
Yes	7.5 (6.0 – 8.3)		1.2 (0.8 – 2.1)	
No	4.4 (2.3 – 7.9)		1.0 (0.7 – 1.6)	
Characteristic	**Correlation coefficient**	**p-value**	**Correlation coefficient**	**p-value**
Time since last chemotherapy	-0.13 (-0.35 – 0.09)	0.24	-0.07 (-0.30 – 0.15)	0.52
Time between preparation and injection [c]	-0.14 (-0.30 – 0.03)	0.10	-0.09 (-0.26 – 0.08)	0.29
Time between injection and SPECT/CT [c]	0.33 (0.17 – 0.48)	<0.01*	0.19 (0.02 – 0.35)	0.03*
Thyroid uptake [c]	0.42 (0.27 – 0.55)	<0.01*	0.38 (0.23 – 0.51)	<0.01*

*[a] Kruskal-Wallis rank sum test, [b] Wilcoxon rank sum, [c] Pearson's product moment correlation. Data are median (Q_1 – Q_3) or ρ (95% CI), * significant at alpha of 0.05*

Discussion

By comparing planar scintigraphy and SPECT/CT, our data suggest that the limit for the lung shunt on SPECT/CT should be 15 Gy (assuming that a 30 Gy limit based on planar scintigraphy is correct). Use of this boundary led to substantial differences in patient selection between planar scintigraphy and SPECT/CT. Of patients with a high lung shunt on SPECT/CT, 44% (8/18) were not identified by planar scintigraphy. These differences were also manifest in the agreement between the two modalities, which was low (see Figure 1), while the reliability was moderate ($ICC_{consistency}$ = 0.69).

Several risk factors were identified on both planar scintigraphy and SPECT/CT: tumor burden, presence of portal or hepatic vein obstruction or thrombus, time between injection and SPECT/CT, and thyroid uptake. These are in agreement with earlier reports (Table 4).[7,16,26–28] Some risk factors were only identified on planar scintigraphy (arterial enhancement and extrahepatic metastasis) but were also found in prior studies.[16,29] On the other hand, in accordance with Gaba et al., this study could not associate SPECT-based lung shunt with tumor type.[7] However, not all results from earlier reports could be validated. An association between a high lung shunt and time since last chemotherapy could not be demonstrated, while Deipolyi et al. did find a positive association.[29] They studied 19 patients with colorectal cancer who received chemotherapy, while this study included 63 colorectal patients of whom retrospective clinical data was only available for 41 patients. This could have influenced our results. A multivariable analysis of risk factors was not considered appropriate because of the low incidence of a high lung shunt (13%, 18/138, Table 2) and because a correction was needed for clustering of data (111 patients supplied 138 cases). In addition, some effect modification was to be expected, for example colorectal tumor types are expected to have a higher number of extrahepatic metastases than hepatocellular carcinomas. The model would have been overfitted and would have resulted in unreliable associations.

Table 4. *Review of literature and all reported associations*

Author	Year of publication	Planar scintigraphy or SPECT	*n*	Characteristic	Lung shunt	Other finding
Leung et al.[3]	1994	Planar	125	Vascularity on angiography	↑	
				Tumor size	–	
Lambert et al. [27]	2010	Planar	90	Kidney or thyroid uptake of ^{99m}Tc	↑	
				Hepatocellular tumor type	–	
Theysohn et al. [30]	2012	Planar[a]	7	Sorafenib	↓	
De Gersem et al. [26]	2013	Planar	4	Time between injection and scan	↑	
Deipolyi et al. [29]	2014	Planar[b]	62	Lung metastases	↑	Higher lung shunt fraction associated with decreased survival
				Mutations present (SNaPshot analysis)	↑	
				Index tumor size	–	
				Overall liver tumor volume	–	
				Received chemotherapy	↓	
Gaba et al. [7]	2014	Planar	141	Tumor type	–	More prevalance of >20% lung shunt for patients with hepatocellular carcinoma In multinomial logistic regression, infiltrative tumor structure, main portal vein invasion, arterioportal shunting increased the lung shunt for HCC
			70	For HCC		
				Infiltrative tumor structure	↑	
				Tumor burden (>50%)	↑	
				Arterioportal shunting on angiography	↑	
				Disease etiology	–	
				Child-Pugh classification	–	
				Index tumor size	–	
				Tumor focality	–	
				Unilobar or bilobar disease	–	
				Portal vein invasion	–	
				Prior therapy	–	
			71	Other tumors		
				Index tumor size	↑	
				Tumor burden (>50%)	↑	
				Tumor type	–	
				Infiltrative tumor structure	–	
				Tumor focality	–	
				Unilobar or bilobar disease	–	
				Portal vein invasion	–	

Table 4. *Continued*

Author	Year of publication	Planar scintigraphy or SPECT	*n*	Characteristic	Lung shunt	Other finding
Olorunsola et al. [28]	2015	Planar	152	Tumor type HCC	↑	Only hepatic venous shunting and presence of either hepatic venous tumor thrombus or occlusion remained significant in multivariable analysis
				Tumor size	↑	
				Hepatic venous shunting	↑	
				Hepatic vein tumor thrombus or compression	↑	
				Tumor focality	–	
				Unilobar or bilobar disease	–	
				Tumor burden	–	
				Infiltrative tumor structure	–	
				Portal venous shunting	–	
				Portal vein tumor thrombus or compression	–	
Powerski et al. [16]	2014	SPECT/CT	233	Arterial enhancement on CT	↑	
				Portal vein occlusion (compression or thrombus)	↑	
				Tumor-to-liver volume	↑[c]	
				Breast cancer tumor type	↓	
this study	2015	SPECT/CT[d]	105	Presence of portal or hepatic vein obstruction or thrombus	↑	
				Burden of disease in target volume	↑	
				Time between injection and scan	↑	
		Planar		Arterial enhancement on CT	↑	
				Extrahepatic metastasis (mCRC only)	↑	
				Thyroid uptake of ^{99m}Tc	↑	

[a] *Not specified, most likely planar because of use geometric mean.* [b] *Not specified, most likely planar because of use fraction.* [c] *Poor association*
[d] *All three factors were also associated on planar scintigraphy*
↑ *Association with increased lung shunt,* – *No association,* ↓ *Association with decreased lung shunt*

The absence of patients with radiation pneumonitis prevents us to conclude whether planar scintigraphy or SPECT/CT is superior. However, we hypothesize SPECT/CT to be more accurate, as it corrects for scatter and attenuation. Also, in 16 patients in whom a procedure was repeated, differences between the two SPECT/CTs were closer to zero than on planar scintigraphy. Our expectation was that the use of SPECT/CT would lead to stronger associations between risk factors and a high lung shunt. However, the opposite was true, as more risk factors were significantly

associated with planar scintigraphy. The SPECT/CT could be less accurate because of its limited field of view. We corrected for this by assuming a fixed lung mass of 1 kg. This could have caused the correlations to disappear.

In addition, two earlier reports concluded that SPECT/CT is more accurate. Yu et al. compared the two modalities in images of 71 patients and found it was necessary to exclude the portions of lungs around the diaphragm to prevent scatter from the liver (which was also done in this study).[14] Even so, planar scintigraphy nearly always resulted in a higher lung dose, with a mean ratio of planar scintigraphy and SPECT/CT of 3.80 (range, 0.86-9.86). Kao et al. described a method to measure the density of the lung parenchyma to better estimate the lung dose.[15] In 30 patients, they found the lung shunt fraction to be overestimated on planar scintigraphy with a mean overestimation of 1.4%. The lung shunt was underestimated on planar scintigraphy compared with SPECT/CT (6.07 Gy vs. 6.48 Gy). However, in the calculations for planar scintigraphy a high lung mass of 1 kg was assumed while the calculation for SPECT/CT was individualized with a low median mass of 736g (range 624-1,024g). This decreased the lung doses for planar scintigraphy.

Even if SPECT/CT is more accurate for quantification, ^{99m}Tc-MAA might not be the right particle to accurately simulate ^{90}Y microspheres. Only one report suggested that it is suitable: Jha et al. reported a Pearson's correlation coefficient of 0.96 in a small cohort of 17 patients in which they compared planar scintigraphy after ^{99m}Tc-MAA with ^{90}Y Bremsstrahlung SPECT.[31] Our findings, however, suggest that degradation of ^{99m}Tc-MAA occurs after injection, which is not expected from ^{90}Y microspheres. Both the lung shunt and the thyroid uptake of free pertechnetate increased with a longer time after injection. A higher thyroid uptake was also correlated with a higher lung shunt. If ^{99m}Tc-MAA would degrade into only free pertechnetate, the thyroid uptake would increase and not the lung shunt. The observation that it does, suggests that ^{99m}Tc-MAA also degrades into small particles that shunt to the lungs. This could also explain the results of Elschot et al., who showed that the use of ^{99m}Tc-MAA SPECT/CT resulted in a greater lung dose (2.5 Gy, range: 1.2-12.3 Gy) than the use of holmium-166 (^{166}Ho) microspheres SPECT/CT (0.02 Gy, range: 0-0.4 Gy).[17] If so, ^{99m}Tc-MAA is unsuitable to estimate the lung shunt after radioembolization.

Based on the results from our study and other insights from literature (Table 4) the following recommendations can be made. First, it is best to minimize the time between injection of ^{99m}Tc-MAA and nuclear imaging. Second, the SPECT field-of-view should include as much of the lungs as possible in particular for patients with lung diseases and/or suspected for a substantial lung shunt. Third, patients with a hypervascular tumor with compression or invasion of the portal or hepatic vein and a high tumor burden are at risk for a high lung shunt.

Future improvements of ^{90}Y quantification using PET/CT might enable direct lung shunt measurements. Because this is already possible with ^{166}Ho microspheres, further research with these microspheres might lead to new findings on the relationship between the lung dose and radiation pneumonitis. Also, the predictive performance of ^{99m}Tc-MAA with respect to the lung shunt after treatment can be investigated.

Conclusion

Planar scintigraphy and SPECT/CT showed marked differences in lung absorbed dose calculations and patient selection. Planar scintigraphy overestimated the lung shunt compared with SPECT/CT. Therefore, we propose a much lower limit for SPECT/CT than conventional for planar scintigraphy, namely 15 Gy instead of 30 Gy. On the other hand it is highly questionable whether dose limits based on ^{99m}Tc-MAA are predictive for radiation pneumonitis. Dose limits should therefore be used with caution. They should be redefined using SPECT/CT and correlated with accurate post-treatment imaging.

References

1. Van Cutsem E, Cervantes A, Nordlinger B, Arnold D, ESMO Guidelines Working Group. Metastatic colorectal cancer: ESMO Clinical Practice Guidelines for diagnosis, treatment and follow-up. Ann Oncol. 2014;25 Suppl 3:iii1–9.
2. Schwarz RE, Abou-Alfa GK, Geschwind JF, Krishnan S, Salem R, Venook AP. Nonoperative therapies for combined modality treatment of hepatocellular cancer: expert consensus statement. HPB. 2010;12(5):313–20.
3. Leung WT, Lau WY, Ho SK, Chan M, Leung NW, Lin J, et al. Measuring lung shunting in hepatocellular carcinoma with intrahepatic-arterial technetium-99m macroaggregated albumin. J Nucl Med. 1994;35(1):70–3.
4. Leung TW, Lau WY, Ho SK, Ward SC, Chow JH, Chan MS, et al. Radiation pneumonitis after selective internal radiation treatment with intraarterial 90yttrium-microspheres for inoperable hepatic tumors. Int J Radiat Oncol Biol Phys. 1995;33(4):919–24.
5. Sirtex Medical Limited. SIR-Spheres package insert (CR1507). North Sydney, NSW, Australia, 2012 [Internet]. [cited 2015 Apr 4]. Available from: http://www.sirtex.com/us/clinicians/package-insert/
6. TheraSphere yttrium-90 glass microspheres [package insert]. Nordion Web site [Internet]. [cited 2015 Apr 4]. Available from: http://www.nordion.com/therasphere/physicians-package-insert/ package-insert-us.pdf
7. Gaba RC, Zivin SP, Dikopf MS, Parvinian A, Casadaban LC, Lu Y, et al. Characteristics of primary and secondary hepatic malignancies associated with hepatopulmonary shunting. Radiology. 2014;271(2):602–12.
8. Lin M. Radiation pneumonitis caused by yttrium-90 microspheres: radiologic findings. AJR Am J Roentgenol. 1994;162(6):1300–2.
9. Ho S, Lau WY, Leung TW, Chan M, Ngar YK, Johnson PJ, et al. Partition model for estimating radiation doses from yttrium-90 microspheres in treating hepatic tumours. Eur J Nucl Med. 1996;23(8):947–52.
10. Salem R, Parikh P, Atassi B, Lewandowski RJ, Ryu RK, Sato KT, et al. Incidence of radiation pneumonitis after hepatic intra-arterial radiotherapy with yttrium-90 microspheres assuming uniform lung distribution. Am J Clin Oncol. 2008;31(5):431–8.
11. Wright CL, Werner JD, Tran JM, Gates VL, Rikabi AA, Shah MH, et al. Radiation pneumonitis following yttrium-90 radioembolization: case report and literature review. J Vasc Interv Radiol. 2012;23(5):669–74.
12. Dobrocky T, Fuerstner M, Klaeser B, Lopez-Benitez R, Wälti YB, Kara L. Regional Radiation Pneumonitis After SIRT of a Subcapsular Liver Metastasis: What is the Effect of Direct Beta Irradiation? Cardiovasc Intervent Radiol. 2015;38(4):1025–30.
13. Ward TJ, Tamrazi A, Lam MGEH, Louie JD, Kao PN, Shah RP, et al. Management of High Hepatopulmonary Shunting in Patients Undergoing Hepatic Radioembolization. J Vasc Interv Radiol. 2015;26(12):1751-60
14. Yu N, Srinivas SM, Difilippo FP, Shrikanthan S, Levitin A, McLennan G, et al. Lung dose calculation with SPECT/CT for (90)Yittrium radioembolization of liver cancer. Int J Radiat Oncol Biol Phys. 2013;85(3):834–9.
15. Kao YH, Magsombol BM, Toh Y, Tay KH, Chow PK, Goh AS, et al. Personalized predictive lung dosimetry by technetium-99m macroaggregated albumin SPECT/CT for yttrium-90 radioembolization. EJNMMI Res. 2014;4:33.
16. Powerski MJ, Erxleben C, Scheurig-Münkler C, Geisel D, Heimann U, Hamm B, et al. Hepatopulmonary shunting in patients with primary and secondary liver tumors scheduled for radioembolization. Eur J Radiol. 2015;84(2):201–7.
17. Elschot M, Nijsen JFW, Lam MGEH, Smits MLJ, Prince JF, Viergever M a, et al. (99m)Tc-MAA overestimates the absorbed dose to the lungs in radioembolization: a quantitative evaluation in patients treated with (166)Ho-microspheres. Eur J Nucl Med Mol Imaging. 2014;41(10):1965–75.
18. Xiao J, Wit TC de, Staelens SG, Beekman FJ. Evaluation of 3D Monte Carlo–Based Scatter Correction for 99mTc Cardiac Perfusion SPECT. J Nucl Med. 2006;47(10):1662–9.

19. Seret A, Nguyen D, Bernard C. Quantitative capabilities of four state-of-the-art SPECT-CT cameras. EJNMMI Res. 2012;2:45.
20. Gulec S a, Mesoloras G, Stabin M. Dosimetric techniques in 90Y-microsphere therapy of liver cancer: The MIRD equations for dose calculations. J Nucl Med. 2006;47(7):1209–11.
21. Kennedy A, Coldwell D, Sangro B, Wasan H, Salem R. Radioembolization for the treatment of liver tumors general principles. Am J Clin Oncol. 2012;35(1):91–9.
22. de Vet HCW, Terwee CB, Knol DL, Bouter LM. When to use agreement versus reliability measures. J Clin Epidemiol. 2006;59(10):1033–9.
23. Bland JM, Altman DG. Statistical methods for assessing agreement between two methods of clinical measurement. Lancet. 1986;1(8476):307–10.
24. Euser AM, Dekker FW, le Cessie S. A practical approach to Bland-Altman plots and variation coefficients for log transformed variables. J Clin Epidemiol. 2008;61(10):978–82.
25. R: A language and environment for statistical computing [Internet]. Vienna, Austria: R Foundation for Statistical Computing; Available from: http://www.r-project.org
26. De Gersem R, Maleux G, Vanbilloen H, Baete K, Verslype C, Haustermans K, et al. Influence of time delay on the estimated lung shunt fraction on 99mTc-labeled MAA scintigraphy for 90Y microsphere treatment planning. Clin Nucl Med. 2013;38(12):940–2.
27. Lambert B, Mertens J, Sturm EJ, Stienaers S, Defreyne L, Asseler Y D'. 99mTc-labelled macroaggregated albumin (MAA) scintigraphy for planning treatment with 90Y microspheres. Eur J Nucl Med Mol Imaging. 2010;37(12):2328–33.
28. Olorunsola OG, Kohi MP, Behr SC, Kolli PK, Taylor AG, Tong RT, et al. Imaging Predictors of Elevated Lung Shunt Fraction in Patients Being Considered for Yttrium-90 Radioembolization. J Vasc Interv Radiol. 2015;26(10):1472-8.
29. Deipolyi AR, Iafrate AJ, Zhu AX, Ergul EA, Ganguli S, Oklu R. High lung shunt fraction in colorectal liver tumors is associated with distant metastasis and decreased survival. J Vasc Interv Radiol. 2014;25(10):1604–8.
30. Theysohn JM, Schlaak JF, Müller S, Ertle J, Schlosser TW, Bockisch A, et al. Selective internal radiation therapy of hepatocellular carcinoma: potential hepatopulmonary shunt reduction after sorafenib administration. J Vasc Interv Radiol. 2012;23(7):949–52.
31. Jha AKA, Zade AA, Rangarajan V, Purandare N, Shah SA, Agrawal A, et al. Comparative analysis of hepatopulmonary shunt obtained from pretherapy 99mTc MAA scintigraphy and post-therapy 90Y Bremsstrahlung imaging in 90Y microsphere therapy. Nucl Med Commun. 2012;33(5):486–90.

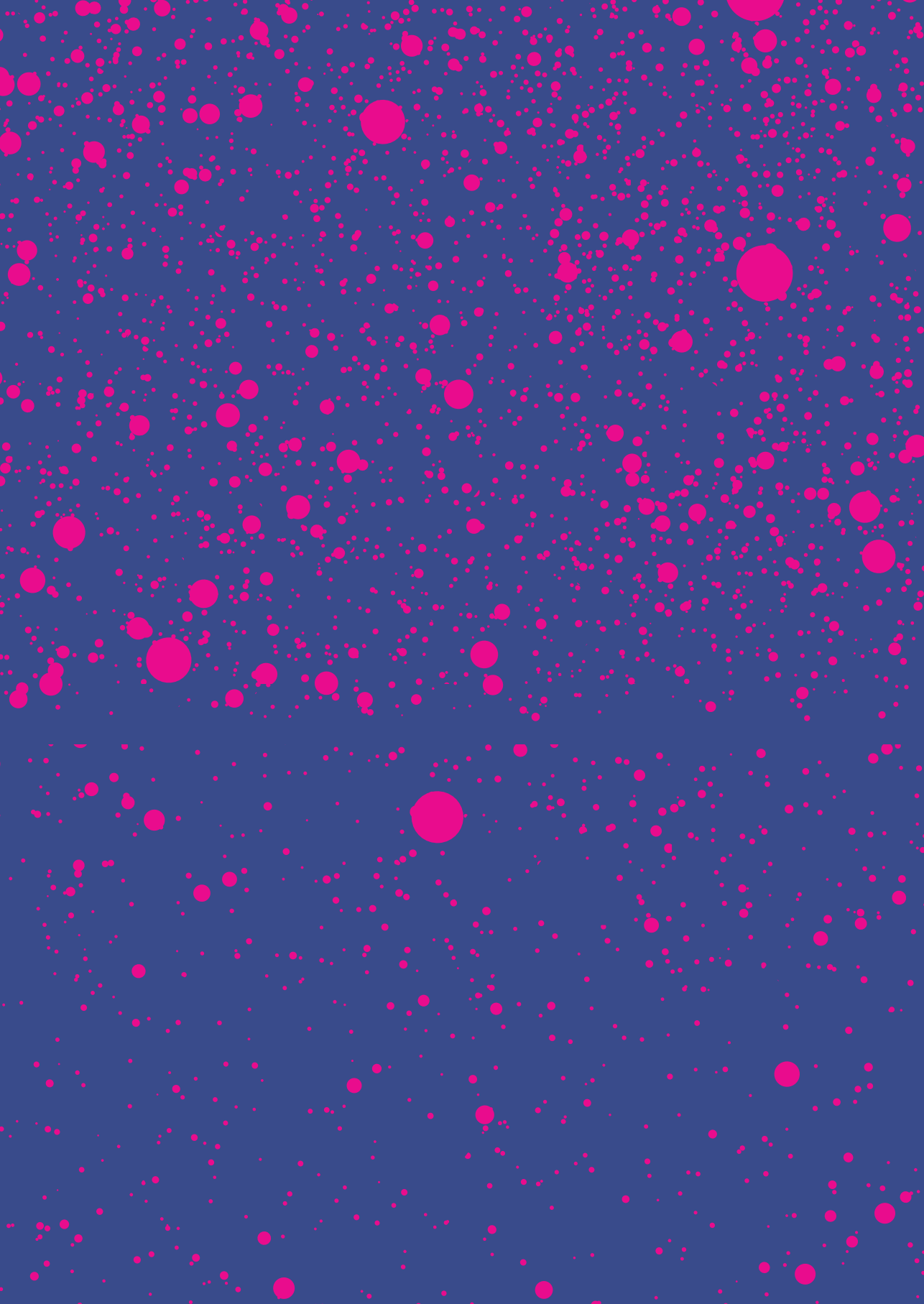

CHAPTER 4

Radiation-induced cholecystitis after hepatic radioembolization: do we need to take precautionary measures?

J.F. Prince
A.F. van den Hoven
M.A.A.J. van den Bosch
M. Elschot
H.W.A.M. de Jong
M.G.E.H. Lam

Journal of Vascular and Interventional Radiology 2014

Abstract

Controversy exists over the need to take precautionary measures during hepatic radioembolization to minimize the risk of radiation-induced cholecystitis. Strategies for a variety of clinical scenarios are discussed on the basis of a literature review. Precautionary measures are unnecessary in the majority of patients and should be taken only when single photon-emission computed tomography (CT; SPECT)/CT shows a significant concentration of technetium-99m macroaggregated albumin in the gallbladder wall. In this case report with quantitative SPECT analysis, it is illustrated how an adjustment of the catheter position can effectively reduce the absorbed dose of radiation delivered to the gallbladder wall by more than 90%.

Introduction

Intra-arterial hepatic radioembolization (RE) has been established as a safe and effective treatment modality for patients with unresectable liver tumors. Although treatment complications are rare, serious clinical toxicity can follow unintentional extrahepatic deposition of radioactive microspheres.[1] Various safety precautions can be taken to minimize this risk, including permanent or temporary occlusion of nontarget vessels, induction of vasospasm with the use of a microwire, choosing a distal catheter position, and us of an anti-reflux infusion system.[1–3] Unfortunately, comparative studies on the efficacy of these precautionary measures are lacking. Therefore, controversy exists as to which of these precautions are appropriate in a variety of clinical scenarios; for example, the need for coil embolization is debated.[4]

Similarly, the need for gallbladder protection remains a matter of debate. It has been reported that deposition of radioactive microspheres in the gallbladder wall may cause radiation-induced cholecystitis, occasionally necessitating surgical interference.[5–11] Therefore, some authors advocate routine prophylactic embolization of the cystic artery before RE.[10,12] A recent survey among European interventional centers revealed that 41% of these centers follow this strategy and always embolize the cystic artery.[13] However, others argue that prophylactic embolization may not be desirable in all patients for the following reasons: (i) in as many as one-third of patients the catheter can be positioned distal to the cystic artery without compromising the intrahepatic microsphere distribution, (ii) only a small fraction of patients in whom a proximal catheter position is chosen will exhibit an increased uptake of technetium-99m (^{99m}Tc) macroaggregated albumin (MAA) and radioactive microspheres in the gallbladder wall, (iii) the occurrence of symptomatic radiation-induced cholecystitis is rare, and (iv) embolization of the cystic artery may incidentally cause ischemic cholecystitis by itself.[14] Remarkably, clinical guidelines for RE do not provide further guidance in this matter.[15–19]

A case is presented here in which a highly perfused gallbladder wall, exhibiting extraordinarily high ^{99m}Tc-MAA activity on single photon-emission computed tomography (CT; SPECT)/CT, is protected by slightly adjusting the catheter position. In addition, strategies that seem most appropriate for a variety of clinical scenarios are discussed, based on the best available evidence.

Case report

A 64-year-old man diagnosed with unresectable colorectal cancer liver metastases, refractory to standard systemic chemotherapy, was referred for RE. Routine pretreatment whole-body (^{18}F) fluorodeoxyglucose positron emission tomography/CT and triphasic liver CT revealed multiple liver metastases, no extrahepatic disease and a variant configuration of the hepatic arterial vasculature: a replaced left hepatic artery (LHA) originating from the left gastric artery vascularizing segments 2/3, and a segment 4 artery (ie, A4 segment) originating from the right hepatic artery (RHA). The patient was considered eligible for RE by multidisciplinary tumor board review. He provided written informed consent to participate in an ongoing clinical phase II trial that is investigating the efficacy of RE performed with holmium-166 (^{166}Ho) microspheres (Radioactive Holmium Microspheres for the Treatment of Unresectable Liver Metastases; clinicaltrials.gov ID, NCT01612325).

In short, ^{166}Ho-poly-(L-lactic acid) microspheres have been developed at our institution to allow for visualization of the in vivo microsphere biodistribution after RE.[20] Quantification of ^{166}Ho-microspheres is feasible on magnetic resonance (MR) imaging and SPECT/CT, by using the paramagnetic properties of holmium or the emission of γ-photon radiation respectively.[21] Patients participating in the aforementioned ongoing phase II trial first receive a workup angiography, during which ^{99m}Tc-MAA is administered. On the day of treatment, a scout dose (60 mg, 250 MBq) and a therapeutic dose (540 mg, varying activities) of ^{166}Ho microspheres are administered sequentially to evaluate the accuracy of ^{166}Ho scout dose imaging. MR imaging and SPECT/CT are acquired after the scout dose and therapeutic dose.

The gastroduodenal artery and right gastric artery were prophylactically coil embolized to minimize the risk of nontarget distribution. Subsequently, the replaced LHA and the RHA, proximal to the origin of the A4 segment (Figure 1A-D), were chosen as planned injection positions. Next, ^{99m}Tc-MAA (52 MBq in the replaced LHA and 95 MBq in the RHA) was administered. SPECT/CT did not reveal significant ^{99m}Tc-MAA activity in the gallbladder wall, but it did reveal a small extrahepatic focus in the duodenum (Figure 2A).

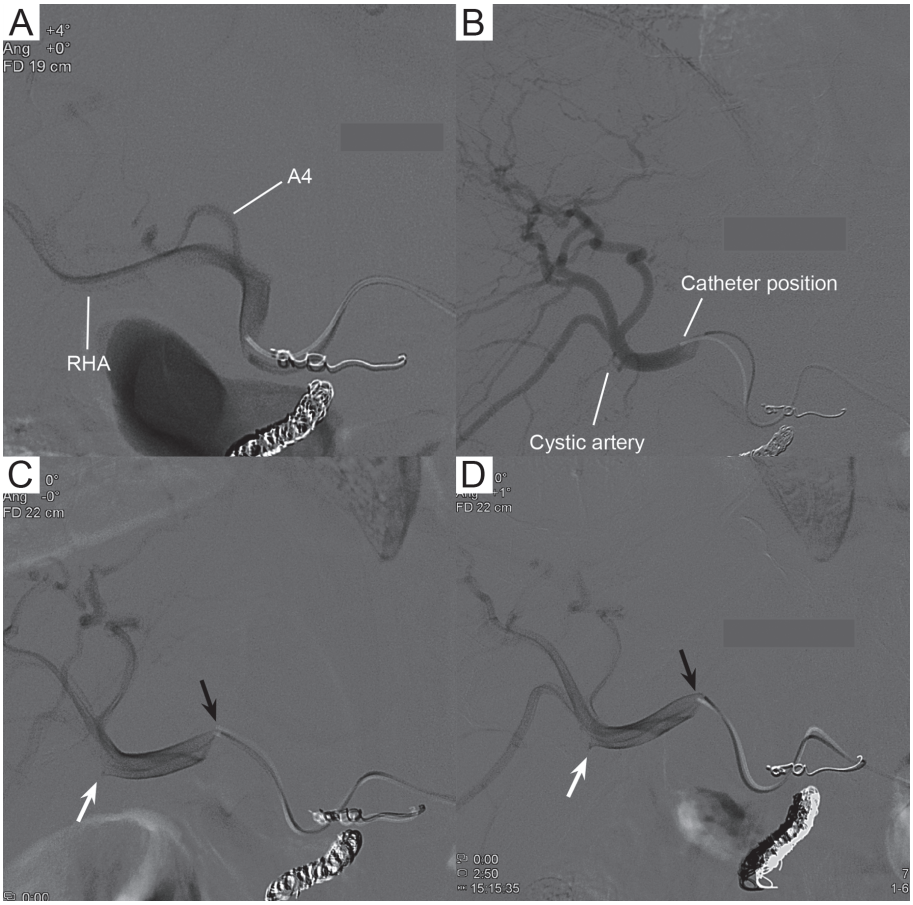

Figure 1 *Injection positions in the RHA during the pretreatment and treatment procedures. The injections in the replaced LHA (originating from the left gastric artery) are not shown. Catheter position during the first work-up angiography (A). The ^{99m}Tc-MAA was administered in the RHA, proximal to the A4 segment. Catheter position during repeat workup angiography (B). The ^{99m}Tc-MAA was administered in the RHA selectively. Note that the cystic artery fills with contrast medium. Adjusted catheter position (black arrow) during the administration of the scout dose of ^{166}Ho-microspheres (C). Identical catheter position (black arrow) during the administration of the therapeutic dose of ^{166}Ho microspheres (D). Note that the cystic artery is not visible (white arrow). Corresponding SPECT/CT images of ^{99m}Tc-MAA and ^{166}Ho microsphere distribution are shown in Figure 2.*

Because of this extrahepatic uptake, the workup angiography was repeated and three selective catheter positions were chosen: the replaced LHA, the A4 segment, and the RHA proximal to the origin of the cystic artery (Figure 1B). In these positions ^{99m}Tc-MAA (34 MBq in the replaced LHA, 23 MBq in the A4 segment and 93 MBq in the RHA) was administered. This time, SPECT/CT did not reveal any extrahepatic deposition. However, the amount of ^{99m}Tc-MAA activity in the gallbladder wall was now extraordinarily high.

With the use of a quantitative SPECT/CT reconstruction[22], the relative amount of activity in the gallbladder was determined, and the gallbladder absorbed dose that would result from treatment was estimated (Table 1). To this purpose, the whole gallbladder and liver were manually delineated by consensus of two authors (J.F.P. and A.F.v.d.H.) by using the low-dose CT of the SPECT/CT examination. A 2-cm margin was added to the segmentation of the liver to account for suboptimal coregistration of SPECT and CT, patient breathing and partial volume effects. The ratio of the ^{99m}Tc-MAA activity in the gallbladder volume of interest (VOI) to the extended liver VOI was multiplied by the administered therapeutic activity (6,866 MBq ^{166}Ho) to provide an estimate of the treatment activity that would have been distributed to the gallbladder. Calculations were performed under the assumptions of complete local energy deposition (15.87 J/GBq of ^{166}Ho-microspheres) and a gallbladder density of 1 kg/L for the volume determined by the gallbladder VOI.

Table 1. *Quantitative SPECT/CT analysis*

Procedure	Infused activity (MBq)	Activity ratio Gallbladder/Liver (%)	(Predicted) Treatment activity Gallbladder (MBq)	(Predicted) Absorbed dose Gallbladder (Gy)
^{99m}Tc-MAA	132	3.3	225	187
^{166}Ho Scout	278	0.7	46	14
^{166}Ho Therapy	6,866	0.5	36	11

The concentration of radioactivity in the gallbladder was six times as high as the mean uptake in the liver, and would have resulted in an estimated treatment absorbed dose of 187 Gy (Table 1, Figure 2B). After considering various prophylactic options, including coil embolization of the cystic artery, it was decided to attempt to avoid targeting of the gallbladder by placing the catheter more in a proximal position in the RHA during the ^{166}Ho-scout procedure. Digital subtraction angiographic images obtained from this position showed a lack of contrast medium filling in the cystic artery (Figure 1C). Subsequently, a scout dose of ^{166}Ho microspheres was administered in three branches (85 MBq in the replaced LHA, 40 MBq in the A4 segment and 175 MBq in the RHA). SPECT/CT showed a lack of activity in the gallbladder, and an adequate intrahepatic biodistribution of ^{166}Ho-microspheres (Figure 2C). Retrospective quantitative analysis with the same VOI approach described earlier estimated an absorbed dose to the gallbladder of 14 Gy (Table 1).

The required ^{166}Ho microsphere treatment activity, calculated for a desired whole liver absorbed dose of 60 Gy, was 8,509 MBq. Stasis of blood flow prohibited a complete administration, resulting in net infused activity of 1,265 MBq in the replaced LHA, 1,262 MBq in the A4 segment and 4,212 MBq in the RHA. Posttreatment SPECT/CT showed a lack of activity in the gallbladder wall, and an adequate intrahepatic ^{166}Ho microsphere biodistribution, comparable to the scout dose distribution (Figure 2D). Quantitative analysis showed that the gallbladder absorbed dose was successfully reduced to 11 Gy, a reduction of more than 90% versus that estimated on the ^{99m}Tc-MAA procedure.

The patient experienced abdominal pain, nausea and vomiting (National Cancer Institute Common Terminology Criteria for Adverse Events [CTCAE] grade 3) during treatment, as part of the post-RE syndrome. Symptoms were treated with analgesic and antiemetic drugs, and resolved 1 day after therapy. Clinical follow-up at 2 weeks and 2 months after treatment showed that the patient was in good clinical condition (World Health Organization performance score of 0) and had no clinical toxicity. Triphasic liver CT at 3 months after treatment showed no abnormalities of the gallbladder.

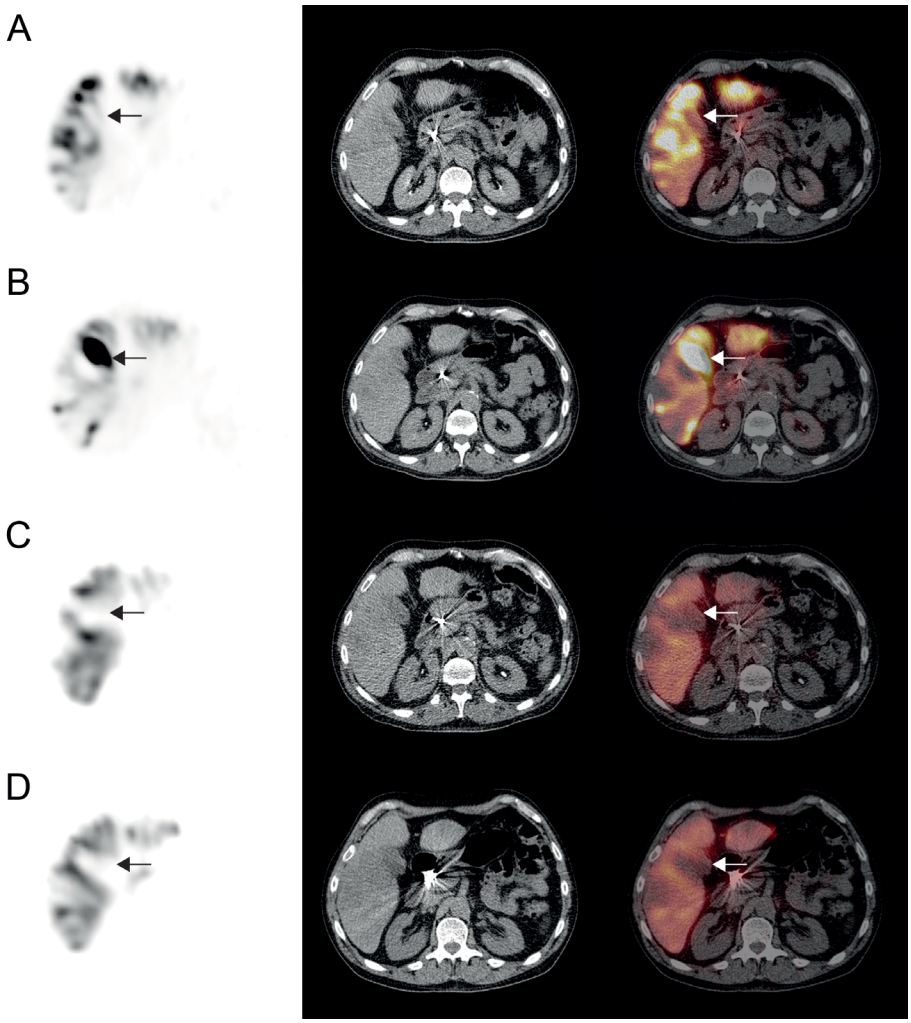

Figure 2 *SPECT/CT images of ^{99m}Tc-MAA and ^{166}Ho microsphere distribution. Note the marked difference in gallbladder wall activity (arrows). The ^{99m}Tc-MAA was administered in the RHA, proximal to the A4 segment (A). During repeat workup angiography, ^{99m}Tc-MAA was administered in the RHA selectively (B). A significant amount of ^{99m}Tc-MAA activity is observed in the gallbladder wall. More proximal catheter position in the RHA during the administration of the scout dose ^{166}Ho microspheres (C). Little to no activity is seen in the gallbladder wall. Identical catheter position during administration of the therapeutic dose of ^{166}Ho microspheres (D).*

Discussion

Uniform criteria for the diagnosis of radiation-induced cholecystitis are currently lacking. Classical symptoms include persistent fever, right upper quadrant pain, nausea and vomiting, occurring shortly after RE treatment.[6] However, these symptoms can also occur as part of the common postembolization syndrome or as a first sign of progressive disease.[23] Unfortunately, physicians cannot rely upon imaging findings, as it has been demonstrated that post-RE gallbladder wall abnormalities on ultrasound, CT and MRI are frequently found in asymptomatic patients, and do not correlate with clinical severity or the need for surgical intervention.[5,24]

In addition, it remains unclear whether the occurrence of symptomatic radiation-induced cholecystitis is correlated with ^{99m}Tc-MAA (reported in 7%-20% of cases[2,14,25]) or yttrium-90 (^{90}Y) activity (reported in 20% of cases[25]) in the gallbladder wall on nuclear imaging (ie, SPECT/CT or positron emission tomography/CT). Therefore, radiation-induced cholecystitis will be diagnosed only when symptoms are refractory to medical therapy and other diagnoses are ruled-out. The reported incidence of radiation cholecystitis varies with grade of severity (grading per CTCAE[26]). The overall incidence, reported by 14 different studies published between 2007 and 2013[2,5,7,8,10,14,24,25,27–32], ranges from 0% to 7%. Symptomatic cholecystitis manageable with medical therapy such as adequate hydration and nutrition, pain medication and antibiotic therapy (CTCAE grade 2) is reported in as many as 4.8% of patients, and severe (CTCAE grade 3) or life-threatening (CTCAE grade 4) cholecystitis requiring surgery is reported in as many as 2.4% of patients. Surgical morbidity rates may be higher for patients with underlying liver disease and recent RE treatment, compared with otherwise healthy patients who undergo cholecystectomy for biliary cholecystitis.[6]

To date, few studies have reported whether any form of gallbladder protection was used during RE. Recently, Theyson et al.[14] compared the incidence of symptomatic cholecystitis after the application of different strategies of gallbladder protection in 295 patients with primary or metastatic liver cancer, undergoing ^{90}Y-RE. The authors reported that they were able to place the catheter distal to the cystic artery in 91 of 295 patients (30.8%) without compromising tumor targeting. In 184 patients (62.4%), a proximal catheter position did not lead to

^{99m}Tc-labeled human serum albumin activity in the gallbladder wall on SPECT/CT, and no further measures were taken to protect the gallbladder. However, in 20 patients (6.8%) a significant accumulation of ^{99m}Tc human serum albumin in the gallbladder wall (higher activity than in the healthy liver tissue) was observed. In these patients, gallbladder protection was performed by temporary occlusion of the cystic artery with Gelfoam (Pharmacia and Upjohn, Kalamazoo, Michigan; n=5), permanent occlusion with coils (n=1), induction of vasospasm in the cystic artery with a microwire (n=4), or alteration the catheter position to change the direction of blood flow (n=10). In only one of these patients, in whom the cystic artery was embolized with Gelfoam, did cholecystitis develop after RE.[14] In another study, McWilliams et al.[10] studied the safety and efficacy of two different methods of cystic artery embolization in 46 patients undergoing ^{90}Y-RE. The cystic artery was temporarily occluded with Gelfoam in 35 patients, and permanently embolized with coils in 10 patients. SPECT/CT did not reveal any ^{99m}Tc-MAA activity in the gallbladder wall, but cholecystitis developed in three patients (6.7%) nevertheless. In each group, CTCAE grade 2 cholecystitis developed in one patient, and grade 3 cholecystitis requiring surgical intervention developed in the coil embolization group.[10] Ahmadzadehfar et al.[2] performed a retrospective cohort study in 76 patients who received preparatory angiography with administration of ^{99m}Tc-MAA. Seven patients showed ^{99m}Tc-MAA activity in the gallbladder wall on SPECT or SPECT/CT, and gallbladder protection was performed before treatment. In six of these patients, the catheter was positioned distal to the origin of the cystic artery, and the cystic artery was coil embolized in one patient. None of these patients exhibited the development of cholecystitis during follow-up.[2] In a cohort study of 15 patients treated with ^{90}Y RE, Garin et al.[25] reported that they did not perform any gallbladder protection and observed ^{99m}Tc-MAA activity in the gallbladder wall on SPECT/CT in three patients (20%), without the occurrence of cholecystitis during follow-up (Table 2).[25]

The use of antibiotic prophylaxis in patients with ^{99m}Tc-MAA activity in the gallbladder wall has previously been described, but its efficacy is yet unknown.[25,27]

In the present report, a case is presented in which repositioning of the catheter reduced the potential gallbladder wall absorbed dose by more than 90%. Partial volume effects and errors in registration, caused by breathing and/or movement, influence these numbers. The absorbed dose is averaged over the gallbladder, a

composite of gallbladder wall and the contained bile, whereas only the dose to the gallbladder wall is relevant for complications. As such, these numbers must be seen as an illustration of the relative reduction of the absorbed dose that is possible by adjusting the injection position.

Repositioning of the catheter can change the position of the tip inside the vessel lumen, not only along the longitudinal axis, but also in the cross-sectional plane of the vessel. This results in different outflow trajectories. Simulations studies show that the particle trajectories are influenced by release position, downstream resistance, type of particle, and timing of release.[33,34] Digital subtraction angiography can be used to confirm lack of flow directed toward the cystic artery. Although catheter manipulation will not have a predetermined effect, marked differences can often be seen between two catheter positions, as shown in the present report. Subsequently, injection of ^{99m}Tc-MAA is used to simulate the distribution of radioactive microspheres.

Based on the summarized evidence, we postulate a scenario-based approach for gallbladder protection during RE (Table 3). The microcatheter can be positioned distal to the cystic artery whenever possible. If, however, a significant concentration of ^{99m}Tc-MAA is observed in the gallbladder wall, the catheter position can be adjusted to alter the direction of blood flow[33], as shown in the present case report and previously described by Theyson et al.[14] The risk of inducing ischemic cholecystitis by taking other measures such as Gelfoam or coil embolization of the cystic artery, should be carefully weighed against the expected risk of symptomatic radiation-induced cholecystitis. We present a case in which we were able to protect a highly perfused gallbladder by slightly adjusting the catheter position. Scientific evidence is scarce for diagnostic features of radiation-induced cholecystitis, its correlation with ^{99m}Tc-MAA and ^{90}Y activity in the gallbladder wall, the efficacy of various precautionary measures, and the efficacy of medical treatment. Researchers are encouraged to report the occurrence and CTCAE grade of radiation-induced cholecystitis as well as (quantitative) findings on nuclear imaging and protective measures taken in these patients, when publishing future RE studies. This way, we can come to a better understanding of this rare but severe treatment complication.

Table 2. *Literature overview on radiation-induced cholecystitis*

Author *Year* (Reference)	**Nr. patients**	**Precautionary measures taken?**	**Gallbladder wall activity on SPECT**	**Overall incidence of symptomatic cholecystitis**	**Symptomatic Cholecystitis** (*CTCAE grade 2*)	**Cholecystitis Requiring Surgery** (*CTCAE grade 3 or 4*)
Peterson *et al. 2013* [27]	112	NR	NR	6% (7/112)	4.5% (5/112)	1.8% (2/112)
Bester *et al. 2013* [28]	427	NR	NR	NR	0.5% (2/427)	0
Bester *et al. 2 2013* [29]	339	NR	NR	1.8% (6/339)	0.6% (2/339) at 1 mo 1.8% (6/339) at 3 mo	0
Theyson *et al. 2013* [14]	295	Yes	6.8% (20/295)	0.03% (1/295)	0.03% (1/295)	0
McWilliwams *et al. 2011* [10]	46	NR	0	6.5% (3/46)	4.3% (2/46)	2.2% (1/46)
Ahmadzadehfar *et al. 2010* [2]	76	Yes	13.1% (10/76)	0	0	0
Cianni *et al. 2010* [32]	110	NR	NR	2.7% (3/110)	2.7% (3/110) at 1 mo	0
Garin *et al. 2010* [25]	15	No	20.0% (3/15)	NR	NR	NR
Cianni *et al. 2009* [30]	41	NR	NR	2.4% (1/41)	2.4% (1/41) at 1 mo	0
Jakobs *et al. 2008* [7]	41	NR	NR	2.4% (1/41)	0	2.4% (1/41)
Atassi *et al. 2008* [5]	327	NR	NR	0.6% (2/327)	0	0.6% (2/327)
Atassi *et al. 2 2008* [24]	130	NR	NR	1.5% (2/130)	0	1.5% (2/130)
Jiao *et al. 2007* [31]	21	NR	NR	4.8% (1/21)	4.8% (1/21)	NR
Miller et al. *2007* [8]	42	NR	NR	2.3% (1/42)	0	2.3% (1/42)

Articles were identified by performing a search in PubMed and EMBASE databases on November 8, 2013. Synonyms for radioembolization were combined with cystic artery, gallbladder or cholecystitis.

CTCAE = Common Terminology Criteria For Adverse Events, NR = Not Reported, SPECT = Single Photon-Emission Computed Tomography

Table 3. *Summary of gallbladder protection integrated in RE procedure*

- Identify cystic artery
- If possible, position microcatheter distal to cystic artery origin
- Inject ^{99m}Tc-MAA and qualitatively assess gallbladder activity on SPECT/CT, if needed:
  1. Adjust microcatheter position, check reduction of cystic artery flow during angiography
  2. Embolize cystic artery using Gelfoam pledgets or coils

References

1. Riaz A, Lewandowski RJ, Kulik LM, Mulcahy MF, Sato KT, Ryu RK, et al. Complications following radioembolization with yttrium-90 microspheres: a comprehensive literature review. J Vasc Interv Radiol. 2009;20(9):1121–30.
2. Ahmadzadehfar H, Sabet A, Biermann K, Muckle M, Brockmann H, Kuhl C, et al. The significance of 99mTc-MAA SPECT/CT liver perfusion imaging in treatment planning for 90Y-microsphere selective internal radiation treatment. J Nucl Med. 2010;51(8):1206–12.
3. van den Hoven AF, Prince JF, Samim M, Arepally A, Zonnenberg BA, Lam MGEH, et al. Posttreatment PET-CT-confirmed intrahepatic radioembolization performed without coil embolization, by using the antireflux Surefire Infusion System. Cardiovasc Intervent Radiol. 2014;37(2):523–8.
4. Hamoui N, Minocha J, Memon K, Sato K, Ryu R, Salem R, Lewandowski RJ. Prophylactic Embolization of the Gastroduodenal and Right Gastric Arteries Is Not Routinely Necessary before Radioembolization with Glass Microspheres. J Vasc Interv Radiol. 2013;24(11):1743-5
5. Atassi B, Bangash AK, Lewandowski RJ, Ibrahim S, Kulik L, Mulcahy MF, et al. Biliary sequelae following radioembolization with Yttrium-90 microspheres. J Vasc Interv Radiol. 2008;19(5):691–7.
6. Hickey R, Lewandowski RJ. Hepatic radioembolization complicated by radiation cholecystitis. Semin Interv Radiol. 2011;28(2):230–3.
7. Jakobs TF, Hoffmann R-T, Dehm K, Trumm C, Stemmler H-J, Tatsch K, et al. Hepatic yttrium-90 radioembolization of chemotherapy-refractory colorectal cancer liver metastases. J Vasc Interv Radiol. 2008;19(8):1187–95.
8. Miller FH, Keppke AL, Reddy D, Huang J, Jin J, Mulcahy MF, et al. Response of liver metastases after treatment with yttrium-90 microspheres: role of size, necrosis, and PET. AJR Am J Roentgenol. 2007;188(3):776–83.
9. Sato KT, Lewandowski RJ, Mulcahy MF, Atassi B, Ryu RK, Gates VL, et al. Unresectable chemorefractory liver metastases: radioembolization with 90Y microspheres–safety, efficacy, and survival. Radiology. 2008;247(2):507–15.
10. McWilliams JP, Kee ST, Loh CT, Lee EW, Liu DM. Prophylactic embolization of the cystic artery before radioembolization: feasibility, safety, and outcomes. Cardiovasc Intervent Radiol. 2011;34(4):786–92.
11. Wee E., Chang W.S., Oo A.M., Shuter B., Lim S.G. Yttrium-90 SIRT for the treatment of unresectable hepatocellular carcinoma: Outcomes of an Asian cohort. Gastroenterology. 2009;136(5):A860.
12. Paprottka PM, Jakobs TF, Reiser MF, Hoffmann RT. Practical vascular anatomy in the preparation of radioembolization. Cardiovasc Intervent Radiol. 2012;35(3):454–62.
13. Powerski MJ, Scheurig-Münkler C, Banzer J, Schnapauff D, Hamm B, Gebauer B, et al. Clinical practice in radioembolization of hepatic malignancies: a survey among interventional centers in Europe. Eur J Radiol. 2012;81(7):e804–11.
14. Theysohn JM, Muller S, Schlaak JF, Ertle J, Schlosser TW, Bockisch A, et al. Selective internal radiotherapy (SIRT) of hepatic tumors: how to deal with the cystic artery. Cardiovasc Intervent Radiol. 2013;36(4):1015–22.
15. ACR-ASTRO-SIR Practice Guideline for Radioembolization with Microsphere Brachytherapy Device (RMDB) for Treatment of Liver Malignancies [Internet]. [cited 2013 Nov 4]. Available from: http://www.acr.org/~/media/D8086059B5F541E9B64E55D68A71693B.pdf
16. Dezarn W a., Cessna JT, DeWerd L a., Feng W, Gates VL, Halama J, et al. Recommendations of the American Association of Physicists in Medicine on dosimetry, imaging, and quality assurance procedures for 90Y microsphere brachytherapy in the treatment of hepatic malignancies. Med Phys. 2011;38(8):4824.
17. Giammarile F, Bodei L, Chiesa C, Flux G, Forrer F, Kraeber-Bodere F, et al. EANM procedure guideline for the treatment of liver cancer and liver metastases with intra-arterial radioactive compounds. Eur J Nucl Med Mol Imaging. 2011;38(7):1393–406.
18. Lewandowski RJ, Sato KT, Atassi B, Ryu RK, Nemcek AA, Kulik L, et al. Radioembolization with 90Y microspheres: angiographic and technical considerations. Cardiovasc Intervent Radiol. 2007;30(4):571–92.
19. Mahnken AH, Spreafico C, Maleux G, Helmberger T, Jakobs TF. Standards of practice in transarterial radioembolization. Cardiovasc Intervent Radiol. 2013;36(3):613–22.

20. Smits ML, Nijsen JF, van den Bosch MA, Lam MG, Vente MA, Mali WP, et al. Holmium-166 radioembolisation in patients with unresectable, chemorefractory liver metastases (HEPAR trial): a phase 1, dose-escalation study. Lancet Oncol. 2012;13(10):1025-34.
21. Smits MLJ, Elschot M, van den Bosch M a a J, van de Maat GH, van het Schip AD, Zonnenberg B a, et al. In vivo dosimetry based on SPECT and MR imaging of 166Ho-microspheres for treatment of liver malignancies. J Nucl Med. 2013;54(12):2093–100.
22. Elschot M, Smits MLJ, Nijsen JFW, Lam MGEH, Zonnenberg B a., van den Bosch M a. a. J, et al. Quantitative Monte Carlo-based holmium-166 SPECT reconstruction. Med Phys. 2013;40(11):112502.
23. Smits MLJ, van den Hoven AF, Rosenbaum CENM, Zonnenberg BA, Lam MGEH, Nijsen JFW, et al. Clinical and laboratory toxicity after intra-arterial radioembolization with (90)y-microspheres for unresectable liver metastases. PloS One. 2013;8(7):e69448.
24. Atassi B, Bangash AK, Bahrani A, Pizzi G, Lewandowski RJ, Ryu RK, et al. Multimodality imaging following 90Y radioembolization: a comprehensive review and pictorial essay. Radiographics. 2008;28(1):81-99.
25. Garin E, Rolland Y, Boucher E, Ardisson V, Laffont S, Boudjema K, et al. First experience of hepatic radioembolization using microspheres labelled with yttrium-90 (TheraSphere): practical aspects concerning its implementation. Eur J Nucl Med Mol Imaging. 2010;37(3):453–61.
26. Trotti A, C olevas AD, Setser A, Rusch V, Jaques D, Budach V, et al. CTCAE v3.0: development of a comprehensive grading system for the adverse effects of cancer treatment. Semin Radiat Oncol. 2003;13(3):176–81.
27. Peterson J L, Vallow LA, Johnson DW, Heckman MG, Diehl NN, Smith AA, et al. Complications after 90Y microsphere radioembolization for unresectable hepatic tumors: An evaluation of 112 patients. Brachytherapy. 2013;12(6):573–9.
28. Bester L, Feitelson S, Milner B, Chua TC, Morris DL. Impact of prior hepatectomy on the safety and efficacy of radioembolization with yttrium-90 microspheres for patients with unresectable liver tumors. Am J Clin Oncol. 2014;37(5):454–60.
29. Bester L, Meteling B, Pocock N, Pavlakis N, Chua TC, Saxena A, et al. Radioembolization versus standard care of hepatic metastases: comparative retrospective cohort study of survival outcomes and adverse events in salvage patients. J Vasc Interv Radiol. 2012;23(1):96–105.
30. Cianni R, Urigo C, Notarianni E, Saltarelli A, Salvatori R, Pasqualini V, et al. Selective internal radiation therapy with SIR-spheres for the treatment of unresectable colorectal hepatic metastases. Cardiovasc Intervent Radiol. 2009;32(6):1179–86.
31. Jiao LR, Szyszko T, Nahhas A Al-, Tait P, Canelo R, Stamp G, et al. Clinical and imaging experience with yttrium-90 microspheres in the management of unresectable liver tumours. Eur J Surg Oncol. 2007;33(5):597–602.
32. Cianni R, Urigo C, Notarianni E, Saltarelli A, Agostini A D', Iozzino M, et al. Radioembolisation using yttrium 90 (Y-90) in patients affected by unresectable hepatic metastases. Radiol Med. 2010;115(4):619–33.
33. Basciano CA, Kleinstreuer C, Kennedy AS, Dezarn WA, Childress E. Computer modeling of controlled microsphere release and targeting in a representative hepatic artery system. Ann Biomed Eng. 2010;38(5):1862–79.
34. Kennedy AS, Kleinstreuer C, Basciano CA, Dezarn WA. Computer modeling of yttrium-90-microsphere transport in the hepatic arterial tree to improve clinical outcomes. Int J Radiat Oncol Biol Phys. 2010;76(2):631–7.

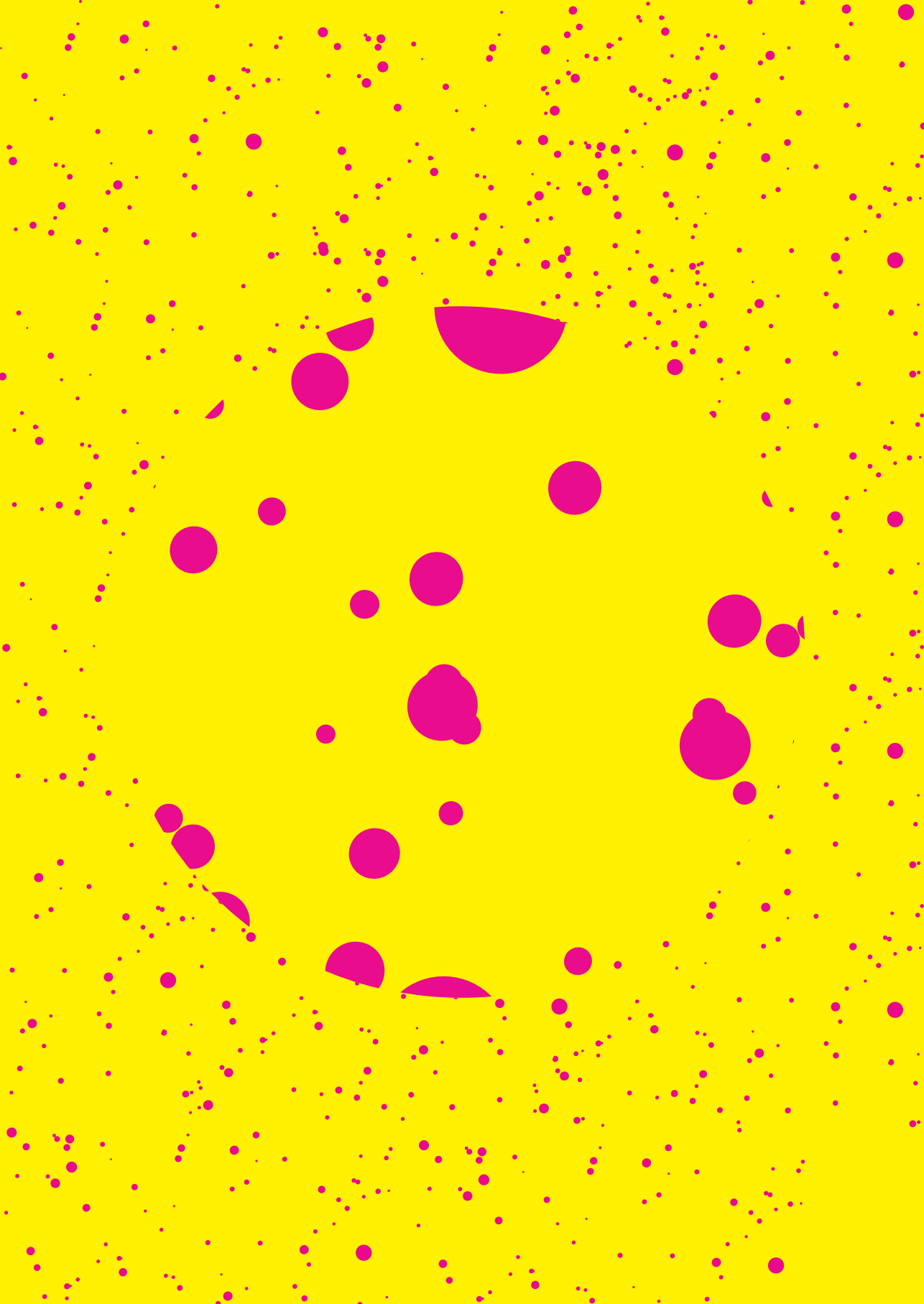

CHAPTER 5

Safety of a scout dose preceding hepatic radioembolization with ^{166}Ho microspheres

J.F. Prince
R. van Rooij
G.H. Bol
H.W.A.M. de Jong
M.A.A.J. van den Bosch
M.G.E.H. Lam

Journal of Nuclear Medicine 2015

Abstract

Purpose

Before holmium-166 (^{166}Ho) radioembolization, a small batch of the same type of microspheres is administered as a scout dose instead of the conventional technetium-99m (^{99m}Tc) macroaggregated albumin (MAA). The ^{166}Ho scout dose provides a more accurate and precise lung shunt assessment. However, in contrast to ^{99m}Tc-MAA, an unintended extrahepatic deposition of this β-emitting scout dose could inflict radiation damage, the extent of which we aimed to quantify in this study.

Methods

All patients eligible for radioembolization in our institute between January 2011 and March 2014 were reviewed. Of the extrahepatic depositions of ^{99m}Tc-MAA on single-photon emission computed tomography (SPECT), the amount and volume were measured. These were used to calculate the theoretic absorbed dose in the case a ^{166}Ho scout dose had been used. The extrahepatic activity was measured as the sum of all voxels of the deposition. Volumes were measured using a threshold technique including all voxels from the maximum voxel intensity up to a certain percentage. The threshold needed to obtain the true volume was studied in a phantom study.

Results

In the phantom study, a threshold of 40% was found to overestimate the volume with the consequence of underestimating the absorbed dose. Of 160 patients, 32 patients (34 cases) of extrahepatic deposition were identified. The depositions contained a median of 1.3% (range, 0.1% - 19.5%) of the administered activity in a median volume of 6.8 mL (range, 1.1 - 42 mL). The use of a scout dose of 250 MBq of ^{166}Ho microspheres in these cases would theoretically have resulted in a median absorbed dose of 6.0 Gy (range 0.9 - 374 Gy). The dose exceeded a limit of 49 Gy (reported by in 2013) in 2 of 34 cases (5.9%, 95% confidence interval, 0.7% – 20.1%), or 2/160 (1.3%, 95% confidence interval, 0.1% – 4.7%) of all patients. In these 2 patients with a large absorbed dose (112 and 374 Gy), the culprit vessel was identified in 1 case.

Conclusion

Extrahepatic deposition of a ^{166}Ho scout dose seems to be theoretically safe in most patients. Its safety in clinical practice is being evaluated in ongoing clinical trials.

Introduction

Radioembolization is a minimally invasive treatment for hepatic malignancies. Millions of radioactive microspheres are injected in the hepatic artery to radiate and embolize malignancies.[1] Deposition of microspheres in gastrointestinal organs can result in ulceration or inflammation of tissue by a combination of embolization and radiation damage.[2–4] To prevent this, vessels leading to gastrointestinal organs may be coil-embolized in patients scheduled for radioembolization treatment, during a pretreatment session using contrast-enhanced images (i.e. digital subtraction angiography complemented by C-arm CT) to identify the culprit vessel.[5] Technetium-99m (^{99m}Tc) macroaggregated albumin (MAA) is administered in this pretreatment session to simulate intrahepatic treatment biodistribution and to assess lung shunting and the possibility of extrahepatic deposition of the microspheres.[6] This procedure is safe because ^{99m}Tc-MAA emits 140 keV γ photons (detectable by scintigraphy) which deposit a negligible dose and the macroaggregated albumin dissolves in the bloodstream in several hours.

Treatment with holmium-166 (^{166}Ho) radioembolization can be preceded by a different scout dose used during the pretreatment session.[7] This scout dose consists of a small batch of microspheres (250 MBq), identical to the treatment ^{166}Ho microspheres. It is expected to better simulate treatment because it shares the same density, size distribution, and morphology with the treatment dose. It was already shown that a ^{166}Ho scout dose was a more reliable predictor of lung shunting than ^{99m}Tc-MAA.[8] However, this scout dose emits electrons due to its β- decay. In the case of unwanted extrahepatic deposition of activity, a ^{166}Ho scout dose may induce ulceration and inflammation of abdominal organs, such as the stomach, duodenum, or pancreas. In prior studies on ^{166}Ho radioembolization of the liver, both ^{99m}Tc-MAA and a ^{166}Ho scout dose preceded treatment.[7] In order to replace ^{99m}Tc-MAA in clinical practice, the risk of extrahepatic deposition of a ^{166}Ho scout dose must be known.

This study uses extrahepatic deposition of ^{99m}Tc-MAA as a surrogate marker for an extrahepatic scout dose, becayse the ^{166}Ho scout dose, used in the Holmium Embolization Particles for Arterial Radiotherapy (HEPAR) trials, was preceded by ^{99m}Tc-MAA injection, which decreased the incidence of extrahepatic deposition to negligible figures. The objective of this study was to calculate the theoretic

absorbed dose of extrahepatic deposition from a ^{166}Ho scout dose by evaluation of the extrahepatic depositions of ^{99m}Tc-MAA as seen in current practice. A phantom study was performed to determine the volume of the depositions on SPECT.

Methods

Study design

In this retrospective cross-sectional study, all pretreatment procedures before radioembolization were reviewed for extrahepatic deposition of ^{99m}Tc-MAA. From these procedures, the amount and volume of the deposition were estimated. The partial volume effect makes absolute quantification of focal uptake challenging, as is known from for example, analysis of standardized uptake values from ^{18}F-FDG-PET.[9] Therefore, likewise as is practice in ^{18}F-FDG-PET, the technique used for volume estimation was first tested in a phantom study. Using the amount and volume, we calculated the potential absorbed dose in the case that a 250 MBq ^{166}Ho scout dose would have been used instead of a 150 MBq ^{99m}Tc-MAA dose. A waiver for informed consent for the retrospective review of these imaging data was obtained from the research ethics committee of our institution.

Phantom equipment

For evaluation of the volume measurement method, the National Electrical Manufacturers Association NU2-2001 image quality phantom, containing 6 spheres of sizes varying between 0.5 and 26.5 mL suspended in a water filled background compartment of 9.7 L, was used. The spheres were filled from a ^{99m}Tc buffer solution of known activity concentration and scanned identically to the ^{99m}Tc-MAA patient protocol.

Patient population

All consecutive patients from January 2011 (SPECT/CT routinely performed since then) until March 2014, who received a ^{99m}Tc-MAA injection as part of radioembolization workup were eligible for inclusion. To obtain a representative sample of the distribution of extrahepatic depositions, if a patient underwent multiple angiography sessions, only the first was included (i.e., if an extrahepatic deposition is corrected in a subsequent angiography it should either disappear or become smaller; the second angiography session probably results in smaller

depositions than the first). If 2 separate extrahepatic depositions were in a single patient, they were evaluated as 2 separate cases.

Procedure

Every patient underwent pretreatment angiography together with injection of 150 MBq ^{99m}Tc-MAA (0.8 mg, Technescan LyoMAA [Mallinckrodt Medical B.V.]) according to published guidelines.[10] The gastroduodenal and/or gastric artery were coil-embolized at the discretion of the interventional radiologists; some preferred to always occlude those arteries while others injected ^{99m}Tc-MAA in a selective, lobar, fashion. The operator confirmed the injection position using dual-subtraction angiography, complimented by C-arm CT. Patients were planned to receive either yttrium resin or holmium microspheres as a whole liver or lobar treatment.

Imaging and reconstruction

All patients were scanned on a Symbia T16 SPECT/CT scanner (Siemens) within an hour after the pretreatment angiography with injection of ^{99m}Tc-MAA. SPECT data of the liver were acquired using a low-energy high-resolution collimator, on a 128 × 128 matrix (zoom, 1.23; pixel size, 3.9 × 3.9 mm) with 120 angles (20 s per projection) over a noncircular 360° orbit and a 140-keV ± 7.5 % photopeak energy window. Low-dose CT data (110 kVp, 40 mAs, adaptive dose modulation with Siemens CARE Dose 4D) were acquired and reconstructed to a voxel size of 1.27 × 1.27 × 5 mm using a smoothing kernel (B08s; Siemens Healthcare). After a CT-derived attenuation map was created (Syngo MI Applications; Siemens Healthcare), SPECT images were reconstructed using 3-dimensional ordered-subset expectation maximization (Flash 3D; Siemens) with: 6 iterations, 8 subsets; 5 mm gaussian smoothing; CT-based attenuation-correction and a window based scatter correction.

Analysis of deposition: activity and volume

The extrahepatic activity was estimated by summation of all voxels within a manual delineation of the deposition. It was delineated using in-house developed software (Volumetool).[11] The margin of delineation was large enough to visually include all focal activity including the displaced counts due to resolution, patient motion, and scatter effects. If the counts in the liver and the displaced counts from the deposition overlapped, the point of the lowest intensity was assumed to be the

best estimate of the boundary between the 2. All voxels within the volume were summed, without use of a threshold, to prevent underestimation of the activity (and absorbed dose). The total administered activity was estimated by a delineation around the liver, which included the deposition but excluded the kidneys, thyroid, stomach, and lungs, because the microspheres used in radioembolization do not shunt to extrahepatic organs in the same way as free pertechnetate from ^{99m}Tc-MAA.[12] The percentage of counts in the deposition relative to the counts in the liver (and deposition) was used to predict the activity in the deposition if ^{166}Ho were to be used as a scout dose.

To determine the volume of an extrahepatic deposition, the limited resolution of the SPECT image needed to be accounted for. As a start, the same manual delineation of the deposition as mentioned before was used, which included the extrahepatic deposition, but excluded the liver. Subsequently, the volume was estimated by selecting only voxels within the start delineation exceeding a certain threshold determined in the phantom study (a percentage of the maximum value in the delineation). These voxels were considered to be contributing to the volume; the voxels with lower values were considered to be a result of the point spread function of the SPECT. The percentage was determined in a phantom study to provide a conservative underestimation of the volume, which would result in an overestimation of the absorbed dose.

Absorbed dose

For theoretic assessment of the potential risk of extrahepatic ^{166}Ho microsphere deposition, the ^{99m}Tc-MAA was assumed to be distributed identically to ^{166}Ho microspheres with regard to the amount and volume of extrahepatic activity.

No adjustments to the prescribed activities were made for high lung shunt fractions. Patients who had contraindications for treatment were not excluded from this analysis. The following formula was used to calculate the dose:

Equation 1 $$Dose\ (Gy) = 15.87\ \left(\frac{mJ}{MBq}\right) \times \frac{extrahepatic\ amount\ (\%) \times 250\ (MBq)}{extrahepatic\ volume\ (cm^3) \times 1.06\ (g/cm^3)}$$

In this formula, 15.87 mJ/Mbq is the total energy absorbed from the total decay of 1 MBq of ^{166}Ho, 250 MBq the activity of injected ^{166}Ho in a scout dose, and a density

of soft tissue of 1.06 g/cm^3 was assumed.[13,14] All energy was assumed to be absorbed in the extrahepatic deposition location, because the mean penetration of the βemission of ^{166}Ho (2.5 mm) is small, compared with the measured volumes.[15]

A safety boundary for the absorbed dose in extrahepatic tissue was reported in the literature by Kao et al.[16,17] After radioembolization with yttrium resin microspheres, the authors quantified the absorbed dose to extrahepatic tissue using PET. An absorbed dose of 18 Gy was deposited in the stomach of 1 patient, after which no complications occurred. In a second patient, extrahepatic deposition was present in the stomach (2x) and duodenum. The patient developed gastritis (stomach), ulceration (stomach), and duodenitis (duodenum) after a mean absorbed dose of 49, 65, and 53 Gy, respectively. For the current study, a 49 Gy boundary was chosen from which toxicity was expected to occur.[16,17]

Statistical analyses

Data were summarized using descriptive statistics suitable for nonnormal distributed data (medians, range). All statistical analyses were performed in R (R Foundation for Statistical Computing).[18] Confidence intervals for proportions were calculated using the adjusted Wald method and displayed as 95% confidence intervals.[19]

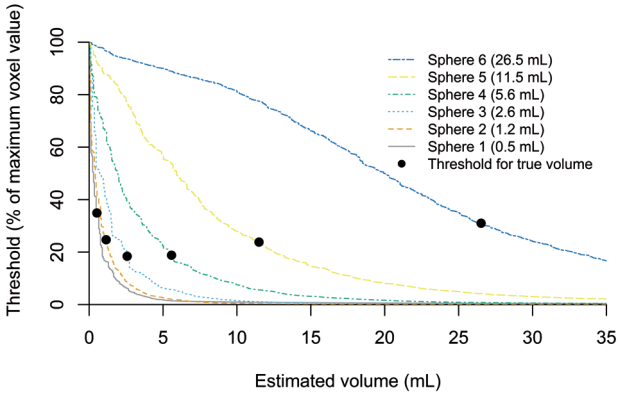

Figure 1 *Volume estimation in phantom study of 6 spheres of different volumes (0.5–26.5 mL). Estimate of volume on SPECT is number of all voxels from threshold up to voxel with maximum value, multiplied by voxel volume; it decreases as threshold increases. True, known, volume of each sphere is indicated by black dot. Higher threshold leads to underestimation while lower threshold leads to overestimation. For all spheres, threshold of 40% leads to underestimation of volume.*

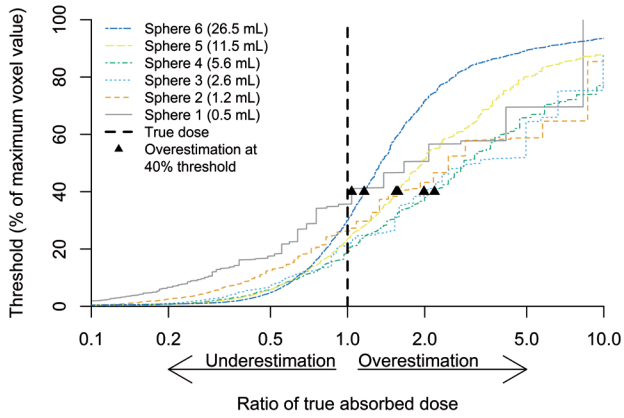

Figure 2 *Absorbed dose estimation in phantom study using 6 spheres of different volumes (0.5–26.5 mL). Absorbed dose is displayed as ratio of true absorbed dose in sphere. Threshold needed to estimate true absorbed dose (dotted line) differs per sphere. Absorbed dose is overestimated in all spheres using a threshold of 40% (black triangles).*

Results

Phantom study

Figure 1 shows the apparent volume for each sphere as a function of threshold level. The thresholds at which the true volumes of the spheres were recovered are denoted

by black dots. The optimal threshold level depends on the sphere size. The volume is underestimated for all spheres if a 40% threshold is used.

Figure 2 shows the 40% threshold estimated absorbed doses relative to their true values in the phantom. To estimate the activity in the spheres, the same method was used as for extrahepatic depositions in patients (i.e., without a threshold to avoid underestimating the activity). The counts in a volume including a single sphere were summed and divided by the sum over the total image containing all spheres. The recovered activities, as a percentage of the true, known, injected activities, were (from smallest sphere to largest) 94%, 89%, 91%, 100%, 100%, and 101%. Combined with the estimated volumes and with Equation 1 applied, the absorbed dose in each sphere was overestimated with (from smallest to largest sphere) 4%, 57%, 99%, 118%, 55%, and 16%.

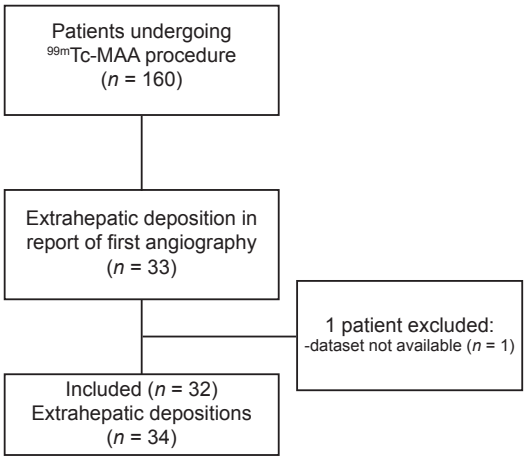

Figure 3 *Flowchart of study design*

Patient population

Of all the 160 patients undergoing a ^{99m}Tc-MAA injection between March 2011 and March 2014, 33 patients were identified with extrahepatic deposition of ^{99m}Tc-MAA. Of these 33 patients, the dataset of 1 procedure was not available due to a technical error. In 2 patients, 2 separate depositions were identified, which were treated as separate cases. In total, 32 patients with 34 extrahepatic depositions were included (Figure 3 provides a flowchart). Baseline characteristics can be found in Table 1. For each of these patients there were contraindications for treatment due

to their extrahepatic deposition, but an additional angiographic procedure allowed treatment in 17 of 32 patients (53%).

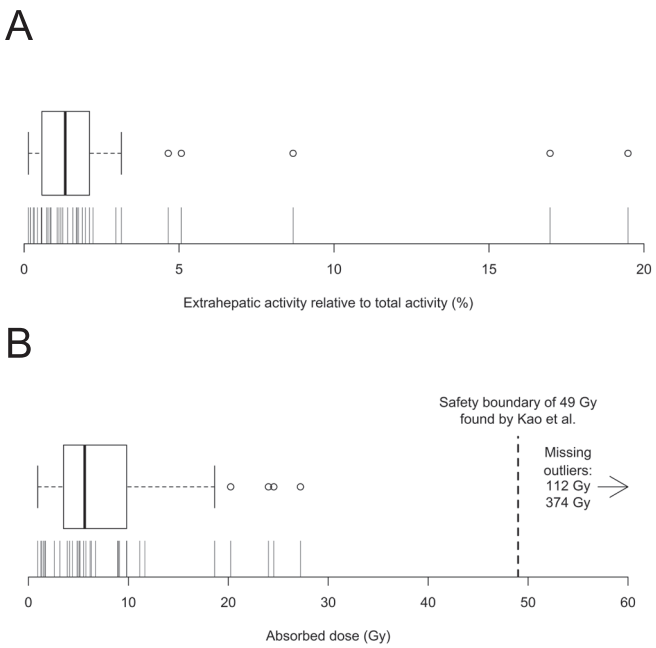

Figure 4 *(A) Box plot and density plot of extrahepatic activity relative to total activity (liver and extrahepatic deposition). Distribution is right-skewed. Each vertical indicates observation. (B) Box plot and density plot of absorbed dose to extrahepatic tissue from 250-MBq ^{166}Ho scout dose, plotted on log-scale (in Gy). Boundary from which complications occurred in study by Kao et al. of 49 Gy is displayed.* [17]

Extrahepatic deposition

Of the infused activity, a median of 1.3% (range 0.1% – 19.5%) was located in the extrahepatic depositions. The distribution of extrahepatic activities was skewed to the right, as can be seen in Figure 4. In the 2 largest outliers, the extrahepatic deposition contained 17.0% and 19.5% of the total administered activity. The median determined volume of the extrahepatic depositions was 6.8 mL (range, 1.1 – 42 mL). The full dataset is available in Supplemental Data A.

Table 1. *Baseline characteristics*

Characteristic	n (%) or median (range)
N / # procedures	32 / 34
Sex	
Male	25 (78%)
Female	7 (22%)
Age (years)	67 (36-80)
Primary tumor	
Colorectal carcinoma	19 (59%)
Cholangiocellular carcinoma	3 (9%)
Hepatocellular carcinoma	3 (9%)
Ocular melanoma	2 (6%)
Adenocarcinoma of unknown primary	1 (3%)
Breast carcinoma	1 (3%)
Gastric carcinoma	1 (3%)
Neuroendocrine tumor	1 (3%)
Papil carcinoma	1 (3%)
Coil-embolization	
Gastroduodenal and right gastric	17 (53%)
Gastroduodenal	6 (19%)
Gastroduodenal and cystic	1 (3%)
Gastroduodenal and pancreatic	1 (3%)
Gastroduodenal and duodenal	1 (3%)
None	6 (19%)
Number of injection positions	
1	17 (53%)
Common	4
Proper	11
Right	1
Replaced left	1
2	14 (44%)
Common + replaced right	1
Common + replaced left	1
Right + left	9
Right + replaced left	1
Replaced right + left	1
Replaced right + left (from SMA)	1
3	1 (3%)
Replaced right and selective (2x) left	1

SMA, superior mesenteric artery

Theoretical absorbed dose after a scout dose ^{166}Ho

If a scout dose of 250 MBq of ^{166}Ho had been administered instead of ^{99m}Tc-MAA, the median absorbed dose to extrahepatic tissue would have been 6.0 Gy (range 0.9 – 374 Gy, right skewed). Two patients would have received absorbed doses at which complications might have developed: 112 and 374 Gy (Figure 4B). The largest absorbed dose of 374 Gy was explained by its large extrahepatic activity (19.5%) in a small volume of only 2.1 mL. This patient had liver metastases of a colorectal carcinoma. He received a first ^{99m}Tc-MAA injection in the proper hepatic artery, after which a large extrahepatic focus was seen on SPECT/CT in the pancreatic region (Figure 5). Subsequent injections in the left and right hepatic artery, during an additional procedure, showed no extrahepatic deposition and he finally was treated with resin ^{90}Y microspheres without complications. The other dose, of 112 Gy, would have received less activity in the deposition (8.7%), but also in a small volume of 3.1 mL. This patient also had liver metastasis from a colorectal carcinoma. He previously underwent a hemihepatectomy of the right liver. A left hepatic artery and middle hepatic artery of small caliber remained, ^{99m}Tc-MAA was injected in both arteries after coil-embolization of the gastroduodenal and right gastric artery. SPECT/CT showed extrahepatic activity in the duodenum (see Figure 6). On repeated angiography, patency of a branch from the proximal gastroduodenal artery was found. Reflux was thought to have occurred because of the small caliber of the vessel after hemihepatectomy. After coil-embolization, treatment was successful. The patient showing 17.0% of extrahepatic activity would not have received a high absorbed dose (only 25 Gy) because of its distribution in a relatively large volume of 27.4 mL.

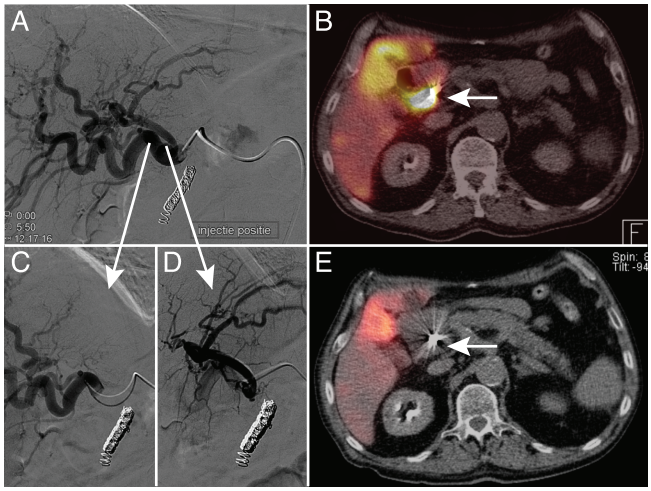

Figure 5 *Extrahepatic deposition of 8.7% of administered activity near duodenum after injection in proper hepatic artery (A, B), which was corrected after selective lobar injection in right (C) and left (D) hepatic artery (E). Had 250-MBq ^{166}Ho scout dose been injected, theoretic extrahepatic absorbed dose would have been 112 Gy.*

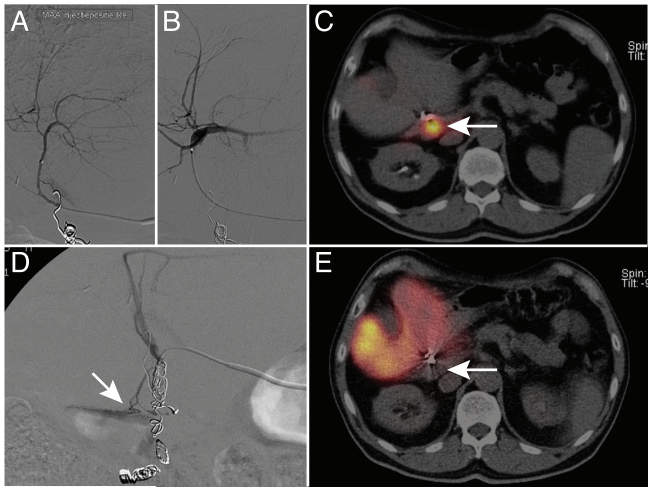

Figure 6 *Extrahepatic deposition in patient, who previously received right hemihepatectomy, after injection in right (A) and left (B) hepatic artery. Deposition (C, white arrow) represents 19.5% of total activity (little activity is seen in liver). During repeat angiography, culprit vessel originated from gastroduodenal artery (D, white arrow). After coil-embolization and single injection in proper hepatic artery, no deposition was seen (E, white arrow). Had 250-MBq ^{166}Ho scout dose been injected, theoretic absorbed dose would have been 374 Gy.*

Discussion

Using a surrogate particle, ^{99m}Tc-MAA, this study shows that the infusion of a scout dose (250 MBq) of therapeutic ^{166}Ho microspheres may theoretically harm extrahepatic tissue by its absorbed dose. In their study, Kao et al. found complications to occur from 49 Gy and upward.[16,17] Of 160 patients, 34 cases with extrahepatic deposition were found. In theory, the boundary of 49 Gy was only exceeded in 1.3% of cases (2/160, 95% confidence interval 0.1 – 4.7%), namely 112 and 374 Gy. In all remaining cases, the absorbed dose would not have exceeded 27.2 Gy (Figure 4B).

A ^{166}Ho scout dose provides an advantage over ^{99m}Tc-MAA mostly because it is superior in predicting the absorbed dose by the lungs. Elschot et al. found that planar scintigraphy after a ^{99m}Tc-MAA injection vastly overestimated the lung shunt.[8] The authors found a median difference of 2.4 Gy (range 1.0 – 12.3 Gy) when they compared estimates of the lung absorbed dose after injection of ^{99m}Tc-MAA and ^{166}Ho microspheres. The relevance of this finding is shown by the incidence of a high lung shunt fraction on ^{99m}Tc-MAA SPECT/CT. In the study population, planar lung shunt fractions were available for 157 of 160 patients. The median lung shunt fraction was 4.9 % (range, 0.3% – 38.7%). Of 157 patients, in 21 patients the lung shunt fraction was greater than 10% (dose reduction advocated), of which 6 were greater than 15% (further reduction) and of which 3 were greater than 20% (contraindication). A possible benefit of a more accurate estimation of the lung shunt by ^{166}Ho microspheres might have been relevant in 13% (21/157) of the patients. The study population was predominantly composed of patients with colorectal liver metastases and it has been suggested that these patients have a lower lung shunt fraction than patients with other primary malignancies.[20] Powerski et al. reported on a population of 233 patients (29% colorectal carcinoma, 27% hepatocellular carcinoma) and found lung shunt fractions to differ between tumor types, showing that patients with hepatocellular carcinoma had higher lung shunt fractions.[21] Incidences of a high lung shunt fraction will vary between institutions as patient populations vary. Gaba et al. reported an incidence of a high lung shunt (>10%) in 40% of patients; 50% of their population of 141 patients consisted of patients with hepatocellular carcinoma.[22] A better estimator of the lung shunt would thus be relevant for clinical practice.

Additionally, it is hypothesized that the predictive value of a ^{166}Ho microsphere scout dose is superior to a ^{99m}Tc-MAA scout dose, because the microspheres of the scout and therapeutic dose are identical. In that case, treatment could be optimized by increasing the radioactive dose in some arteries (e.g., with a high tumor-to-nontumor ratio) and by limiting it in others, possibly leading to a higher efficacy and lower toxicity. Imaging of both ^{99m}Tc-MAA and ^{166}Ho can be performed by SPECT/CT. ^{99m}Tc emits 140 keV γ rays with a radiation abundance of 89%, while ^{166}Ho emits 81 keV gamma rays with an abundance of 7%.[23] Although spatial resolution, contrast recovery, and sensitivity are worse for ^{166}Ho than ^{99m}Tc-MAA, injection of 250 MBq of ^{166}Ho microspheres is sufficient to provide images that allow for the evaluation of lung shunt and extrahepatic deposition.[24,25] Another benefit of ^{166}Ho microspheres, and a principal reason for their development[26], is the possibility of their multimodal detection: an 81-keV photopeak for nuclear imaging[24], high magnetic susceptibility for MR imaging[27], and a high mass attenuation coefficient for X-ray CT imaging[28]. The most promising modality, MR imaging, could enable MR-guided treatment, as has been performed ex vivo in rabbits.[29]

The absorbed doses presented in this study should be considered with care, as they are most likely dose overestimations (4% - 118% in the phantom study). The dose calculations are dependent on the activity and volume estimations. The latter depends on the chosen threshold, as seen in Figure 1. The accuracy of SPECT is influenced by detrimental breathing effects, limited resolution, scatter, and septal penetration. Furthermore, volume estimations of small volumes (< 1 mL) may be less precise, which can be seen in Figure 1 by the density of the curves for the smaller spheres. Our phantom study consisted of homogeneously filled spheres, whereas extrahepatic depositions may be more cylindric and consist of heterogeneous clusters of microspheres. Because our measurements could not be exact, an underestimation of the theoretic absorbed dose had to be avoided, as this could lead us to conclude that a ^{166}Ho scout dose was safe while it might not be. In our phantom study, we showed that a threshold of 40% will underestimate the volume (Figure 1) and thereby overestimate the absorbed dose (Figure 2).

The preliminary published threshold of 49 Gy is based on 1 publication, a case series in which extrahepatic depositions from radioembolization were quantified. This threshold might be an underestimation, as the same absorbed dose in a different volume might lead to a different clinical outcome, for example, high

doses in a large volume might be more toxic than in a small volume. It might also be an overestimation, as the threshold on external radiotherapy was found to be much lower.[30] Although absorbed doses from external radiotherapy are not comparable to radioembolization (due to differences in biologic effective doses) and literature on complications of the stomach and small bowels is scant, data on external radiotherapy do provide a clue. A risk of 5% for toxicities within 5 y was estimated after partial stomach or small-bowel irradiation with 50 Gy. However, stereotactic body radiation therapy achieves higher absorbed doses per fraction, and might be more comparable to radioembolization; Kavanagh et al. advise to minimize the maximum absorbed point dose in 5 mL of stomach to less than 30 Gy and minimize the amount of small-bowel volume irradiation with more than 12.5 Gy to less than 30 mL. A study by Streitparth et al., investigating 1-time high-dose-rate brachytherapy of liver malignancies, found a threshold absorbed dose of 11 Gy in a 1-mL volume of stomach wall for gastric toxicities.[31] The authors noted that findings from high-dose-rate brachytherapy (irradiation time: 20-40 min) vary from external radiotherapy, as the latter is probably less toxic. For ^{166}Ho, with a half-life of 26.8 h, 90% of the dose is deposited over 89 h. In our study, the large difference between the outliers (112 and 374 Gy) and the highest safe absorbed dose (27.2 Gy) shows that the safety threshold of 49 Gy need not be very accurate for this study to draw the same conclusions. If accurate dosimetry studies on radioembolization become available, the data from this study can be reevaluated (all data are available in Supplemental Table 1).

Extrahepatic deposition after radioembolization treatment can cause ulceration or inflammation, probably because of both embolization and radiation damage. We investigated only the latter. An animal study in 9 pigs by Bilbao et al. [2] showed that nonradioactive microspheres only induce ulceration when aggregated, and embolization of small distal vessels alone does not cause ulceration. Blood flow was regenerated by the appearance of new vessels or recanalization of occluded vessels. A report by Ogawa et al. of 3 patients who developed gastroduodenal complications after hepatic radioembolization suggested that the changes in the gastroduodenal region were similar in histologic appearance and timing to radiation-induced damage.[3] Murthy et al. noted that some ulcers do not contain microspheres on histopathologic examination and posed another causative mechanism: Bremsstrahlung of adjacent liver tissue treated with radioembolization.[4] After extrahepatic deposition, it seems likely embolization has an additional negative

effect, the extent of which is unknown. Embolization is also dependent on different variables, including microsphere composition and size. It is therefore not incorporated in this study.

An analysis of the causes of extrahepatic depositions is beyond the scope of this study. However, our cohort is in accordance with findings by Lam et al.[32], who found that a proximal injection can be a cause; we found ^{99m}Tc-MAA was often injected in a proximal, whole liver (47%, 15/32) fashion. Another factor the authors mentioned that is, stasis during injection, did not occur, because ^{99m}Tc-MAA has little embolic effect. Paradoxically, we found that most patients underwent prophylactic occlusion of one or more arteries, even though coil-embolization is no longer routinely performed in our center. Unfortunately, after introduction of C-arm CT in our institute, extrahepatic depositions still occurred. A preventive effect hereof could not be tested for in the present analysis. The high incidence of extrahepatic activity on ^{99m}Tc-MAA SPECT/CT (33/160 patients) may have been related to a learning curve (e.g. administration in the proper hepatic artery vs. more selective administration) and the late introduction of technical innovations (e.g., C-arm CT). When the incidence of extrahepatic activity decreases because of either, the relative benefit of a ^{166}Ho scout dose increases, as it has superior lung shunt estimation and probably allows for a more accurate dosimetry-based treatment planning. Not all extrahepatic deposition could be corrected and only 53% of patients were ultimately treated with radioembolization.

A ^{166}Ho scout dose of 250 MBq was used for assessment, because it is currently used in clinical studies. By decreasing this activity, the absorbed dose can be decreased. The current activity was chosen after several preclinical studies to find a balance between toxicity and detectability. The potential lung dose of a ^{166}Ho scout dose is for example far below a clinically relevant absorbed dose of 30 Gy.[33] To reduce this activity would render it safer, but reduce its detectability.

In this study, the incidence of an extrahepatic deposition of a ^{166}Ho scout dose that is high enough to cause complications after injection is low (<2%). The high absorbed doses found in this theoretic analysis do not necessarily translate to complications in practice. From a risk-benefit perspective, an injection of ^{99m}Tc-MAA is preferred over a ^{166}Ho scout dose in the absence of significant benefits. However, a better estimation of the lung dose (and anticipated treatment

individualization) seems to outweigh the risk. Additionally, improved pretreatment imaging and additional C-arm CT imaging may decrease the risk and severity of extrahepatic depositions.[5,34] The workup for ^{166}Ho radioembolization in 2 clinical studies that recently started recruitment in our center has now been changed. A digital subtraction angiography and C-arm CT are always performed from every injection position, and a ^{99m}Tc-MAA scout dose was replaced by a ^{166}Ho scout dose (Surefire Infusion System vs. Standard Microcatheter Use During Holmium-166 Radioembolization study, NCT02208804; HEPAR Plus study, NCT02067988). The safety a ^{166}Ho scout dose is continuously evaluated in these prospective clinical trials.

Conclusion

Theoretic analysis of the potential risk of a 250 MBq ^{166}Ho scout dose resulted in a low incidence (1.3%, 95% confidence interval 0.1% – 4.7%) of potentially harmful extrahepatic deposition. Because its clinical benefits, which include a more accurate estimate of the lung shunt, seem to outweigh its potential risk, the ^{99m}Tc-MAA injection was replaced by a ^{166}Ho scout dose in ongoing clinical trials on ^{166}Ho radioembolization. Its safety is evaluated further in clinical practice.

References

1. Seidensticker R, Denecke T, Kraus P, Seidensticker M, Mohnike K, Fahlke J, et al. Matched-Pair Comparison of Radioembolization Plus Best Supportive Care Versus Best Supportive Care Alone for Chemotherapy Refractory Liver-Dominant Colorectal Metastases. Cardiovasc Intervent Radiol. 2011;35(5):1066–73.
2. Bilbao JI, de Martino A, de Luis E, Diaz-Dorronsoro L, Alonso-Burgos A, Martinez de la Cuesta A, et al. Biocompatibility, inflammatory response, and recannalization characteristics of nonradioactive resin microspheres: histological findings. Cardiovasc Intervent Radiol. 2009;32(4):727–36.
3. Ogawa F, Mino-Kenudson M, Shimizu M, Ligato S, Lauwers GY. Gastroduodenitis associated with yttrium 90-microsphere selective internal radiation: an iatrogenic complication in need of recognition. Arch Pathol Lab Med. 2008;132(11):1734–8.
4. Murthy R, Brown DB, Salem R, Meranze SG, Coldwell DM, Krishnan S, et al. Gastrointestinal complications associated with hepatic arterial Yttrium-90 microsphere therapy. J Vasc Interv Radiol. 2007;18(4):553–61.
5. Heusner TA, Hamami ME, Ertle J, Hahn S, Poeppel T, Hilgard P, et al. Angiography-based C-arm CT for the assessment of extrahepatic shunting before radioembolization. ROFO. 2010;182(7):603–8.
6. Lau WY, Leung TWT, Ho S, Chan M, Leung NWY, Lin J, et al. Diagnostic pharmaco-scintigraphy with hepatic intraarterial technetium-99m macroaggregated albumin in the determination of tumour to non-tumour uptake ratio in hepatocellular carcinoma. Br J Radiol. 1994;67(794):136–9.
7. Smits ML, Nijsen JF, van den Bosch MA, Lam MG, Vente MA, Mali WP, et al. Holmium-166 radioembolisation in patients with unresectable, chemorefractory liver metastases (HEPAR trial): a phase 1, dose-escalation study. Lancet Oncol. 2012;13(10):1025-34.
8. Elschot M, Nijsen JFW, Lam MGEH, Smits MLJ, Prince JF, Viergever M a, et al. (99m)Tc-MAA overestimates the absorbed dose to the lungs in radioembolization: a quantitative evaluation in patients treated with (166)Ho-microspheres. Eur J Nucl Med Mol Imaging. 2014;41(10):1965–75.
9. Boellaard R, Krak NC, Hoekstra OS, Lammertsma A a. Effects of noise, image resolution, and ROI definition on the accuracy of standard uptake values: a simulation study. J Nucl Med. 2004;45:1519–27.
10. Kennedy A, Nag S, Salem R, Murthy R, McEwan AJ, Nutting C, et al. Recommendations for radioembolization of hepatic malignancies using yttrium-90 microsphere brachytherapy: a consensus panel report from the radioembolization brachytherapy oncology consortium. Int J Radiat Oncol Biol Phys. 2007;68(1):13–23.
11. Bol GH, Kotte ANTJ, van der Heide UA, Lagendijk JJW. Simultaneous multi-modality ROI delineation in clinical practice. Comput Methods Programs Biomed. 2009;96(2):133–40.
12. Sabet A, Ahmadzadehfar H, Muckle M, Haslerud T, Wilhelm K, Biersack H-J, et al. Significance of oral administration of sodium perchlorate in planning liver-directed radioembolization. J Nucl Med. 2011;52(7):1063–7.
13. Vente M a D, Nijsen JFW, de Wit TC, Seppenwoolde JH, Krijger GC, Seevinck PR, et al. Clinical effects of transcatheter hepatic arterial embolization with holmium-166 poly(L-lactic acid) microspheres in healthy pigs. Eur J Nucl Med Mol Imaging. 2008;35(7):1259–71.
14. Bethesda MD. Internation Commission on Radiation Units and Measurements (ICRU). Tissue Substitutes in Radiation Dosimetry and Measurements. ICRU report 44. 1989.
15. Bult W, Kroeze SGC, Elschot M, Seevinck PR, Beekman FJ, de Jong HW a M, et al. Intratumoral administration of holmium-166 acetylacetonate microspheres: antitumor efficacy and feasibility of multimodality imaging in renal cancer. PloS One. 2013;8(1):e52178.
16. Kao Y-H, Steinberg JD, Tay Y-S, Lim GK, Yan J, Townsend DW, et al. Post-radioembolization yttrium-90 PET/CT - part 1: diagnostic reporting. EJNMMI Res. 2013;3(1):56.
17. Kao Y-H, Steinberg JD, Tay Y-S, Lim GK, Yan J, Townsend DW, et al. Post-radioembolization yttrium-90 PET/CT - part 2: dose-response and tumor predictive dosimetry for resin microspheres. EJNMMI Res. 2013;3(1):57.
18. R: A language and environment for statistical computing [Internet]. Vienna, Austria: R Foundation for Statistical Computing; Available from: http://www.r-project.org
19. Agresti A, Coull B a. Approximate Is Better than "Exact" for Interval Estimation of Binomial Proportions. Am Stat. 1998;52(2):119–26.

20. Gates V, Salem R. Reply to "hepatic radioembolization as a true single-session treatment." J Vasc Interv Radiol. 2014;25(7):1144–6.

21. Powerski MJ, Erxleben C, Scheurig-Münkler C, Geisel D, Heimann U, Hamm B, et al. Hepatopulmonary shunting in patients with primary and secondary liver tumors scheduled for radioembolization. Eur J Radiol. 2015;84(2):201–7.

22. Gaba RC, Zivin SP, Dikopf MS, Parvinian A, Casadaban LC, Lu Y, et al. Characteristics of primary and secondary hepatic malignancies associated with hepatopulmonary shunting. Radiology. 2014;271(2):602–12.

23. Elschot M, Nijsen JFW, Dam AJ, de Jong HWAM. Quantitative evaluation of scintillation camera imaging characteristics of isotopes used in liver radioembolization. PloS One. 2011;6(11):e26174.

24. Elschot M, Smits MLJ, Nijsen JFW, Lam MGEH, Zonnenberg B a., van den Bosch M a. a. J, et al. Quantitative Monte Carlo-based holmium-166 SPECT reconstruction. Med Phys. 2013;40(11):112502.

25. de Wit TC, Xiao J, Nijsen JFW, van het Schip FD, Staelens SG, van Rijk PP, et al. Hybrid scatter correction applied to quantitative holmium-166 SPECT. Phys Med Biol. 2006;51(19):4773–87.

26. Mumper RJ, Ryo UY, Jay M. Neutron-activated holmium-166-poly (L-lactic acid) microspheres: a potential agent for the internal radiation therapy of hepatic tumors. J Nucl Med. 1991;32(11):2139–43.

27. van de Maat GH, Seevinck PR, Elschot M, Smits MLJ, de Leeuw H, van Het Schip AD, et al. MRI-based biodistribution assessment of holmium-166 poly(L-lactic acid) microspheres after radioembolisation. Eur Radiol. 2013;3(23):827–35.

28. Seevinck PR, Seppenwoolde J-H, de Wit TC, Nijsen JFW, Beekman FJ, van Het Schip AD, et al. Factors affecting the sensitivity and detection limits of MRI, CT, and SPECT for multimodal diagnostic and therapeutic agents. Anticancer Agents Med Chem. 2007;7(3):317–34.

29. Nijsen JFW, Seppenwoolde J-H, Havenith T, Bos C, Bakker CJG, van het Schip AD. Liver tumors: MR imaging of radioactive holmium microspheres–phantom and rabbit study. Radiology. 2004;231(2):491–9.

30. Kavanagh BD, Pan CC, Dawson L a., Das SK, Li XA, Haken RK Ten, et al. Radiation Dose-Volume Effects in the Stomach and Small Bowel. Int J Radiat Oncol Biol Phys. 2010;76(3 SUPPL.):101–7.

31. Streitparth F, Pech M, Böhmig M, Ruehl R, Peters N, Wieners G, et al. In vivo assessment of the gastric mucosal tolerance dose after single fraction, small volume irradiation of liver malignancies by computed tomography-guided, high-dose-rate brachytherapy. Int J Radiat Oncol Biol Phys. 2006;65(5):1479–86.

32. Lam MGEH, Banerjee S, Louie JD, Abdelmaksoud MHK, Iagaru AH, Ennen RE, et al. Root cause analysis of gastroduodenal ulceration after yttrium-90 radioembolization. Cardiovasc Intervent Radiol. 2013;36(6):1536–47.

33. Dezarn W a., Cessna JT, DeWerd L a., Feng W, Gates VL, Halama J, et al. Recommendations of the American Association of Physicists in Medicine on dosimetry, imaging, and quality assurance procedures for 90Y microsphere brachytherapy in the treatment of hepatic malignancies. Med Phys. 2011;38(8):4824.

34. van den Hoven AF, van Leeuwen MS, Lam MGEH, van den Bosch M a a J. Hepatic Arterial Configuration in Relation to the Segmental Anatomy of the Liver; Observations on MDCT and DSA Relevant to Radioembolization Treatment. Cardiovasc Intervent Radiol. 2015;38(1):100-11.

Supplemental Table 1

Case number	Second deposition	Sex	Age	Tumor	Arteries coil-embolized	Injection positions (#)	Injection positions (location)	C-arm CT used	Treated with radioembolization after correction	Volume of extrahepatic deposition (mL)	Activity in extrahepatic deposition (%)	Absorbed dose of extrahepatic deposition (Gy)
1	No	M	77	Colorectal carcinoma	GDA	1	PHA	No	Yes	3.1	8.7%	112.1
2	No	F	80	Hepatocellular carcinoma	GDA	2	RHA and LHA	Yes	No	3.0	0.7%	9.8
3	Yes	F	80	Hepatocellular carcinoma	GDA	2	RHA and LHA	Yes	No	4.3	3.0%	27.2
4	No	M	61	Colorectal carcinoma	-	1	PHA	No	Yes	6.0	0.1%	0.9
5	No	F	55	Colorectal carcinoma	GDA, RGA	1	PHA	No	No	7.7	1.8%	9.0
6	No	M	68	Ocular melanoma	-	1	RHA	No	No	3.4	0.8%	8.9
7	No	M	61	Colorectal carcinoma	GDA	2	CHA and rLHA	Yes	Yes	11.5	0.4%	1.5
8	No	M	65	Colorectal carcinoma	GDA, RGA	1	CHA	Yes	Yes	6.7	0.2%	1.2
9	No	M	75	Hepatocellular carcinoma	-	1	rLHA	No	No	14.6	1.9%	5.1
10	No	M	65	Colorectal carcinoma	GDA	1	PHA	No	No	32.3	2.1%	2.6
11	No	M	62	Colorectal carcinoma	-	1	PHA	No	Yes	27.4	17.0%	24.6
12	No	M	57	Cholangio carcinoma	GDA, RGA	2	RHA and LHA	No	No	4.3	1.3%	11.7
13	No	M	66	Colorectal carcinoma	GDA	2	RHA and LHA	No	Yes	6.9	1.6%	9.1
14	No	F	73	Colorectal carcinoma	GDA, RGA	3	rRHA and LHA (2x)	No	Yes	15.2	1.7%	4.4
15	No	M	69	Colorectal carcinoma	GDA, RGA	1	PHA	No	Yes	7.0	2.0%	11.1
16	No	M	55	Hepatocellular carcinoma	GDA, RGA	2	RHA and LHA	Yes	No	3.7	0.6%	6.2
17	No	F	66	Cholangio carcinoma	GDA, RGA	1	CHA	No	No	4.8	1.2%	9.8

Supplemental Table 1 *Continued*

Case number	Second deposition	Sex	Age	Tumor	Arteries coil-embolized	Injection positions (#)	Injection positions (location)	C-arm CT used	Treated with radioembolization after correction	Volume of extrahepatic deposition (mL)	Activity in extrahepatic deposition (%)	Absorbed dose of extrahepatic deposition (Gy)
18	No	M	71	Colorectal carcinoma	GDA, RGA	1	PHA	No	Yes	10.1	1.4%	5.5
19	No	M	80	Colorectal carcinoma	GDA, RGA	1	CHA	No	No	13.0	0.6%	1.7
20	No	M	67	Colorectal carcinoma	GDA, RGA	2	RHA and LHA	No	Yes	2.1	19.5%	373.8
21	No	F	73	Colorectal carcinoma	GDA, duodenal branch	1	PHA	No	No	18.1	1.9%	4.1
22	No	M	54	Papil carcinoma	-	1	PHA	No	No	1.1	0.6%	20.2
23	No	M	80	Colorectal carcinoma	GDA, RGA	2	RHA and LHA	No	No	6.0	0.9%	5.8
24	No	M	75	Cholangio carcinoma	GDA	2	rRHA and rLHA	No	No	41.3	5.1%	4.9
25	Yes	M	75	Cholangio carcinoma	GDA	2	rRHA and rLHA	No	No	11.5	1.1%	3.9
26	No	M	66	Neuroendocrine tumor	GDA, RGA	2	rRHA and CHA	No	Yes	7.9	0.3%	1.6
27	No	M	75	Colorectal carcinoma	GDA, pancreatic artery	2	RHA and LHA	Yes	Yes	6.7	3.1%	18.6
28	No	M	58	Colorectal carcinoma	GDA, RGA	1	PHA	No	Yes	3.7	0.3%	3.1
29	No	M	64	Colorectal carcinoma	GDA, RGA	2	RHA and rLHA	Yes	Yes	6.3	0.2%	1.3
30	No	M	68	Gastric carcinoma	-	2	RHA and LHA	No	No	17.1	2.2%	5.2
31	No	M	75	Ocular melanoma	GDA, RGA	1	PHA	No	Yes	6.7	1.1%	6.3
32	No	M	81	Adenocarcinoma of unknown primary	GDA, RGA	1	CHA	No	Yes	7.7	4.7%	24.0

Supplemental Table 1 *Continued*

Case number	Second deposition	Sex	Age	Tumor	Arteries coil-embolized	Injection positions (#)	Injection positions (location)	C-arm CT used	Treated with radioembolization after correction	Volume of extrahepatic deposition (mL)	Activity in extrahepatic deposition (%)	Absorbed dose of extrahepatic deposition (Gy)
33	No	F	36	Colorectal carcinoma	GDA, cystic artery	2	rRHA and LHA	No	Yes	5.0	0.8%	6.7
34	No	F	61	Breast carcinoma	GDA, RGA	2	RHA and LHA	No	No	13.7	1.7%	5.0

GDA, gastroduodenal artery. RGA, right gastric artery. CHA, common hepatic artery. PHA, proper hepatic artery. RHA, right hepatic artery. LHA, left hepatic artery. r, replaced.

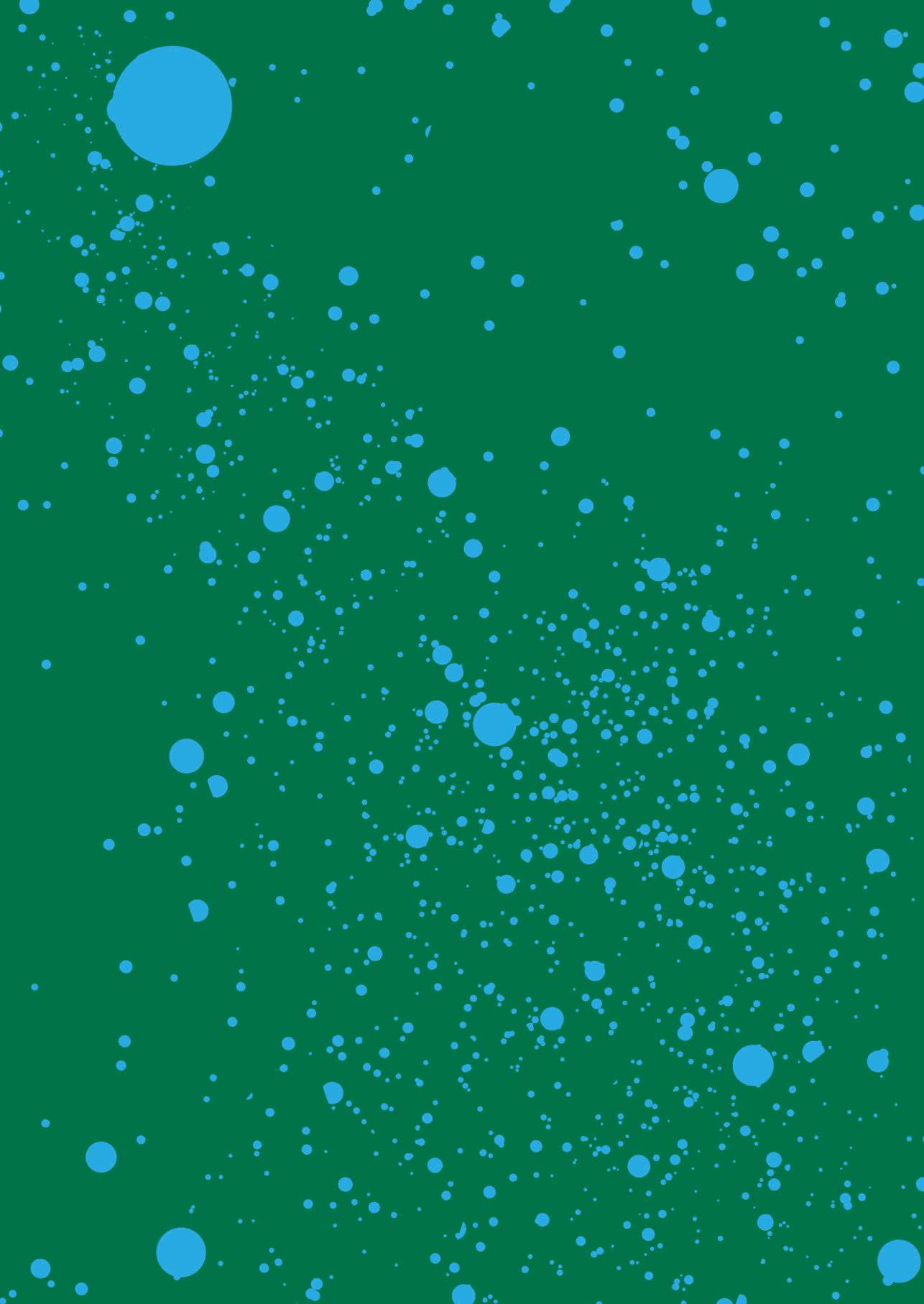

CHAPTER 6

Efficacy of radioembolization with ^{166}Ho microspheres in liver metastases

J.F. Prince
M.A.A.J. van den Bosch
J.F.W. Nijsen
M.L.J. Smits
A.F. van den Hoven
F.J. Wessels
R.C.G. Bruijnen
M.N.G.J. Braat
G.C. Krijger
M.G.E.H. Lam
B.A. Zonnenberg

Manuscript in preparation

Abstract

Background

Radioembolization of liver malignancies can be performed with microspheres loaded with either yttrium-90 or holmium-166 (^{166}Ho). ^{166}Ho microspheres have better imaging qualities and are proven safe in a dose-escalation study. The purpose of this study was to investigate their efficacy.

Methods

In this nonrandomized single-arm trial, 56 patients were enrolled with liver metastases refractory to systemic therapy and ineligible for surgical resection. Radioembolization was performed with a dose of 60 Gy to the liver (equal to 3.8 GBq [103 mCi]/kg liver tissue). The primary outcome was tumor response of two target lesions on triphasic liver CT scans, 3 months after therapy using RECIST 1.1 criteria as evaluated by three raters.

Results

After treatment of 38 patients, the target lesions showed disease control in 73% after three months (95% confidence interval [CI], 57 to 85%). The median overall survival was 15.3 months (95% CI, 9.1 to ∞ months). Grade 3 or 4 toxic events (according CTC v4.03 criteria) after treatment included abdominal pain (in 18% of patients), nausea (9%), ascites (3%), gastric stenosis (3%), liver abscesses (3%), paroxysmal atrial tachycardia (3%), radioembolization induced liver disease (3%), thoracic pain (3%), upper gastrointestinal hemorrhage (3%), and vomiting (3%). Laboratory examination after treatment showed grade 3 or 4 toxicities in alkaline phosphatase (70%), gammaGT (78%), lymphocytes (11%), and ALAT (4%).

Conclusions

Radioembolization with ^{166}Ho microspheres induced a tumor response with an acceptable toxicity profile in patients with liver metastases.

Introduction

Radioembolization can delay the progression of colorectal liver metastases. During radioembolization, radioactive microspheres are injected into the liver's arteries to radiate and embolize metastases. Its effects on patients' overall survival is not yet determined, although several retrospective studies and randomized controlled trials have been published.[1–4] To increase efficacy and reduce toxicity, physicians started treating liver lobes or segments instead of the whole liver.[5,6] Also, the administered doses have been tailored per artery and intensified.[6,7] The evaluation of these adapted treatments requires more accurate imaging than the currently used radioactive isotope, yttrium-90 (^{90}Y), can provide.

To improve upon this, a microsphere with holmium-166 (^{166}Ho) has been developed.[8] ^{90}Y can be quantified on PET/CT, but only after a full treatment dose.[9] ^{166}Ho differs from ^{90}Y in two imaging aspects. First, its paramagnetic properties allow visualization on MR imaging and thus imaging in real-time, or later when the microspheres are no longer radioactive.[10,11] Second, the emission of gamma rays allows visualization on SPECT/CT with higher sensitivity, which becomes apparent when treating selectively (with lower activities).[12] It has already been shown that a small scout dose improves dosimetry for the lungs, something for which 40% of patients have their treatment adapted.[13,14] Furthermore, it is expected that a scout dose can better predict the intrahepatic distribution and further aid in the individualization of treatment. It is unknown if these microspheres have the same efficacy as microspheres loaded with ^{90}Y.

A previous dose-escalation trial investigated the first human use of ^{166}Ho microspheres and showed that administration with an aimed liver dose of up to 60 Gy is safe.[15] Even though patients were treated with different doses in that study, 9 patients showed partial response or stable disease of their target lesions. In this study, the efficacy of ^{166}Ho radioembolization was investigated.

Methods

Study Design and Treatment

The Holmium Embolization Particles for Arterial Radiotherapy II (HEPAR II) trial was a single-arm, single-center trial for patients with unresectable liver metastasis of any primary origin who were unable to undergo systemic treatment. The study was conducted in accordance with the Declaration of Helsinki. The study protocol was approved by the local research ethics committee. All patients provided written informed consent. Every 3 months, both an independent data monitoring committee and the Dutch Health Care Inspectorate (IGZ) independently assessed the side effects that were observed in this study.

Patients received a single treatment session of radioembolization with ^{166}Ho microspheres. Laboratory examinations were performed every 3 weeks up to 3 months, from which imaging was performed every 3 months. Patients were followed until progression of their liver metastasis was found on imaging, up to a maximum of 12 months.

The primary outcome was the response rate of target lesions after 3 months according to Response Evaluation Criteria in Solid Tumors (RECIST), version 1.1, on contrast-enhanced CT.[16]many investigators, cooperative groups, industry and government authorities have adopted these criteria in the assessment of treatment outcomes. However, a number of questions and issues have arisen which have led to the development of a revised RECIST guideline (version 1.1 Secondary outcomes included the overall tumor response, response on ^{18}F-FDG-PET/CT, tumor markers, overall and progression-free survival, toxicity, quality of life, and quantification of ^{166}Ho on SPECT/CT, MRI, and PET/CT.

Academic investigators designed the study, collected the data, and analyzed them. All data were verified by an independent monitor. The trial was sponsored by a grant from the Dutch Cancer Society (KWF Kankerbestrijding), which had no other role in the study. The trial was registered in ClinicalTrials.gov (NCT01612325).

Patients

Patients were eligible if diagnosed with metastatic liver lesions and limited disease outside the liver, had a life expectancy of >3 months, had measureable disease

on CT (RECIST 1.1), had adequate liver, renal and bone marrow function, and had a WHO performance score of ≤2. They were excluded if they received prior radiotherapy to the liver, chemotherapy or major surgery within the previous 4 weeks. Also if they had unresolved toxicity of prior treatment greater than grade 2, had an increased chance of liver toxicity, suffered from psychiatric disorders, did not use an acceptable method of contraception or could not undergo contrast injection or MR imaging. Patients were recruited from the multidisciplinary tumor board in our hospital or from referring oncologists.

Treatment

Treatment was performed as described earlier.[15] A preparatory angiography was performed in which extra-hepatic vessels were embolized and ^{99m}Tc-MAA (150 MBq, 0.8 mg, Technescan LyoMAA®; Mallinckrodt Medical B.V., Petten, the Netherlands) was administered to assess the safety and the intra-hepatic distribution of subsequent administrations. ^{166}Ho microspheres were administered as a scout dose (250 MBq) and treatment dose, with imaging using SPECT and MRI after both injections. The total dose of radioactivity was adjusted to the targeted liver mass measured on CT (aimed absorbed dose, 60 Gy or 3.8 GBq/kg liver tissue) and was contained in a fixed amount of microspheres (600 mg).

Assessments

The primary outcome, the response of (up to 2) target lesions per RECIST 1.1 after 3 months, was scored independently by three raters (FW, RB, MB). They were asked to identify target lesions on an anonymized and randomized set of baseline scans. These lesions were propagated to the follow up scans by one of the investigators (JP) after which all scans (baseline and follow up) were anonymized and randomized and the raters measured the longest diameters. To complete the RECIST measurements for the secondary outcome, they assessed the progression of non-target lesions or the presence of new lesions as in clinical practice (unblinded). The outcome was determined by the majority (≥2) of outcomes or imputed as 'not evaluable' (which was imputed as progression in the primary analysis). Disease control was defined as any category other than progressive disease.

Response on ^{18}FDG-PET/CT was determined by a single rater (JP) using the PERCIST 1.0 criteria.[17] Relevant tumor markers were only collected in follow up if baseline markers were elevated and represented as a percentage of baseline.

Analyses for survival and disease progression were performed on October 7, 2015. Both were performed with the Kaplan-Meier method. Time was measured from administration of ^{166}Ho microspheres. Adverse events were assessed every visit and graded according to the National Cancer Institute Common Terminology Criteria for Adverse Events (CTCAE), version 4.03.[18] The quality of life was assessed using the European Organisation for Research and Treatment of Cancer core (QLQ-C30) and liver metastasis questionnaires (QLQ-LMC21) at baseline, 6 weeks and every 3 months. After 11 treated patients, a questionnaire after 1 week was added to better reflect patients' transient symptoms. Quantification of the amount of ^{166}Ho microspheres on SPECT/CT was performed by a single rater who segmented the liver on low-dose CT and added a margin for scatter (2, 3, or 4 cm in all directions, depending on the amount of scatter). Quantification was performed on in-house developed Monte Carlo reconstructions (UMCS) and using in-house developed software (Volumetool).[12,19] MR quantification was based on the impact on relaxation rate of the T_2 signal on multi-gradient echo sequences and performed on in house developed software similar to earlier reports (Quirem Medical, The Netherlands).[10]

Sequential design and stopping criteria

Stopping boundaries were defined beforehand to ensure a power of 90% and a type I error of 4.5% (one-sided) if the true proportion of patients with disease control was 0.4 (instead of 0.2). We aimed to include 30 to 48 patients with interim analyses after 30, 36, and 42 patients became evaluable for the primary outcome. The stopping boundaries after analysis of the first 30 patients were 5 (for futility) and 11 (for efficacy). The criteria for efficacy were surpassed at the first interim analysis: 24 of the first 30 showed disease control of their target lesions.

Statistical analysis

Descriptive statistics were calculated as medians and the range, means and SDs, or percentages and frequencies. Outcomes analyses were performed on an imputed case analysis, in which patients who were not evaluable or available were imputed as having progressive disease. Confidence intervals were displayed as the Adjusted Wald, not corrected for interim analysis because of current controversy.[20] Statistical tests were performed with a two-sided α of 0.05. For testing of laboratory values the Bonferroni correction was used. Analyses were performed using R statistical software (R version 3.2.1 for Windows).

Results

Patients

From May 2012 until March 2015, 56 patients with various primary tumors were enrolled, 38 of whom received treatment with ^{166}Ho microspheres (Figure 1). Follow up was available up to 3 months for 17 patients, up to 6 months for 11 patients, up to 9 months for 5 patients and up to 12 months for 3 patients. Two patients did not reach the first moment of imaging (3 months) because of recurrence of their primary tumor or rapid progression of disease. One patient informed us after 3 months that she had been using Tamoxifen and was excluded from analysis. Most patients were in adequate physical health (WHO 0, Child Pugh A, Table 1).

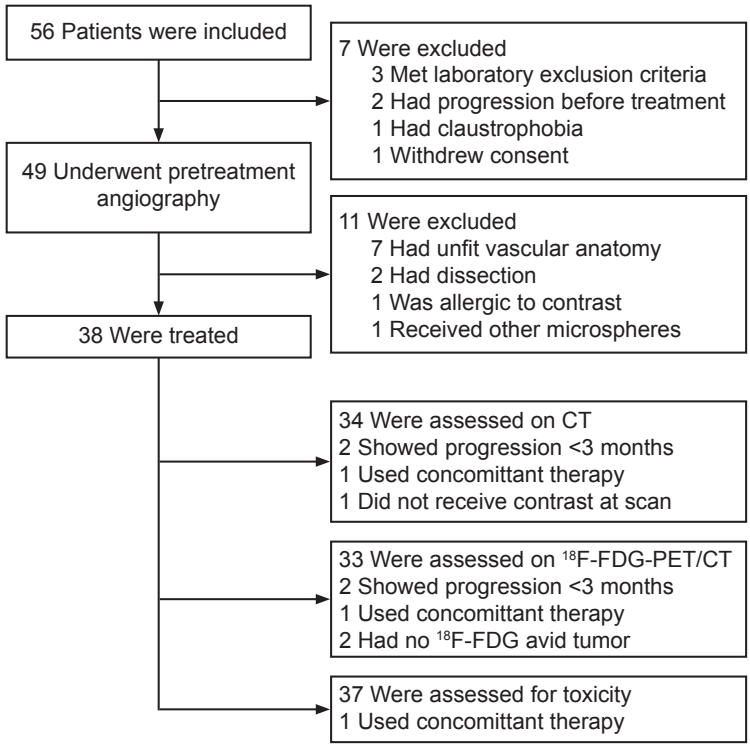

Figure 1 *Flowchart of study*

Table 1. *Baseline characteristics of 38 treated patients*

Characteristic	Value
n	38
Age (years)	
Median	66
range	41-84
Sex – no. (%)	
Male	22 (58%)
Female	16 (42%)
WHO performance status – no. (%)	
0	29 (83%)
1	5 (14%)
2	1 (3%)
Primary malignancy – no. (%)	
Colorectal	23 (61%)
Breast	4 (11%)
Cholangiocarcinoma	4 (11%)
Neuroendocrine tumor	2 (5%)
Uveal melanoma	2 (5%)
Other*	3 (8%)
Time since diagnosis (months)	
Median	28
Range	4-95
Time to metastases – no. (%)	
Synchronous	17 (45%)
Metachronous	21 (55%)
Time since liver metastases (months)	
Median	18
Range	3-92
Chemotherapy (colorectal) – no. (%)	
n	23
Capecitabine	21 (91%)
Oxaliplatin	19 (83%)
Bevacizumab	13 (57%)
Irinotecan	10 (43%)
5-Fluorouracil	7 (30%)
Panitumumab	3 (13%)
Cetuximab	1 (4%)
Dabrafenib	1 (4%)
Child Pugh Score – no. (%)	
A	38 (100%)
Extrahepatic disease – no. (%)	12 (58%)
Elevated tumor marker – no. (%)	15 (65%)†

* *Pancreatic cancer, stomach cancer, and thymoma, † Unknown for 15 patients*

Treatment

Of the 38 patients, 2 were treated in separate treatment sessions for the right and left liver lobe (total, 40 sessions). The scout dose could be fully administered (>90%) in 29/35 patients (83%, median delivery 93%, range, 80 - 98%), because some residue remained in the vial (which was already accounted for because 10% more than the prescribed activity was ordered). The therapy dose could be fully administered in 28/37 patients (76%, median delivery 96%, range, 41 – 99%), because stasis occurred or patients experienced pain. In 38 scout procedures, the median infused radioactivity was 258 MBq (range, 103 – 313) and in 38 treatment procedures, the median infused radioactivity was 5.970 MBq (range, 3.667 – 13.189). In 37 patients, a median of 604 mg (range, 288 – 886) of microspheres were infused.

Efficacy

The target lesions showed disease control in 27/37 patients after 3 months (73%, 95% confidence interval [CI], 57 to 85%, Table 2), in 13/37 (35%) after 6 months, in 4/37 (11%) after 9 months, and in 2/37 (5%) after 12 months. The proportion of agreement between the three raters was 81% for the assessment of progression of target lesions after 3 months. The target lesions of the colorectal cancer patients showed disease control in 16/22 (73%) patients (95% CI, 56 to 90%). The median progression free survival of the target lesions was 6 months (95% CI, 6 to ∞ months). In available case analysis, 27/31 (87%) of patients showed disease control of their target lesions after 3 months. On ^{18}F-FDG-PET/CT, disease control in the liver was achieved in 19/36 (53%) of patients after 3 months (95% CI, 37 to 68%). For colorectal cancer patients, this was achieved in 14/23 (61%) of patients (95% CI, 41 to 78%).

Table 2. *Response 3 months after ^{166}Ho radioembolization*

Category of response	Contrast-enhanced CT			PET/CT*	
	Target lesions	Liver specific	Abdomen	Liver specific	Whole body
Complete response	-	-	-	1 (3%)	-
Partial response	5 (14%)	5 (14%)	5 (14%)	9 (25%)	7 (19%)
Stable disease	22 (59%)	13 (35%)	9 (24%)	9 (25%)	4 (11%)
Progressive disease†	10 (27%)	19 (51%)	23 (62%)	17 (47%)	25 (69%)
Total	37 (100%)	37 (100%)	37 (100%)	36 (100%)	36 (100%)

*Imputed case analysis. Number of patients (percentage of total). * The PERCIST 1.0 reproducibility criteria were met in 47% (42/89) of PET/CT scans, for more details see Supplemental Table S1, † Not evaluable and/or missing patients imputed as progressive disease*

The median overall survival was 15.3 months (95% CI, 9.1 to ∞ months, Figure 2A). The overall survival analysis was based on 24 deaths (63%) after a median follow up of 12.1 months (range 2.8 to 35.5 months). For colorectal cancer patients, the median overall survival was 14.4 months (95% CI, 8.3 - ∞ months, Figure 2B). No significant difference in median survival was seen if patients showed disease control in their target lesions on CT (15 vs 8 months, p = 0.11) or in their liver on ^{18}F-FDG-PET (16 vs 7 months, p = 0.21).

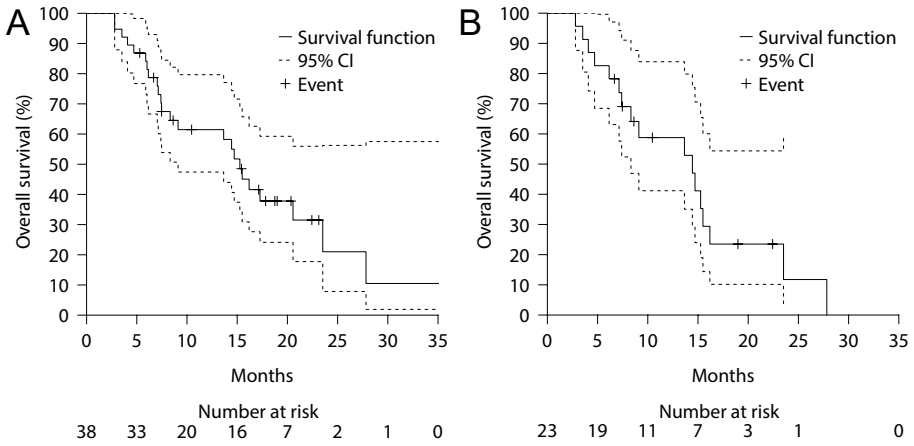

Figure 2 *The Kaplan-Meier estimate of median overall survival was 15.3 months (95% CI, 9.1 to ∞ months) for all patients (A) and 14.4 months (95% CI, 8.3 - ∞ months) for colorectal cancer patients (B)*

Toxicity

The most common adverse events during follow up were manageable gastrointestinal disorders which are part of the post radioembolization syndrome (Table 3). At any time after treatment, nausea of any grade occurred in 79% of patients, abdominal and back pain in 79%, vomiting in 68%, fatigue in 66%, and anorexia in 26%. Severe toxicity (grade 3 or 4) included mostly abdominal pain (18%) and nausea (8%). In addition, one patient developed liver abscesses which were treated with percutaneous drainage and i.v. antibiotics. Because that patient could have been predisposed by the prior pylorus-preserving pancreaticoduodenectomy, it was added to the list of exclusion criteria. Another patient was hospitalized 9 weeks after radioembolization for a duodenal ulceration, which was successfully treated with local endoscopic coagulation and adrenaline.

Table 3. *Adverse events with incidence of >10% or grade 3 or 4 regardless of relation with ^{166}Ho radioembolization*

Adverse Event	Any time during follow up	≤1 week after treatment	Grade 3 or 4
Nausea	79% (30)	71% (27)	8% (3)
Abdominal Pain	71% (27)	68% (26)	18% (7)
Vomiting	68% (26)	58% (22)	3% (1)
Fatigue	66% (25)	26% (10)	3% (1)
Back Pain	39% (15)	24% (9)	0
Constipation	29% (11)	5% (2)	0
Anorexia	26% (10)	13% (5)	0
Fever	18% (7)	11% (4)	0
Allergic reaction	16% (6)	13% (5)	0
Dizziness	16% (6)	11% (4)	0
Edema limbs	16% (6)	0	0
Shoulder pain	13% (5)	5% (2)	0
Arthralgia	13% (5)	3% (1)	0
Hematoma	11% (4)	5% (2)	0
Dysgeusia	11% (4)	3% (1)	0
Chills	11% (4)	0	0
Dyspnea	11% (4)	0	0
Ascites	8% (3)	0	3% (1)
Thoracic pain	3% (1)	3% (1)	3% (1)
Gastric stenosis	3% (1)	0	3% (1)
Liver abscesses	3% (1)	0	3% (1)
Paroxysmal atrial tachycardia	3% (1)	0	3% (1)
Radioembolization induced liver disease	3% (1)	0	3% (1)
Upper gastrointestinal hemorrhage	3% (1)	0	3% (1)

Hematologic laboratory tests were first performed 3 weeks after treatment and showed a significant difference in hemoglobin (decrease), mean corpuscular hemoglobin concentration (decrease), leukocytes (decrease), lymphocytes (decrease) and monocytes (increase, Table 4). The decrease in lymphocytes remained significant after 3 months, at which time the platelet count had also significantly decreased while the thrombin time had significantly increased. These changes could have been caused by splenomegaly because of portal hypertension after treatment; spleen size increased from a mean of 256 mL to 359 mL ($p < 0.001$) after 3 months. Nonhematologic laboratory tests that differed after 3 weeks were alkaline phosphatase (increased), gamma-glutamyl transpeptidase (increased), alanine aminotransferase (increased), and albumin (decreased). All remained changed after 3 months, at which time both the bilirubin and aspartate aminotransferase level were also increased.

Table 4 *Laboratory toxicity for values with significant difference from baseline*

	Baseline	3 weeks	3 months
		median (range)	
Bilirubin (μmol/L)	8 (5 - 23)	8.5 (5 - 19)	13 (6 - 31)*
ALP (U/L)	144 (55 - 418)	265.5 (130 - 828)*	324 (150 - 1000)*
GGT (U/L)	117.5 (17 - 1361)	255 (89 - 895)*	344 (140 - 1624)*
AST (U/L)	42 (17 - 135)	50.5 (23 - 396)	66 (38 - 276)*
ALT (U/L)	28 (11 - 90)	40.5 (13 - 445)*	56 (15 - 304)*
Albumin (g/L)	40.6 (32.3 - 46.9)	36.25 (28.5 - 42.4)*	37.1 (29 - 44.9)*
Hemoglobin (mmol/L)	8.6 (6.3 - 10.7)	8.2 (5.3 - 10.2)*	8.95 (5.8 - 10.7)
MCHC (mmol/L)	20.9 (19.9 - 22)	20.6 (19.3 - 21.9)*	20.7 (19.6 - 22.9)
Leukocytes ($x10^9$/L)	7.75 (4.5 - 12.6)	6.45 (3.9 - 12.7)*	6.9 (4 - 12.2)
Lymphocytes ($x10^9$/L)	1.45 (0.79 - 3.18)	0.79 (0.43 - 1.52)*	1.045 (0.25 - 2.32)*
Monocytes ($x10^9$/L)	0.525 (0.02 - 1.2)	0.79 (0.41 - 1.38)*	0.59 (0.02 - 1.14)
Platelet count ($x10^9$/L)	226.5 (143 - 456)	227 (98 - 491)	190 (107 - 308)*
TT (sec)	16.5 (14.2 - 22.8)	NA	17.8 (15.3 - 96.5)*

ALP: alkaline phosphatase, GGT: gamma-glutamyl transferase, AST: aspartate aminotransferase, ALT: alanine aminotransferase, MCHC: mean corpuscular hemoglobin concentration, TT: thrombin time
** Significant at $p < 0.00088$ (Bonferroni correction for 57 hypotheses)*
For more data see Supplemental Table S2

Three deaths occurred shortly after treatment. The first was a patient who returned with vomiting, anorexia and weight loss. A gastroscopy showed recurrence of the primary malignancy, gastric cancer. An expendable gastric stent was placed for palliation. The patient died 2.8 months after treatment. The second death was of a patient who developed liver failure accompanied by ascites, dyspnea and jaundice (bilirubin 266 μmol/L, albumin 29.3 g/L). Diagnostic studies (including ^{18}F-FDG-PET/CT) showed severe disease progression from which he died 2.8 months after treatment. Lastly, the third patient died 4.1 months after treatment following a collapse at home. His liver functions had been declining (bilirubin 38 μmol/L, albumin 27.2 g/L), and after developing ascites, he had undergone several paracenteses. A combination of radioembolization induced liver disease and disease progression was suspected.

^{166}Ho radioembolization decreased the global health status temporary from 83 (IQR 67 – 83) at baseline to 42 (25 – 71) after 1 week. It recovered after 6 weeks (67 [58 – 83]). The most affected functional scales were physical, role, and social functioning (Figure 3A). The worst symptoms were fatigue, eating, pain, and emotional problems, all of which peaked after 1 week (Figure 3B). All scores can be found in Supplemental Table S3.

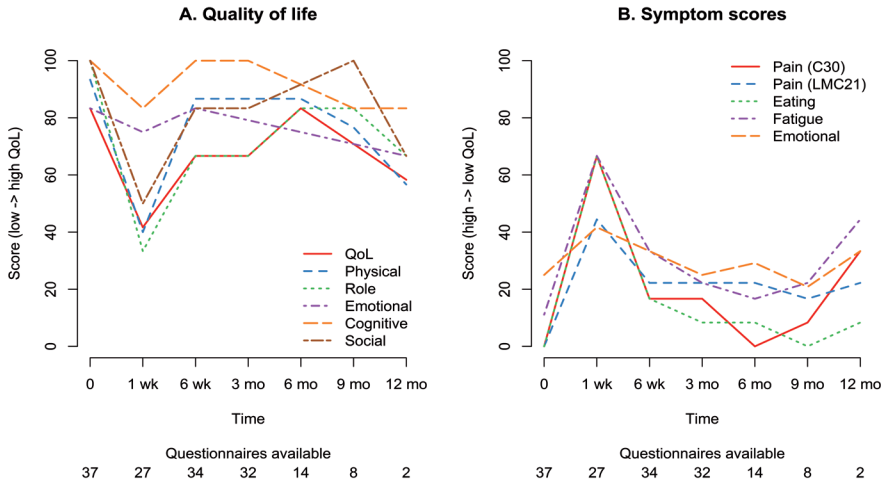

Figure 3 *Quality of life (QoL). Values are median per time point. A higher score in A indicates a better quality of life. A higher score in B indicates a worse quality of life. Only symptoms with a high score are displayed in B, for all scores see Supplemental Table S3.*

Imaging

Of 40 treatments in 38 patients, the SPECT/CT was available after treatment in 38 cases. A mean of 105.1±6.3% of all ^{166}Ho activity was recovered in the liver (example in Figure 4A, B). The scout dose of ^{166}Ho microspheres could be detected with a mean recovery of 102.2±5.7% of the injected activity in 38 patients. A median amount of 0.02% (range, 0 – 0.8%) of the administered ^{166}Ho was present in the lungs after treatment. The lung shunt of both the scout dose of ^{99m}Tc-MAA and ^{166}Ho microspheres did not correlate with the lung shunt after treatment (spearman correlation coefficient, 0.07 [p = 0.71] and 0.26 [p = 0.17]). The median lung shunt was 3.2% (range, 0.01 – 19.3%) after ^{99m}Tc-MAA injection and 0.01% (range, 0 – 0.3%) after a scout dose of ^{166}Ho microspheres. Using MR quantification, a median of 51% (range, 11 – 92%) of all Ho was detected in the livers of 26 patients for which imaging was available (Figure 4C, D). This was partly caused by an inability to calculate the R2*, which could be partly improved by adjustment of the signal threshold. This led to a median detection of 68% of Ho (range, 6 – 99%).

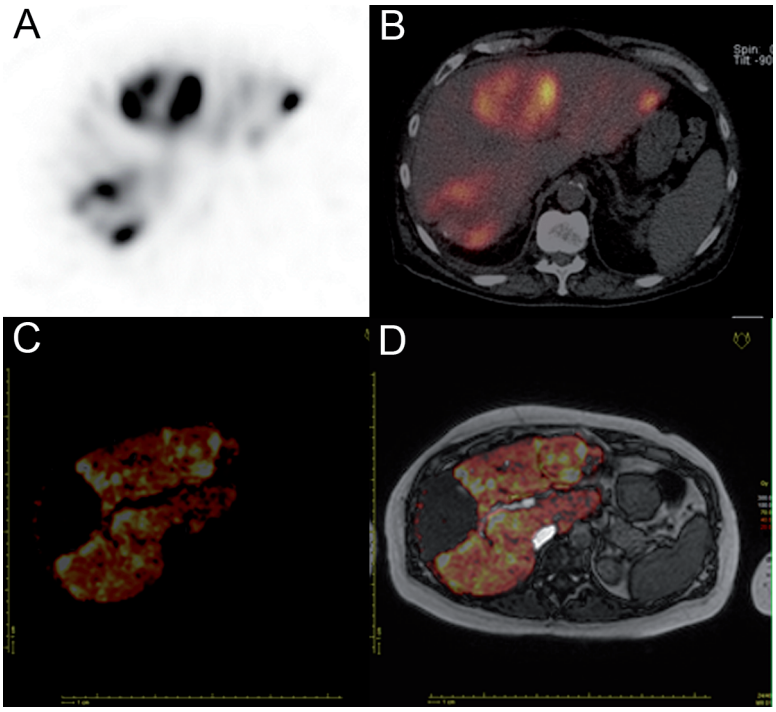

Figure 4 *^{166}Ho microspheres can be seen on SPECT (A), combined with CT (B) or on MR imaging (C) combined with anatomical T2w images (D). Note that AB are not from the same patient as CD.*

Discussion

The aim of this study was to study the efficacy of ^{166}Ho radioembolization in patients with liver metastasis of any primary origin for whom no other treatments were available. The target lesions of 73% of patients (95% CI, 57 to 85%) showed disease control after 3 months, which, in this cohort of patients with chemorefractory disease and no surgical treatment options, is a clear indicator of efficacy.

To avoid any bias, three radiologist independently evaluated the tumor response using RECIST guidelines on anonymized and randomized images. The procedure was set up akin to an independent central review, which can introduce other biases and often decreases response rates.[21] There was sufficient agreement (81%) regarding the progression of target lesions. The ^{18}F-FDG-PET images provide additional proof of efficacy, because the same percentage of disease control in the

liver is seen (49% for CT and 53% for PET). However, not all images were deemed reproducible by PERCIST. Even so, when only reproducible images were taken into account, the same percentage of disease control was seen (42%, Supplemental Table S1).

Radioembolization is commonly performed with ^{90}Y microspheres, which have shown to be an effective treatment for patients with colorectal liver metastasis who have limited treatment options.[3,4] Because ^{166}Ho also emits beta radiation, it was expected ^{166}Ho microspheres would show comparable results. We have shown that ^{166}Ho microspheres are able to stop progression of liver metastasis in a substantial number of patients (49%). A direct comparison between ^{90}Y and ^{166}Ho microspheres from the literature is difficult, most ^{90}Y cohorts are retrospective and prospective studies combined radioembolization with chemotherapy. A prospective study in patients with liver metastases from colorectal cancer (n = 61) showed a rate of partial response and stable disease of 59%, which is comparable to this study (45% for colorectal cancer patients).[22] The amount of extrahepatic disease was higher in our study (58% vs 35%). The median overall survival after radioembolization was longer in this study (14.4 months versus 8.8 months for colorectal patients). The rate of adverse events was comparable. The occurrence of grade 3 or 4 (abdominal) pain was 18% in this study versus 13% in the ^{90}Y study. The rates of nausea (8%), vomiting (3%) and fatigue (3%) were also comparable (1%, 3% and 3%).

Radioembolization with ^{166}Ho microspheres was associated with a low number of adverse events of grade 3 or higher, most of which were transient and manageable: abdominal pain and nausea were most common (18% and 8%). The same trend was seen in the quality of life questionnaires: quality of life decreased 1 week after treatment but recovered after 6 weeks. No data could be found to compare this short time frame with current literature. Most symptoms were resolved after 6 weeks (when most studies report their quality of life score). Only by adding the questionnaire after 1 week could we identify pain, nutrition problems, fatigue, and emotional problems as the most burdensome complaints. We advise any prospective study into radioembolization to add this time point.

The lack of randomization restrains any conclusive statements about efficacy. However, no adequate control group could be formed, because limited

other treatment options were available to these patients who were refractory to chemotherapy and unable to undergo surgery (mostly phase 1 trials with systematic treatment). Alternatively, this trial could have been performed as a non-inferiority trial compared with ^{90}Y microspheres. However, the sample size would have been larger and the 3 years it took to complete this study would have increased, delaying decisions about continuing development.

Because efficacy was found, two new trials were started which both use ^{166}Ho microspheres and its imaging capabilities: the SIM trial (NCT02208804) and the HEPAR PLUS trial (NCT02067988). Because we saw the catheter position is crucial to the agreement of the accordance of the scout and therapy dose, the SIM trial assesses if an anti-reflux catheter improves this agreement. The HEPAR PLUS trial was developed to assess if radioembolization also improves response rates of radiolabeled somatostatin analogues in patients with neuroendocrine tumors.

An important benefit of ^{166}Ho microspheres is the ability to better estimate the lung shunt after radioembolization. Currently, ^{99m}Tc-MAA is used as a scout dose, but ^{166}Ho has been proven to be more reliable in its estimation.[13] Even though beta radiation is emitted, an extrahepatic deposition will probably not lead to a high extrahepatic dose and toxicity.[23] In addition, imaging after a treatment dose can check if an adequate administration occurred. If patients complain of abdominal pain shortly after treatment, it can be used to check for an extrahepatic deposition (the isotope can be imaged 4-6 days after treatment). In future, the scout dose may be used to predict the treatment distribution. The infusion per artery can be adapted accordingly instead of a crude target such as 60 Gy to the liver. This can increase efficacy and reduce toxicity. Also, the paramagnetic properties of holmium allow MR guided radioembolization, or assessing the stability of microspheres after radioactivity has decayed. Last, the dose rate of ^{90}Y (half-life 64h) and ^{166}Ho (27h) probably produces different biologic effects, although details are currently unknown.

In conclusion, radioembolization with ^{166}Ho microspheres was efficacious in patients with metastatic liver malignancies which were refractory to chemotherapy and unable to undergo surgery. Common adverse events such as abdominal pain and nausea were transient and manageable.

Acknowledgements

The authors would like to acknowledge Tjitske Bosma, Remmert de Roos, Hugo de Jong, Bastiaan van Nierop, Rob van Rooij, Gerrit van der Maat and Lenny Verkooijen for their efforts in this trial.

References

1. Gray B, Hazel GV, Hope M, Burton M, Moroz P, Anderson J, et al. Randomised trial of SIR-Spheres® plus chemotherapy vs. chemotherapy alone for treating patients with liver metastases from primary large bowel cancer. Ann Oncol. 2001;12(12):1711–20.
2. Van Hazel G, Blackwell A, Anderson J, Price D, Moroz P, Bower G, et al. Randomised phase 2 trial of SIR-Spheres plus fluorouracil/leucovorin chemotherapy versus fluorouracil/leucovorin chemotherapy alone in advanced colorectal cancer. J Surg Oncol. 2004;88(2):78–85.
3. Hendlisz A, Eynde MV den, Peeters M, Maleux G, Lambert B, Vannoote J, et al. Phase III Trial Comparing Protracted Intravenous Fluorouracil Infusion Alone or With Yttrium-90 Resin Microspheres Radioembolization for Liver-Limited Metastatic Colorectal Cancer Refractory to Standard Chemotherapy. J Clin Oncol. 2010;28(23):3687–94.
4. Seidensticker R, Denecke T, Kraus P, Seidensticker M, Mohnike K, Fahlke J, et al. Matched-Pair Comparison of Radioembolization Plus Best Supportive Care Versus Best Supportive Care Alone for Chemotherapy Refractory Liver-Dominant Colorectal Metastases. Cardiovasc Intervent Radiol. 2011;35(5):1066–73.
5. Riaz A, Gates VL, Atassi B, Lewandowski RJ, Mulcahy MF, Ryu RK, et al. Radiation Segmentectomy: A Novel Approach to Increase Safety and Efficacy of Radioembolization. Int J Radiat Oncol. 2011;79(1):163–71.
6. Kao YH, Hock Tan AE, Burgmans MC, Irani FG, Khoo LS, Gong Lo RH, et al. Image-guided personalized predictive dosimetry by artery-specific SPECT/CT partition modeling for safe and effective 90Y radioembolization. J Nucl Med. 2012;53(4):559–66.
7. Garin E, Rolland Y, Edeline J, Icard N, Lenoir L, Laffont S, et al. Personalized Dosimetry with Intensification Using 90Y-Loaded Glass Microsphere Radioembolization Induces Prolonged Overall Survival in Hepatocellular Carcinoma Patients with Portal Vein Thrombosis. J Nucl Med. 2015;56(3):339–46.
8. Mumper RJ, Ryo UY, Jay M. Neutron-activated holmium-166-poly (L-lactic acid) microspheres: a potential agent for the internal radiation therapy of hepatic tumors. J Nucl Med. 1991;32(11):2139–43.
9. Gates VL, Esmail AAH, Marshall K, Spies S, Salem R. Internal pair production of 90Y permits hepatic localization of microspheres using routine PET: proof of concept. J Nucl Med. 2011;52:72–6.
10. van de Maat GH, Seevinck PR, Elschot M, Smits MLJ, de Leeuw H, van Het Schip AD, et al. MRI-based biodistribution assessment of holmium-166 poly(L-lactic acid) microspheres after radioembolisation. Eur Radiol. 2013;3(23):827–35.
11. Nijsen JFW, Seppenwoolde J-H, Havenith T, Bos C, Bakker CJG, van het Schip AD. Liver tumors: MR imaging of radioactive holmium microspheres–phantom and rabbit study. Radiology. 2004;231(2):491–9.
12. Elschot M, Smits MLJ, Nijsen JFW, Lam MGEH, Zonnenberg B a., van den Bosch M a. a. J, et al. Quantitative Monte Carlo-based holmium-166 SPECT reconstruction. Med Phys. 2013;40(11):112502.
13. Elschot M, Nijsen JFW, Lam MGEH, Smits MLJ, Prince JF, Viergever M a, et al. (99m)Tc-MAA overestimates the absorbed dose to the lungs in radioembolization: a quantitative evaluation in patients treated with (166)Ho-microspheres. Eur J Nucl Med Mol Imaging. 2014;41(10):1965–75.
14. Gaba RC, Zivin SP, Dikopf MS, Parvinian A, Casadaban LC, Lu Y, et al. Characteristics of primary and secondary hepatic malignancies associated with hepatopulmonary shunting. Radiology. 2014 May;271(2):602–12.
15. Smits ML, Nijsen JF, van den Bosch MA, Lam MG, Vente MA, Mali WP, et al. Holmium-166 radioembolisation in patients with unresectable, chemorefractory liver metastases (HEPAR trial): a phase 1, dose-escalation study. Lancet Oncol. 2012;13(10):1025-34.
16. Eisenhauer EA, Therasse P, Bogaerts J, Schwartz LH, Sargent D, Ford R, et al. New response evaluation criteria in solid tumours: revised RECIST guideline (version 1.1). Eur J Cancer. 2009;45:228–47.
17. Wahl RL, Jacene H, Kasamon Y, Lodge M a. From RECIST to PERCIST: Evolving Considerations for PET response criteria in solid tumors. J Nucl Med. 2009;50 Suppl 1(5):122S – 50S.
18. Bethesda MD: Cancer Therapy Evaluation Program. Common Terminology Criteria for Adverse Events v4.03 (CTCAE) [Internet]. 2010 [cited 2011 Oct 7]. Available from: http://evs.nci.nih.gov/ftp1/CTCAE/CTCAE_4.03_2010-06-14_QuickReference_5x7.pdf

19. Bol GH, Kotte ANTJ, van der Heide UA, Lagendijk JJW. Simultaneous multi-modality ROI delineation in clinical practice. Comput Methods Programs Biomed. 2009;96(2):133–40.
20. Todd S, Whitehead A, Stallard N, Whitehead J. Interim analyses and sequential designs in phase III studies. Br J Clin Pharmacol. 2001;51(5):394–9.
21. Ford R, Schwartz L, Dancey J, Dodd LE, Eisenhauer E a, Gwyther S, et al. Lessons learned from independent central review. Eur J Cancer. 2009;45(2):268–74.
22. Benson AB, Geschwind J-F, Mulcahy MF, Rilling W, Siskin G, Wiseman G, et al. Radioembolisation for liver metastases: Results from a prospective 151 patient multi-institutional phase II study. Eur J Cancer. 2013;49(15):3122–30.
23. Prince JF, van Rooij R, Bol GH, de Jong HWAM, van den Bosch MAAJ, Lam MGEH. Safety of a Scout Dose Preceding Hepatic Radioembolization with 166Ho Microspheres. J Nucl Med. 2015;56(6):817–23.

Supplemental Appendix

Table S1 *Response on PET/CT*

	Reproducible for PERCIST 1.0 % (*n*)	Not reproducible for PERCIST 1.0 % (*n*)	All patients % (*n*)
Liver specific response			
3 months			
Complete metabolic response	0% (0)	5% (1)	3% (1)
Partial metabolic response	25% (3)	30% (6)	28% (9)
Stable metabolic disease	17% (2)	35% (7)	28% (9)
Progressive metabolic disease	58% (7)	30% (6)	41% (13)
Total	38% (12)	63% (20)	100% (32)
6 months			
Partial metabolic response	67% (2)	0% (0)	13% (2)
Stable metabolic disease	33% (1)	23% (3)	19% (3)
Progressive metabolic disease	0% (0)	77% (10)	69% (11)
Total	19% (3)	81% (13)	100% (16)
9 months			
Stable metabolic disease	0% (0)	60% (3)	50% (3)
Progressive metabolic disease	100% (1)	40% (2)	50% (3)
Total	17% (1)	83% (5)	100% (6)
12 months			
Stable metabolic disease	0% (0)	100% (1)	100% (1)
Total	0% (0)	100% (1)	100% (1)
Whole body response			
3 months			
Partial metabolic response	17% (2)	25% (5)	22% (7)
Stable metabolic disease	8% (1)	15% (3)	13% (4)
Progressive metabolic disease	75% (9)	60% (12)	66% (21)
Total	38% (12)	63% (20)	100% (32)
6 months			
Partial metabolic response	33% (1)	0% (0)	6% (1)
Stable metabolic disease	0% (0)	8% (1)	6% (1)
Progressive metabolic disease	67% (2)	92% (12)	88% (14)
Total	19% (3)	81% (13)	100% (16)
9 months			
Stable metabolic disease	0% (0)	20% (1)	17% (1)
Progressive metabolic disease	100% (1)	80% (4)	83% (5)
Total	17% (1)	83% (5)	100% (6)
12 months			
Progressive metabolic disease	0% (0)	100% (1)	100% (1)
Total	0% (0)	100% (1)	100% (1)

Table S2 *Laboratory toxicity*

	Baseline	3 weeks	3 months
		median (range)	
Sodium (mmol/L)	137.5 (131 - 141)	NA	137 (130 - 140)
Potassium (mmol/L)	4 (3.2 - 4.6)	NA	4.1 (3.4 - 4.9)
Chloride (mmol/L)	103 (97 - 107)	NA	101.5 (98 - 106)
Bicarbonate (mmol/L)	25.8 (21.7 - 31.3)	NA	26.35 (21.6 - 31.8)
Ionized calcium (mmol/L)	1.19 (1.06 - 1.37)	NA	1.2 (1.12 - 1.53)
Magnesium (mmol/L)	0.8 (0.4 - 1.04)	0.65 (0.65 - 0.65)	0.805 (0.65 - 0.92)
Phosphorus (mmol/L)	1.02 (0.4 - 1.39)	NA	1 (0.78 - 1.28)
Urea (mmol/L)	5.45 (3.2 - 10.3)	5.5 (5.5 - 5.5)	5.05 (2.4 - 11.5)
Creatinine (μmol/L)	72 (45 - 153)	69 (47 - 137)	67 (47 - 136)
Bilirubin (μmol/L)	8 (5 - 23)	8.5 (5 - 19)	13 (6 - 31)*
ALP (U/L)	144 (55 - 418)	265.5 (130 - 828)*	324 (150 - 1000)*
GGT (U/L)	117.5 (17 - 1361)	255 (89 - 895)*	344 (140 - 1624)*
AST (U/L)	42 (17 - 135)	50.5 (23 - 396)	66 (38 - 276)*
ALT (U/L)	28 (11 - 90)	40.5 (13 - 445)*	56 (15 - 304)*
LD (U/L)	264.5 (122 - 2350)	243 (161 - 972)	290 (187 - 861)
Albumin (g/L)	40.6 (32.3 - 46.9)	36.25 (28.5 - 42.4)*	37.1 (29 - 44.9)*
Total protein (g/L)	74 (66 - 86)	NA	75 (66 - 87)
Ammonia (μmol/L)	28.5 (18 - 47)	26.5 (15 - 40)	32 (17 - 63)
Hemoglobin (mmol/L)	8.6 (6.3 - 10.7)	8.2 (5.3 - 10.2)*	8.95 (5.8 - 10.7)
Hemotocrit (L/L)	0.41 (0.31 - 0.52)	0.39 (0.27 - 0.5)	0.43 (0.29 - 0.5)
Erytrocytes ($x10^{12}$/L)	4.57 (3.62 - 5.86)	4.31 (3.18 - 5.75)	4.68 (3.44 - 6.06)
MCV (fL)	90 (78 - 100)	91 (81 - 102)	90 (78 - 102)
MCH (fmol)	1.895 (1.58 - 2.21)	1.845 (1.6 - 2.12)	1.88 (1.54 - 2.19)
MCHC (mmol/L)	20.9 (19.9 - 22)	20.6 (19.3 - 21.9)*	20.7 (19.6 - 22.9)
Leukocytes ($x10^9$/L)	7.75 (4.5 - 12.6)	6.45 (3.9 - 12.7)*	6.9 (4 - 12.2)
Eosinophils ($x10^9$/L)	0.14 (0 - 1.44)	0.14 (0.03 - 0.84)	0.105 (0.01 - 0.75)
Basophils ($x10^9$/L)	0.04 (0 - 0.07)	0.02 (0 - 0.08)	0.03 (0 - 0.1)
Neutrophils ($x10^9$/L)	5.615 (2.25 - 10.2)	4.47 (2.16 - 10.7)	4.785 (2.42 - 9.82)
Lymphocytes ($x10^9$/L)	1.45 (0.79 - 3.18)	0.79 (0.43 - 1.52)*	1.045 (0.25 - 2.32)*
Monocytes ($x10^9$/L)	0.525 (0.02 - 1.2)	0.79 (0.41 - 1.38)*	0.59 (0.02 - 1.14)
Platelet count ($x10^9$/L)	226.5 (143 - 456)	227 (98 - 491)	190 (107 - 308)*
PT (sec)	13.75 (12.4 - 33.2)	NA	13.8 (12.6 - 37.4)
APTT (sec)	36.5 (25 - 69)	NA	37 (32 - 71)
TT (sec)	16.5 (14.2 - 22.8)	NA	17.8 (15.3 - 96.5)*
INR (ratio)	1.06 (0.93 - 2.62)	NA	1.06 (0.93 - 4.35)

*ALP: alkaline phosphatase, GGT: gamma-glutamyl transferase, AST: aspartate aminotransferase, ALT: alanine aminotransferase, LD: lactate dehydrogenase, MCV: mean corpuscular volume, MCH: mean corpuscular hemoglobin, MCHC: mean corpuscular hemoglobin concentration, PT: prothrombin time, APTT: activated partial thromboplastin time, TT: thrombin time, INR: international normalized ratio. * Significant at $p < 0.00088$ (Bonferroni correction for 57 hypotheses)*

Table S3. *Quality of life*

Scale	Baseline (*n*=37)	1 week (27)	6 weeks (34)	3 months (32)	6 months (14)	9 months (8)	12 months (2)
QLQ-C30							
QoL	83 (67 - 83)	42 (25 - 71)	67 (58 - 83)	67 (58 - 83)	83 (67 - 90)	71 (54 - 88)	58
Physical Functioning	93 (87 - 100)	40 (20 - 83)	87 (67 - 93)	87 (67 - 100)	87 (77 - 93)	77 (63 - 95)	57
Role Functioning	100 (83 - 100)	33 (0 - 42)	67 (50 - 100)	67 (62 - 100)	83 (67 - 100)	83 (62 - 100)	67
Emotional Functioning	83 (75 - 92)	75 (54 - 96)	83 (67 - 100)	79 (67 - 92)	75 (67 - 92)	71 (62 - 83)	67
Cognitive Functioning	100 (83 - 100)	83 (67 - 100)	100 (83 - 100)	100 (83 - 100)	92 (67 - 100)	83 (75 - 100)	83
Social Functioning	100 (67 - 100)	50 (33 - 83)	83 (67 - 100)	83 (67 - 100)	92 (71 - 100)	100 (62 - 100)	67
Fatigue	11 (0 - 22)	67 (44 - 100)	33 (22 - 50)	22 (22 - 56)	17 (3 - 31)	22 (8 - 56)	50
Nausea and vomiting	0 (0 - 0)	33 (17 - 67)	0 (0 - 17)	0 (0 - 17)	0 (0 - 12)	0 (0 - 17)	8
Pain	0 (0 - 0)	67 (33 - 83)	17 (0 - 33)	17 (0 - 33)	0 (0 - 29)	8 (0 - 42)	33
Dyspnoea	0 (0 - 33)	0 (0 - 33)	0 (0 - 33)	0 (0 - 33)	33 (0 - 67)	33 (0 - 33)	67
Insomnia	0 (0 - 33)	33 (0 - 67)	17 (0 - 33)	0 (0 - 33)	17 (0 - 33)	33 (25 - 42)	33
Appetite loss	0 (0 - 0)	33 (33 - 100)	0 (0 - 33)	0 (0 - 33)	0 (0 - 33)	0 (0 - 8)	0
Constipation	0 (0 - 0)	33 (0 - 67)	0 (0 - 0)	0 (0 - 0)	0 (0 - 0)	0 (0 - 0)	0
Diarrhoea	0 (0 - 33)	0 (0 - 0)	0 (0 - 0)	0 (0 - 33)	0 (0 - 33)	17 (0 - 33)	17
Financial difficulties	0 (0 - 0)	0 (0 - 0)	0 (0 - 0)	0 (0 - 0)	0 (0 - 0)	0 (0 - 0)	17
QLQ-LMC21							
Eating	0 (0 - 17)	67 (38 - 83)	17 (0 - 33)	8 (0 - 33)	8 (0 - 46)	0 (0 - 17)	8
Fatigue	11 (0 - 33)	67 (44 - 94)	33 (14 - 44)	22 (6 - 39)	17 (11 - 33)	22 (11 - 53)	44
Pain	0 (0 - 11)	44 (22 - 67)	22 (0 - 33)	22 (0 - 36)	22 (11 - 33)	17 (11 - 39)	22
Emotional problems	25 (17 - 42)	42 (17 - 58)	33 (17 - 42)	25 (17 - 42)	29 (19 - 40)	21 (17 - 44)	33
Weight loss	0 (0 - 0)	0 (0 - 0)	0 (0 - 0)	0 (0 - 0)	0 (0 - 33)	0 (0 - 33)	0
Taste	0 (0 - 0)	0 (0 - 67)	0 (0 - 33)	0 (0 - 33)	0 (0 - 25)	0 (0 - 8)	0
Dry mouth	0 (0 - 33)	0 (0 - 50)	0 (0 - 33)	0 (0 - 33)	0 (0 - 33)	33 (0 - 67)	33

Table S3. *Continued*

Scale	Baseline (*n*=37)	1 week (27)	6 weeks (34)	3 months (32)	6 months (14)	9 months (8)	12 months (2)
QLQ-LMC21							
Sore mouth/ tongue	0 (0 - 0)	0 (0 - 0)	0 (0 - 0)	0 (0 - 0)	0 (0 - 0)	0 (0 - 0)	17
Peripheral neuropathy	33 (0 - 33)	0 (0 - 33)	33 (0 - 67)	17 (0 - 33)	0 (0 - 33)	0 (0 - 33)	33
Jaundice	0 (0 - 0)	0 (0 - 0)	0 (0 - 0)	0 (0 - 0)	0 (0 - 0)	0 (0 - 0)	0
Contact with friends	0 (0 - 0)	33 (0 - 67)	0 (0 - 0)	0 (0 - 33)	0 (0 - 33)	0 (0 - 33)	33
Talking about feelings	0 (0 - 0)	0 (0 - 0)	0 (0 - 0)	0 (0 - 33)	0 (0 - 25)	17 (0 - 33)	17
Sex life	0 (0 - 33)	17 (0 - 67)	33 (0 - 33)	33 (0 - 33)	33 (0 - 50)	50 (8 - 67)	33

Data are median (IQR). QLQ-C30: quality of life questionnaire – common 30, QLQ-LMC21: quality of life – colorectal liver metastases 21

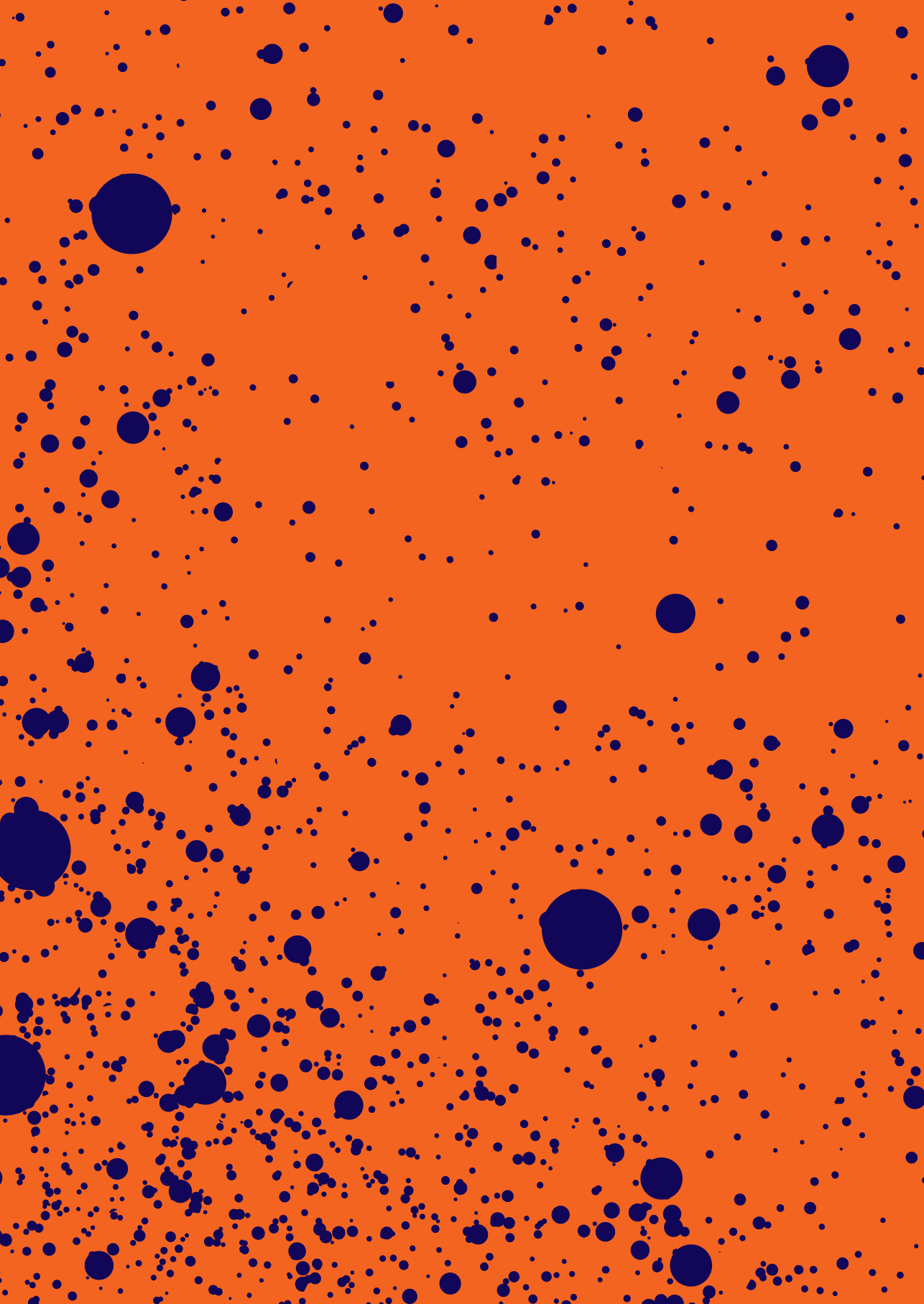

CHAPTER 7

Radiation emissions from patients treated with holmium-166 radioembolization

J.F. Prince
M.L.J. Smits
G.C. Krijger
B.A. Zonnenberg
M.A.A.J. van den Bosch
J.F.W. Nijsen
M.G.E.H. Lam

Journal of Vascular and Interventional Radiology 2014

Abstract

Purpose

To assess the radiation exposure to individuals coming from patients after treatment with holmium-166 (^{166}Ho) microspheres.

Materials and methods

^{166}Ho radioembolization (RE) with escalating whole-liver doses of 20 Gy, 40 Gy, 60 Gy, and 80 Gy was administered to 15 patients. Exposure rates (μSv/h) from patients were measured at 1.0 m distance from a lateral and frontal position at 0, 3, 6, 24, and 48 hours after infusion. The total effective dose equivalent (TEDE) to a maximally exposed contact was calculated in accordance with guidelines of the U.S. Nuclear Regulatory Commission (NRC). Results were extrapolated to a whole liver dose of 60 Gy used in future treatments.

Results

The median exposure rate at discharge, 48 hours after infusion, measured from a lateral position was 26 μSv/h (range, 7 – 45 μSv/h). Extrapolated to a whole liver dose of 60 Gy, none of the exposure rates for the NRC contact scenario, at any time, frontal or lateral, would lead to a TEDE ≥ 5 mSv; all patients may be released directly after treatment. Release after 6 hours is possible without contact restrictions for patients who received up to 7 GBq.

Conclusions

The TEDE to a contact of patients treated with ^{166}Ho-RE would not exceed the NRC limit of 5 mSv. Contact restrictions 6 hours after treatment are unnecessary for infused activities < 7 GBq.

Introduction

The two most commonly used types of microspheres for hepatic radioembolization (RE) are resin microspheres that chelate yttrium-90 (^{90}Y) (SIR-Spheres; Sirtex Medical Limited, North Sidney, New South Wales, Australia), and glass microspheres containing ^{90}Y (Theraspheres; BTG International Ltd., London, United Kingdom). A different kind of microsphere for RE has been developed, consisting of a poly(L-lactic acid) matrix containing holmium-166 (^{166}Ho), that can be visualized in vivo with both single photon-emission computed tomography (SPECT) and magnetic resonance imaging.[1] These properties can be used to analyze accurately the distribution of microspheres after treatment.[2] For instance, a scout dose of ^{166}Ho microspheres might improve the safety of the procedure by omitting technetium-99m macroaggregated albumin (^{99m}Tc-MAA) for distribution assessment because ^{99m}Tc-MAA is a poor predictor, especially regarding lung shunt fraction.[3] By prediction of distribution during treatment, a dose could be individualized based on damage to healthy liver parenchyma or tumors.

All three microsphere products are loaded with a high-energy beta-emitting isotope. For resin and glass microspheres, the isotope ^{90}Y emits a beta particle with a maximum energy of 2.28 MeV with an abundance of 99%. The half-life is 64.1 hours. Holmium-166 (^{166}Ho) emits beta radiation at two main energies (beta particle maximum energy = 1.74 MeV and 1.85 MeV; intensity = 48.7% and 50.0%) and has a half-life of 26.8 hours. Because the beta energy of ^{166}Ho is lower than ^{90}Y and its physical half-life is significantly shorter, the energy released per unit of activity is 15.87 J/GBq for ^{166}Ho and 49.67 J/GBq for ^{90}Y.[4] An approximately three times higher activity of ^{166}Ho is required to obtain an absorbed dose similar to the dose from a given activity of ^{90}Y. For both ^{90}Y and ^{166}Ho, low-energy photons (bremsstrahlung) are also emitted indirectly as a result of deceleration of the beta particles in tissue. The direct gamma radiation of ^{166}Ho (81 keV, abundance 6.2%) can be used for dosimetry with SPECT. However, from a radiation safety point of view, the direct gamma emission of ^{166}Ho, including a low intensity (abundance 0.93%) 1,379-keV gamma emission, increases the radiation exposure to individuals surrounding the patient in the first days after treatment.

The U.S. Nuclear Regulatory Commission (NRC) has set regulations for the release of patients after administration of radioactive materials. Using the scenario described by the NRC, the limit of the total effective dose equivalent (TEDE) to individuals surrounding patients treated with radioactive materials is 5 mSv, above which patients cannot be discharged.[5] When the TEDE to surrounding individuals is > 1 mSv, the patients should be given written instructions how to keep exposure to other individuals ALARA ("as low as reasonably achievable"; ie, contact restrictions).

The purpose of the present study was to assess the potential radiation exposure to other individuals coming from patients treated with ^{166}Ho-RE and to evaluate what radiation safety precautions are necessary after treatment.

Materials and methods

Study design

In this phase 1 study, the safety and toxicity profile of ^{166}Ho-microspheres were evaluated in patients with unresectable, chemorefractory liver metastases. The primary endpoint was the maximum tolerated radiation dose to the liver. Patients were treated in four cohorts, with escalating radioactivity of ^{166}Ho, to accomplish a targeted whole-liver dose of 20 Gy (n=6), 40 Gy (n=3), 60 Gy (n=3) and 80 Gy (n=3). All patients provided written informed consent before enrollment in the study. This trial was approved by the institutional review board and is registered with ClinicalTrials.gov (NCT01031784). The toxicity and treatment results of this study were published previously.[6]

Study population

All patients were ineligible for surgery or chemotherapy or refused these treatments because of their side effects. Inclusion criteria consisted of liver-dominant metastases and an estimated life expectancy of > 3 months. Patients were excluded if they had impaired hematological, renal, or liver function. All patients were treated at our institution. Baseline characteristics are summarized in Table 1; more details can be found in the publication of the primary study outcome.[6]

Table 1. *Baseline characteristics*

Characteristic	Value
n	15
Male	9 (60%)
Age (years)	54 (49 – 60)
BMI	24.9 (24.0 – 26.4)
Primary tumor type	
Colorectal carcinoma	6 (40%)
Ocular melanoma	6 (40%)
Cholangiocarcinoma	2 (13%)
Breast carcinoma	1 (7%)
Previous treatments	
Systemic	11 (73%)
Locoregional	5 (33%)
WHO performance status	
0	13 (87%)
1	2 (13%)

Values are a number (%) or median (95% CI). BMI = body mass index; WHO = World Health Organization

Treatment procedure

After coil embolization of nonhepatic vessels during angiography performed before treatment, ^{99m}Tc-MAA was administered in relevant arteries leading to liver parenchyma. No segmental or lobular treatments were performed; all patients received whole-liver RE in a single session. If no significant lung shunting or extrahepatic deposition was observed on SPECT/CT imaging, patients received a scout (approximately 60 mg, 250 MBq) and therapy (approximately 540 mg, varying activities) dose of ^{166}Ho microspheres. The size of these microspheres ranged from 15 – 60 μm. The scout dose was performed as a second check for extrahepatic deposition or lung shunting and was part of an investigation into distribution differences between microspheres and MAA particles. The treatment details are provided in Table 2.

Release and follow-up

Patients were retained in the nuclear medicine ward for 48 hours after treatment. After discharge, patients were given contact restrictions for another 48 hours (see Appendix 1).

Table 2. *Treatment Details*

Characteristic	Value
Whole-liver treatment	15 (100%)*
Liver volume (mL)	1,807 (1,654–2344)
Targeted mean liver dose (Gy)†	40 (20–60)
Activity prepared (MBq)†	4,707 (2,361–7,141)
Residual activity in vial (MBq)	274 (161–363)
Net infused activity (MBq)†	4,510 (2,162–6,856)
Actual mean liver dose (Gy)†	35 (18–59)
Lung shunt fraction (%)‡	6.9 (3.9–8.1)

Values are median (95% confidence interval) except where noted. The activities using holmium-166 are higher compared with yttrium-90 for compensation of the lower energy release (J/Bq). Number (%). †Summary of four cohorts; for separate values see Smits et al.[6] ‡Based on scintigraphy after technetium-99m macroaggregated albumin infusion, 1 missing value (n = 14).*

Planning the activity to be administered

Dosimetry to the liver was calculated using a method analogous to the medical internal radiation dosimetry pamphlet number 17.[7] Targeted whole-liver radiation absorbed doses were 20 Gy, 40 Gy, 60 Gy, and 80 Gy. For calculation of necessary radioactivity of ^{166}Ho, the following formula was used:

$$A_{Ho166}(\mathrm{MBq}) = Dose_{\ Liver}(\mathrm{Gy}) \times 63 \left(\frac{\mathrm{MBq}}{\mathrm{J}}\right) \times \mathrm{M}_{Liver}\ (\mathrm{kg}) \quad [Equation\ 1]$$

Where A_{Ho166} is the activity of ^{166}Ho in MBq to be administered, the absorbed energy is the activity-to-dose conversion of ^{166}Ho assuming that all energy of the emitted beta particles is absorbed in the liver, and the M_{Liver} is the mass calculated by delineating the liver on computed tomography software developed in house (Volumetool)[8], assuming a liver tissue density of 1.0 g/cm^3. Activities for each cohort were 1.3 GBq/kg, 2.5 GBq/kg, 3.8 GBq/kg, and 5.0 GBq/kg (liver weight). The lung shunt fraction is not included in this formula.

Net administered activity measurement

Before treatment, the activity of the vial containing the microspheres was measured using a validated dose calibrator (VDC405 or VDC404, Veenstra Instruments, Houre, The Netherlands). On completion of therapy, the remnant radioactivity in the vial was measured again. The difference was used as the net activity with which the patient was treated and used in further dose calculations.

Radiation emission after treatment

The radiation emitted by the patient after treatment was studied in two ways. First, the exposure to other individuals was calculated from the exposure rates at 1.0 m distance from the patient. Second, all exposures were extrapolated to a scenario where each patient received a targeted whole-liver absorbed dose of 60 Gy.

Estimated effective dose to others based on infused activity

Using the net administered activity and the gamma ray constant, the TEDE to others from the direct gamma radiation after discharge can be estimated. All ^{166}Ho was assumed to remain in the liver.[9] Biological half-life was neglected, and only the physical half-life of ^{166}Ho was taken into account. The bremsstrahlung and the fraction of metastable ^{166}Ho were neglected for the estimated exposure to others. The exposure to others is described as "effective dose", or more officially the TEDE. The effective dose was calculated using the following formula:[5]

$$D(\infty) = \frac{34.6\ \Gamma\ Q_0\ t_{1/2}\ E}{(1.0)^2} \qquad [Equation\ 2]$$

Where D(∞) is the effective dose (mSv), 34.6 is a conversion factor (24h/d * 1/ln(2)), Γ the specific gamma ray dose constant (mSv/GBq-h at 1.0 m), Q_0 is the activity at the time of release (GBq), $t_{1/2}$ the half-life (d), E the occupancy factor, and 1.0 the average distance from the patient (m). The specific gamma ray dose constant for ^{166}Ho is 0.00627 mSv/GBq-hr at 1.0 m.[10] The half-life of ^{166}Ho is 26.8 hours. No significant beta emission is expected outside of the human body due to the maximal tissue penetration of 8.7 mm and mean tissue penetration of 2.5 mm of beta radiation from ^{166}Ho.[11,12] The formula can be rewritten as:

$$D(\infty) = 0.242\ Q_0\ E \quad [Equation\ 3]$$

Where D(∞) is the effective dose (mSv) from activity Q_0 (GBq) until final decay, with a presence E (range 0% - 100%) at 1.0 m. E was conservatively set to 1 (continuous presence) for the analyses of this study because the half-life of ^{166}Ho is relatively short. Effective dose was calculated for the four most relevant time points that were also used for measurements in this study (ie, 0, 6, 24, and 48 h after infusion).

Measurements of exposure rates and calculation of effective doses

Exposure rates were measured after treatment with ^{166}Ho-RE from two positions at five different times. Measurements were performed from a right lateral and frontal position at 1.0 m distance from the patient. A portable exposure rate meter was used (Radiagem 2000; Canberra Industries, Inc, Meriden, Connecticut). This calibrated dose rate meter was sensitive for gamma radiation only (range, 40 keV – 1.5 MeV). It was aimed at the center of the liver. The measurements were performed shortly after infusion of microspheres (t_0), and at 3 (t_3), 6 (t_6), 24 (t_{24}), and 48 (t_{48}) hours after infusion. The exact times of the measurements were noted, to allow correction for decay. Immediately after angiography, patients were required to remain in the supine position to allow the vascular access site to heal, so frontal measurements were not performed at t_0.

Exposure rates were measured at different times. To allow comparison, all dose rates from the same patient and position were extrapolated to exposure rate at time of infusion. The mean of these exposure rates was used to calculate mean effective doses at t_0 per patient. To assess the validity of this method, the mean of the decay-corrected exposure rate at t_0 and the resulting effective dose of each patient were examined for a correlation with the infused activity. Pearson correlation coefficient (r^2, r, and corresponding P value for H_0: r = 0) was calculated. A linear model was made with two independent variables (infused activity and body mass index) to assess the added value of body mass index on the prediction of the resulting effective dose. If possible, this model was reduced by backward stepwise selection based on the Akaike information criterion. The slope of the correlation line was used to determine a new constant that included attenuation to replace the hypothetical constant of 0.242 mSv/GBq in Equation 3. The newly determined constant was used to determine whether contact restrictions were necessary for different release times and varying amounts of infused activity.

The effective dose to other individuals was calculated from measured exposure rates in accordance with published guidelines of the NRC.[5] The following equation, which is also used by McCann et al.[13]19 glass, was used to calculate the effective dose to others:

$$D(\infty) = 34.6\ R_0\ T_P\ \mathrm{E} \qquad [Equation\ 4]$$

Where D(∞) is the effective dose (in mSv), 34.6 is the conversion factor of 24 h/d times the total integration of decay (1/ln(2) = 1.44) and R_0 is the dose rate measured at 1.0 m from the patient (in mSv/h), T_P is the physical half-life in days (1.115 d for ^{166}Ho), and E is the occupancy factor.

Extrapolation to a 60-Gy aimed whole liver absorbed dose

In the present dose-escalation study, the whole-liver absorbed doses ranged from 14.7 - 78.3 Gy. Based on the maximum tolerated absorbed dose established in this study, 60 Gy will be the targetec whole-liver absorbed dose for future ^{166}Ho RE treatments (equivalent to 3.8 GBq/kg).[6] Because the liver absorbed doses in the patients of this study varied widely, measured exposure rates and effective doses were extrapolated to a scenario where each patient received a whole-liver dose of 60 Gy, assuming a linear relation.

Contact scenarios

Using Equation 3, the effective dose for different contact scenarios was calculated, as suggested by Gulec and Siegel.[14] Besides the basic scenario in which the occupancy factor (E) was 1 (continuous presence) and the distance (d) was 1.0 m, scenarios for household members (E = 0.25, d = 1); caregivers (E = 0.25, d = 0.3); givers of significant care (E = 0.5, d = 0.3); and for infants, children, or pregnant women (E = 0.042, d = 0.1) were calculated. The applied distance correction factor was not the inverse square but a multiplication of 3/d, where d is the distance in meters. This correction factor is more appropriate for distances closer than 1.0 m owing to the source of radiation (ie, the liver) resembling a line more than a point source.[14]

Results

Estimated effective dose to others based on infused activity

Based on the net administered activity, the estimated median effective dose to other individuals from patients treated with ^{166}Ho-RE was 0.93 mSv (range 0.33 – 2.13 mSv) assuming an occupancy factor of 1 (continuous presence at 1.0 m during total decay) starting at the moment that patients are discharged (6 h after treatment). The effective dose for the other time points are presented in Table 3.

Table 3. *Estimated and Measured Effective Doses to Others Exposed to Patients Treated with Holmium-166 Radioembolization Starting from Different Time Points*

(A) Estimated Effective Dose				
	Dose T_0(mSv)	Dose T_6(mSv)	Dose T_{24}(mSv)	Dose T_{48}(mSv)
Cohort 20 Gy	0.52 (0.39–1.09)	0.45 (0.33–0.93)	0.28 (0.21–0.59)	0.15 (0.11–0.31)
Cohort 40 Gy	0.84 (0.84–1.33)	0.72 (0.72–1.14)	0.45 (0.45–0.71)	0.24 (0.24–0.38)
Cohort 60 Gy	1.92 (1.65–2.31)	1.64 (1.41–1.98)	1.03 (0.89–1.24)	0.55 (0.48–0.67)
Cohort 80 Gy	1.74 (1.66–2.49)	1.49 (1.42–2.13)	0.94 (0.89–1.34)	0.50 (0.48–0.72)
(B) Measured Effective Dose				
	Dose T_0(mSv)	Dose T_6(mSv)	Dose T_{24}(mSv)	Dose T_{48}(mSv)
Cohort 20 Gy	0.32 (0.27–0.65)	0.27 (0.24–0.55)	0.17 (0.15–0.35)	0.09 (0.08–0.19)
Cohort 40 Gy	0.62 (0.56–0.85)	0.53 (0.48–0.73)	0.33 (0.30–0.46)	0.18 (0.16–0.25)
Cohort 60 Gy	1.25 (1.18–1.32)	1.07 (1.01–1.13)	0.67 (0.64–0.71)	0.36 (0.34–0.38)
Cohort 80 Gy	1.56 (0.93–1.82)	1.34 (0.80–1.56)	0.84 (0.50–0.98)	0.45 (0.27–0.52)

(A) Estimated effective dose to individuals near patients after radioembolization as calculated from the administered activities by Equation 3. Reported data are median (range). (B) Effective doses to individuals near patients after radioembolization as calculated from the measured dose rates by Equation 4. Reported data are median (range).

Measured exposure rates and calculated effective doses

Of 135 exposure rate measurements in 15 patients, 6 were missing (4.4%; 1 lateral and 5 frontal measurements in 5 different patients). The median lateral exposure rates at discharge, 6 hours after infusion, measured from 1.0 m distance were 8 μSv/h (range, 4 - 17 μSv/h), 13 μSv/h (11 – 18 μSv/h), 26 μSv/h (22 – 39 μSv/h), and 37 μSv/h (23 – 38 μSv/h) for the 20-Gy, 40-Gy, 60-Gy and 80-Gy cohorts. The exposure rates and resulting effective doses for each cohort are presented in Figure 1. After correction for decay, there was a strong correlation between mean exposure rate at t_0 for each patient and the infused activity for the lateral measurements (r^2 = 0.89, r = 0.94, P < .01) and for the frontal measurements (r^2 = 0.85, r = 0.92, P < .01) (Figure 2A). Because the lateral exposure rate measurements correlated slightly better with infused activity than the frontal measurements, the lateral exposure

rates were used for further calculations. Body mass index did not improve the fit of the model, leaving only the infused activity as an independent variable. The median effective dose to other individuals assuming an occupancy factor of 1 starting 6 hours after treatment was 0.55 mSv (range, 0.24 – 1.56 mSv). The effective doses for the other time points are displayed in Table 3.

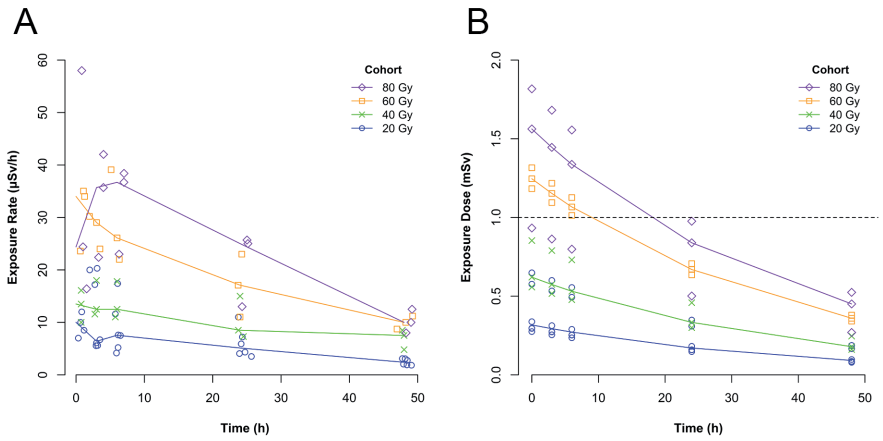

Figure 1 *Measured exposure rates in microSv/h for each patient categorized per cohort (A) and subsequently calculated effective doses in mSv (B). The median exposure rates and median effective doses per cohort are connected by lines. The black reference line in B represents the 1.0 mSv threshold above which contact restrictions are necessary for release*

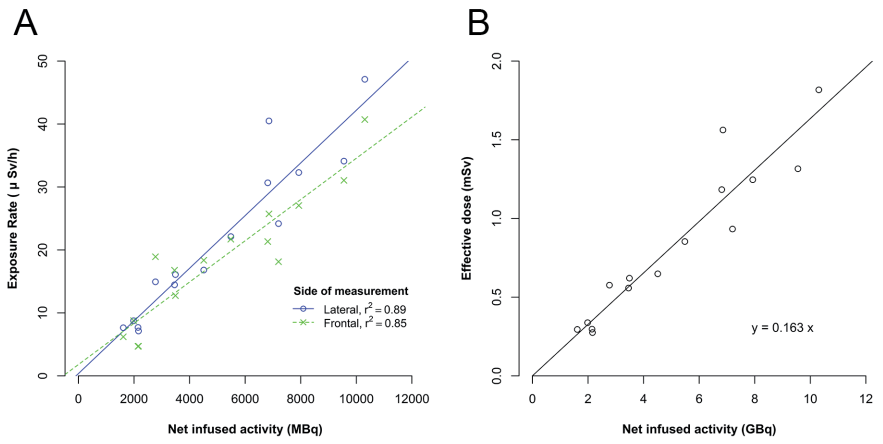

Figure 2 *Scatter plots of the infused activity versus (A) the lateral and frontal exposure rates, and (B) the effective dose based on the lateral exposure rates. The constant of 0.163 mSv/GBq was derived from the trendline without intercept in B. Reported R^2 values are Pearson's correlation coefficients*

The calculated effective dose for a person standing at 1.0 m distance on the right side of the patient for continuous presence from t_0 correlated well with the infused activity (r^2 = 0.89) with a constant of 0.163 mSv/GBq (Figure 2B). This constant was used to create a chart that indicates whether contact restrictions are necessary for different release times (Figure 3). According to these calculations, for the basic contact scenario, release without contact restrictions 6 hours after treatment is appropriate for all patients who receive up to 7 GBq of ^{166}Ho. All patients who receive up to 11 GBq of ^{166}Ho can be released without instructions 24 hours after therapy.

Extrapolation to a 60 Gy targeted whole-liver absorbed dose

Extrapolation of the measured exposure rates to 60 Gy (3.8 GBq/kg) resulted in median exposure rates of 31 μSv/h, 29 μSv/h, 27 μSv/h, 18 μSv/h, and 9 μSv/h for the lateral measurements, at 0, 3, 6, 24, and 48 hours. Assuming continuous presence (occupancy factor = 1) starting 6 hours after infusion, the median effective dose to a person standing at 1.0 m in the right lateral position was estimated to be 1.03 mSv (range, 0.61-1.76 mSv). The median effective dose to a person at 1.0 m distance, lateral from the patient, starting immediately after treatment is 1.20 mSv (range, 0.71-2.06 mSv). None of the extrapolated exposure rates for the basic scenario, at any time, frontal or lateral, would lead to an effective dose ≥ 5 mSv. For the caregivers and givers of significant care scenarios, the effective dose could be ≥ 5 mSv. The mean effective dose to individuals for these other contact scenarios is displayed in Table 4.

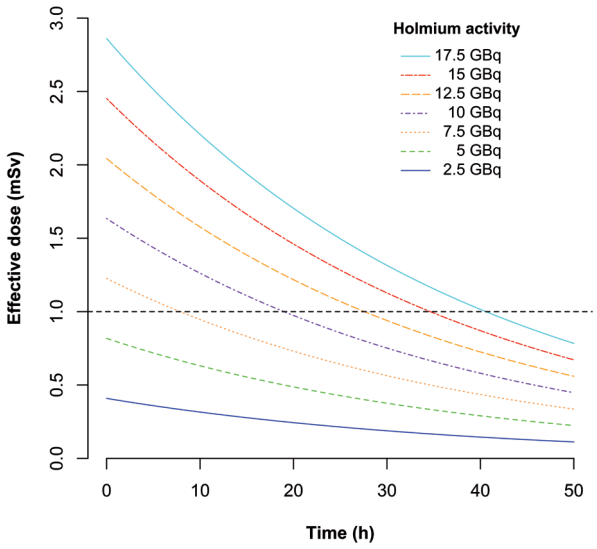

Figure 3 *Total effective dose equivalent (TEDE) for different infused activities and release times after infusion. Contact restrictions are necessary if the TEDE exceeds 1.0 mSv (dashed reference line). Whether release without contact restrictions is appropriate can be checked by following the line for the activity administered to the patient and the time of release on the x-axis. If the value is below 1.0 mSv, release without contact restrictions is appropriate*

Table 4. *Maximum effective doses for a 60-Gy whole liver absorbed dose scenario combined with different contact scenarios*

	Dose T_0 (mSv)	Dose T_6 (mSv)	Dose T_{24}(mSv)	Dose T_{48} (mSv)
Basic scenario (E=1, d=1)	1.20 (0.71-2.06)	1.03 (0.61-1.76)	0.64 (0.38-1.11)	0.35 (0.21-0.59)
NRC contact scenario: Household members (E=0.25, d=1)	0.30 (0.18-0.51)	0.26 (0.15-0.44)	0.16 (0.10-0.28)	0.09 (0.05-0.15)
Caregivers (E=0.25, d=0.3)	3.00 (1.79-5.15)	2.57 (1.53-4.41)	1.61 (0.96-2.76)	0.87 (0.52-1.48)
Givers of significant care (E=0.5, d=0,3)	6.00 (3.57-10.29)	5.13 (3.06-8.81)	3.22 (1.92-5.53)	1.73 (1.03-2.97)
Infants / children / pregnant women (E=0.042, d=0.1)	1.51 (0.90-2.59)	1.29 (0.77-2.22)	0.81 (0.48-1.39)	0.44 (0.26-0.75)

Reported data are median (range).

Discussion

The gamma emission by ^{166}Ho is beneficial for imaging purposes[1,4] but may raise concerns regarding radiation exposure to others. This study describes the exposure rate coming from patients treated with ^{166}Ho RE and the subsequent potential effective dose to others. The effective doses to others were first estimated using the gamma ray constant and were then calculated based on the measured exposure rates. As expected, the estimated effective doses were higher than the measured effective doses because attenuation was not taken into account for the estimated effective doses. There was an excellent correlation between the infused activity and the effective doses based on the lateral measurements at 1.0 m distance ($r^2 = 0.89$) with a constant of 0.163 mSv/GBq of ^{166}Ho. We used this constant to extrapolate the measured values to a whole-liver dose of 60 Gy (3.8 GBq/kg) to gain insight into the radiation exposure of future patients who will be treated with a targeted whole-liver absorbed dose of 60 Gy. Potential effective doses for a range of contact scenarios were calculated, of which some posed a concern (significant caregivers).[14]

A similar study was performed in patients treated with resin or glass ^{90}Y-microspheres.[13] In that study, there was a poor correlation between infused activity of resin microspheres and exposure rates at 1.0 m ($r^2 = 0.21$). This discrepancy may be due to the fact that the measured exposure rate in patients treated with ^{90}Y consists of bremsstrahlung only, and the amount of bremsstrahlung leaving the body is highly dependent on distribution and attenuation; this has less influence on the direct gamma emission from ^{166}Ho. As expected, the exposure rates and effective doses to others from patients treated with ^{166}Ho are higher than for ^{90}Y-RE.[14] Nevertheless, patients treated with ^{166}Ho RE can still be discharged directly after treatment according to the NRC contact scenario. In addition, contact restrictions are necessary only for patients who are discharged within 6 hours after treatment or who received > 7 GBq.

The U.S. NRC guidelines were used as a reference because these regulations apply to the entire United States where a large number of RE-treatments are performed. The threshold for release of patients and need for contact restrictions may be different in other countries. Figure 3 may be used to define restrictions based on administered activity. Although contact restrictions are not required in most

cases, the effective doses should still be minimized by employing all reasonable methods according to the radiation safety ALARA principle.

Despite the limited number of patients in this study, the measurements consistently showed a strong correlation between infused activity and exposure rate and effective dose. Also, as part of this phase 1 dose-escalation study, patients received a wide range of activities. This wide range helped to establish the relationship between infused activity and effective dose and to extrapolate more accurately to higher amounts of activity. The future treatment dose of 60 Gy might be subject to change. It is shown that the dose can be increased (eg, for individualization of treatment based on damage to healthy liver parenchyma) without concerns for radiation safety.

The estimated effective dose to others was limited by the fact that bremsstrahlung radiation and metastable ^{166}Ho were neglected. These components were expected to be much smaller than the exposure from the direct gamma emission. Bremsstrahlung and metastable ^{166}Ho were part of the measured exposure rates and calculated effective doses. True exposure rates were nevertheless underestimated by these measurements because of the limited range of the exposure rate meter (range, 40 keV – 1.5 MeV), especially in the 0-40 keV range. The lower limit is especially relevant for measuring bremsstrahlung because low-energy photons constitute a significant part of the bremsstrahlung spectrum.[15]

Both lateral and frontal exposure rate measurements were performed. For the frontal measurements, the patient needed to sit up in bed, which was impossible shortly after closure of the arterial access site for angiography. The lateral dose rate measurements were easier to perform, were more comfortable for the patient and proved to be more accurate.

Another limitation of this study was the assumption that all radiation was emitted by ^{166}Ho from inside the liver. Similar to resin ^{90}Y-microspheres, it is known that trace amounts of ^{166}Ho may leach into the vascular system.[6,16] Body fluids, especially urine, can be contaminated. Because the lung shunt in the study population, determined by ^{166}Ho SPECT after treatment, was low (≤ 0.7 Gy lung dose), it can be neglected in the analysis.[3]

In conclusion, according to the NRC contact scenario, the effective dose to a contact of a patient treated with ^{166}Ho RE at a targeted 60 Gy whole-liver absorbed dose would not exceed the NRC limit of 5 mSv, not even when the patients is discharged immediately after treatment. Contact restrictions 24 hours after treatment are unnecessary for infused activities < 11 GBq according to the contact scenario and threshold of 1 mSv set by the NRC. Other aspects of radiation safety concerning ^{166}Ho RE, such as the dose to personnel and release through body fluids, need to be studied further.

Acknowledgment

The authors thank epidemiologist Dr. H.M. Verkooijen, for her contribution to the statistical analyses.

References

1. Smits MLJ, Elschot M, van den Bosch M a a J, van de Maat GH, van Het Schip AD, Zonnenberg B a, et al. In Vivo Dosimetry Based on SPECT and MR Imaging of 166Ho-Microspheres for Treatment of Liver Malignancies. J Nucl Med. 2013;54(12):2093–100.
2. Elschot M, Smits MLJ, Nijsen JFW, Lam MGEH, Zonnenberg B a., van den Bosch M a. a. J, et al. Quantitative Monte Carlo-based holmium-166 SPECT reconstruction. Med Phys. 2013;40(11):112502.
3. Elschot M, Nijsen JFW, Lam MGEH, Smits MLJ, Prince JF, Viergever M a, et al. (99m)Tc-MAA overestimates the absorbed dose to the lungs in radioembolization: a quantitative evaluation in patients treated with (166)Ho-microspheres. Eur J Nucl Med Mol Imaging. 2014;41(10):1965-75
4. Elschot M, Nijsen JF, Dam AJ, de Jong HW. Quantitative evaluation of scintillation camera imaging characteristics of isotopes used in liver radioembolization. PLoS One. 2011;6(11):e26174.
5. Nuclear Regulatory Commission, NRC-10 CFR 35.75. Available at http://www.nrc.gov/reading-rm/doc-collections/cfr/part035/part035-0075.html. Accessed October 3, 2012.
6. Smits ML, Nijsen JF, van den Bosch MA, Lam MG, Vente MA, Mali WP, et al. Holmium-166 radioembolisation in patients with unresectable, chemorefractory liver metastases (HEPAR trial): a phase 1, dose-escalation study. Lancet Oncol. 2012;13(10):1025-34.
7. Bolch WE, Bouchet LG, Robertson JS, Wessels BW, Siegel JA, Howell RW, et al. MIRD Pamphlet No. 17: The Dosimetry of Nonuniform Activity Distributions - Radionuclide S Values at the Voxel Level. J Nucl Med. 1999;40(17):11S – 36S.
8. Bol GH, Kotte ANTJ, van der Heide U a, Lagendijk JJW. Simultaneous multi-modality ROI delineation in clinical practice. Comput Methods Programs Biomed. 2009;96(2):133–40.
9. van de Maat GH, Seevinck PR, Elschot M, Smits MLJ, de Leeuw H, van Het Schip AD, et al. MRI-based biodistribution assessment of holmium-166 poly(L-lactic acid) microspheres after radioembolisation. Eur Radiol. 2013;3(23):827–35.
10. INC R consulting and services from IEM. Gamma Ray Dose Constant [Internet]. [cited 2014 Jul 3]. Available from: http://www.iem-inc.com/toolgam.html
11. Bult W, Kroeze SGC, Elschot M, Seevinck PR, Beekman FJ, de Jong HW a M, et al. Intratumoral administration of holmium-166 acetylacetonate microspheres: antitumor efficacy and feasibility of multimodality imaging in renal cancer. PloS One. 2013;8(1):e52178.
12. Breitz HB, Wendt RE, Stabin MS, Shen S, Erwin WD, Rajendran JG, et al. 166Ho-DOTMP radiation-absorbed dose estimation for skeletal targeted radiotherapy. J Nucl Med. 2006;47(3):534–42.
13. McCann JW, Larkin AM, Martino LJ, Eschelman DJ, Gonsalves CF, Brown DB. Radiation emission from patients treated with selective hepatic radioembolization using yttrium-90 microspheres: are contact restrictions necessary? J Vasc Interv Radiol. 2012;23(5):661–7.
14. Gulec S a, Siegel J a. Posttherapy radiation safety considerations in radiomicrosphere treatment with 90Y-microspheres. J Nucl Med. 2007;48(12):2080–6.
15. Rault E, Staelens S, Van Holen R, De Beenhouwer J, Vandenberghe S. Fast simulation of yttrium-90 bremsstrahlung photons with GATE. Med Phys. 2010;37(6):2943–50.
16. Lambert B, Sturm E, Mertens J, Oltenfreiter R, Smeets P, Troisi R, et al. Intra-arterial treatment with (90)Y microspheres for hepatocellular carcinoma: 4 years experience at the Ghent University Hospital. Eur J Nucl Med Mol Imaging. 2011;38(12):2117–24.

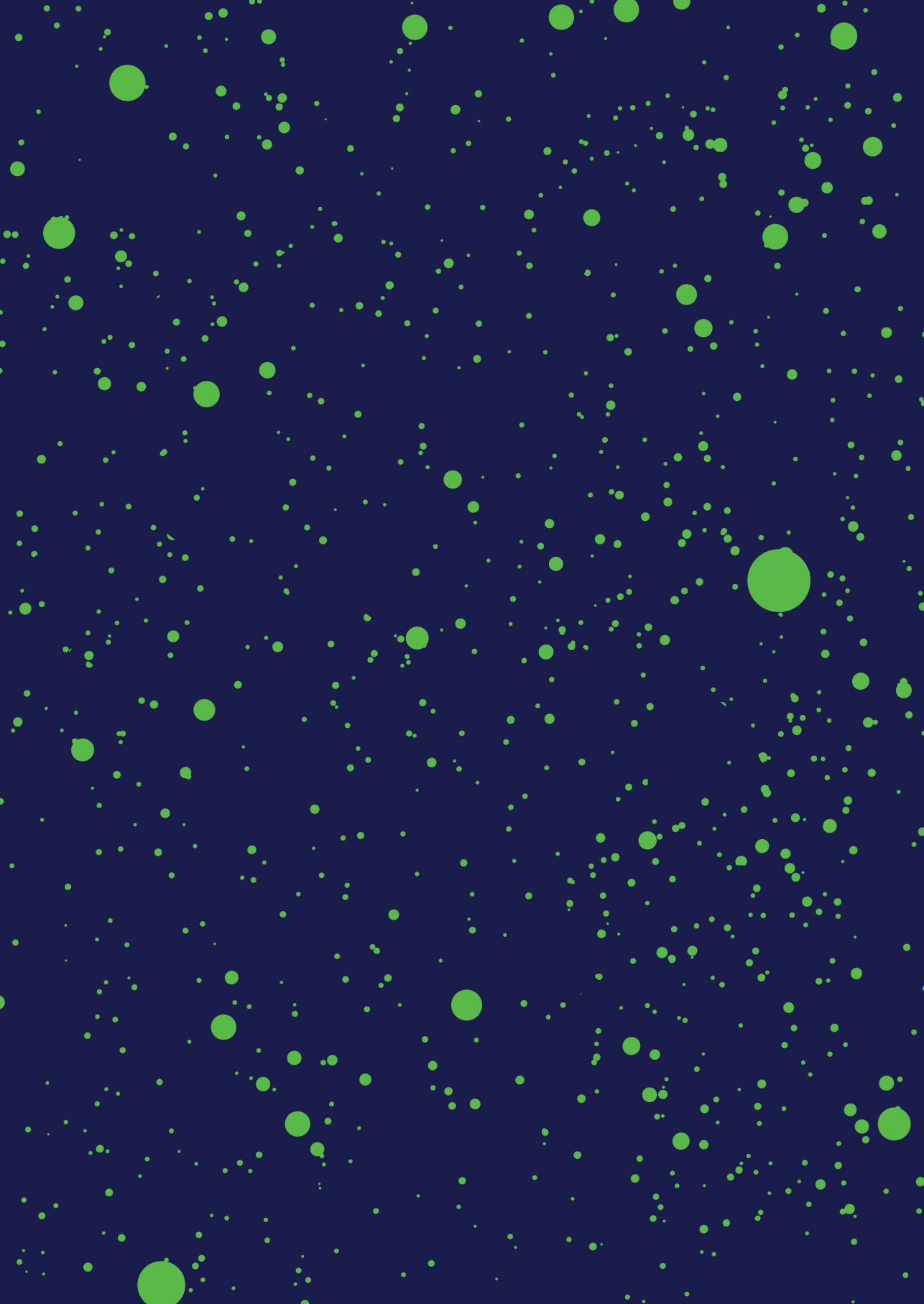

CHAPTER 8

General Discussion

To put our research into context, the position of radioembolization and ^{166}Ho microspheres in current treatment algorithms is discussed. Also, the differences with other microspheres are highlighted. Starting with the benefit ^{166}Ho microspheres can provide, future improvements to radioembolization are discussed.

Is radioembolization effective?

Yes, although the current evidence is limited. The effectiveness seems to differ for each type of cancer and for the timing of treatment initiation (first-line or salvage setting). Some types of cancer are more suitable for liver-directed treatment, because they metastasize to the liver first, such as colorectal cancer. Because this is the largest group of eligible patients, the effectiveness is discussed for this particular patient population. Other tumor types may be eligible for radioembolization, but either the evidence is limited or these tumor types were not included in the studies for ^{166}Ho microspheres (e.g., hepatocellular carcinoma). All effectiveness studies in literature have, thus far, been performed with ^{90}Y microspheres (for colorectal cancer mostly with resin microspheres [SIR-Spheres, SIRTeX Medical Ltd., Australia]).

Two small randomized controlled trials showed a benefit for performing radioembolization in patients who could still undergo treatment with chemotherapy. In studies by Gray et al.[1] and Hazel et al.[2], patients were randomized to receive radioembolization in addition to hepatic arterial infusion of floxuridine or intravenous infusion of fluorouracil/leucovorin respectively. Radioembolization caused a significant delay in the progression of liver tumors in both trials, but a significant extension of survival in the second trial only (intravenous fluorouracil/leucovorin ± radioembolization). In addition, the interim results of a more recent, and much larger, randomized controlled trial, the SIRFLOX trial, also showed a delay in progression of liver tumors, but not in progression of tumors at other sites.[3] The survival data of the SIRFLOX trial are expected in 2017. At this moment, these results provide enough evidence to warrant clinical trials, but not enough to incorporate radioembolization in the treatment paradigm as first-line treatment for colorectal cancer.

In salvage patients, for whom best supportive care is the only alternative, radioembolization is supported by more evidence. In a recent systematic review, Rosenbaum et al. concluded that radioembolization can increase survival. Approximately 50% of patients survive more than 12 months.[4] Two

trials are noteworthy. First, Hendlisz et al. performed a randomized trial to compare a patient group with and without radioembolization (with ^{90}Y resin microspheres) in addition to intravenous fluorouracil.[5] Radioembolization was given after patients became refractory to standard chemotherapy. The progression free survival in the liver was extended (from 2.1 to 5.5 months, p = 0.003), but survival was not (from 7.3 to 10.0 months, p = 0.80). However, the study was small (n = 44) and 10 of 21 patients crossed over and received radioembolization at a later stage. Second, Seidensticker et al. matched 29 patients who received radioembolization with 29 of over 500 other patients based on prior treatments, tumor burden, timing of metastases (synchronous or metachronous), alkaline phosphatase and carcinoembryonic antigen. They concluded that radioembolization did extend the median survival, by 4.8 months (from 3.5 to 8.3 months, p < 0.001).[6] These results provide enough evidence to offer radioembolization to salvage patients to extend their survival with relatively few side-effects.[7]

Is radioembolization with ^{166}Ho microspheres effective?

Yes, both because the mode of action is comparable to ^{90}Y resin microspheres and because we found comparable efficacy in the HEPAR 2 trial. Although differences exist, the microspheres are in the same order of magnitude of: size, number of microspheres, energy of beta radiation, and aimed absorbed dose to the liver (Table 1).[8] The shared properties imply that the microspheres roughly distribute identically in the liver, and deposit roughly the same amount of energy to induce comparable cell damage.

Accordingly, the HEPAR 2 trial showed an effect in 38 salvage patients with metastatic disease; 49% of patients responded for at least 3 months (45% of colorectal cancer patients). The metabolic response, measured on ^{18}F-FDG-PET/CT, showed a comparable response of 53%, strengthening the claim of efficacy. For colorectal cancer patients, a response was seen in 59% of patients in the study by Seidensticker et al.[6] and in 86% in the study by Hendlisz et al.[5] Rosenbaum et al. concluded in their review that a response was seen in 29-90% of patients.[4] The median overall survival for colorectal patients was 14.4 months, which compares favorably with studies mentioned earlier (range, 2.1 – 10.0 months) and fits well in the range of survival data from other radioembolization studies (8.3 – 15.2 months).[4]

The data from the HEPAR 2 were deliberately planned to be collected in a small scale phase 2 study in a short time frame. Only efficacy in a relatively small study could justify further up scaling of expenditures. Within three years, efficacy was shown and a CE marking was obtained. Further studies on the efficacy of ^{166}Ho radioembolization deserve to be more resource intensive, for example by randomizing patients to compare treatment with either a placebo (or best supportive care), chemotherapy, or other microspheres.

Currently, radioembolization with ^{166}Ho microspheres is indicated for salvage patients, preferably in a research setting. If, for example, the SIRFLOX trial shows a benefit of adding ^{90}Y radioembolization to first-line chemotherapy, a non-inferiority trial can potentially test if ^{166}Ho radioembolization offers the same benefit without repeating the same investments.[9]

Table 1. *Microsphere characteristics*

Characteristic	^{166}Ho microspheres	SIR-Spheres	TheraSphere
Isotope	Holmium-166	Yttrium-90	
Half-life (h)	26.8	64.1	
Deposited energy (J/GBq)	15.9	49.4	
Maximum β⁻energy (MeV)	1.85 (50.0%) 1.77 (48.7%)	2.28 (100%)	
γ-energy (keV)	80.6 (6.6%) 1,379 (0.9%)	none[1]	
Decay product	Erbium-166	Zirconium-90	
Matrix material	Poly(L-lactic acid)	Resin	Glass
Diameter (μm)	30±15	32.5±2.5	25±10
Density (g/mL)	1.4	1.6	3.3
Number per dose	33,000,000	50,000,000	4,000,000
Activity/microsphere (Bq)	300-330	40-70	2,400-2,700

[1] *Abundance of gamma photons is very low, 0.02% (1,761 keV)*

What side effects can be expected after ^{166}Ho radioembolization?

Transient side effects occur in the majority of patients.[8] In the hours after treatment, patients often report an abdominal pressure or pain, frequently accompanied by nausea (± vomiting), which can be managed by analgesic and/or antiemetic medication.[10] These complaints usually subside within 24 hours after treatment, at which time patients are released. At home, some patients report that these complaints reoccur temporary and in a lesser degree. The onset of complaints is often during or immediately after treatment, indicating that embolization induced ischemia is probably the cause, similar to chemoembolization.[11]

Radiation damage accumulates during the following hours and days, whereupon cells go into apoptosis. At that time, increasing pain, nausea and vomiting which limit activities of daily living can indicate extra hepatic deposition of microspheres, and are an indication for acquiring a SPECT/CT (possible up to 4-6 days after treatment). The microsphere distribution can be assessed to evaluate the risk of gastrointestinal ulceration or pancreatitis. After a week, patients often start to be fatigued, which slowly subsides after 2-4 weeks. Pain, loss of appetite, and fatigue were also the most affected symptoms on the quality of life questionnaires of the HEPAR 2. These symptoms showed an increase after 1 week and were almost at baseline levels at 6 weeks.

For 4-8 weeks after treatment, the physician should be aware of radioembolization induced liver disease (REILD), a rare complication with an increased mortality rate which is signaled by jaundice (increasing bilirubin levels) and ascites.[12] Long term toxicity data are sparse for ^{166}Ho microspheres, however, there is no conclusive evidence for any long term toxicities.

Which type of microspheres should be used for radioembolization?

Radioembolization is currently performed with ^{90}Y microspheres, either glass (TheraSphere®, BTG, Canada) or resin microspheres (SIR-Spheres®, SIRTeX Medical Ltd., Australia). The choice between them is based on published trials and the preference of the treating physician. For ^{90}Y resin microspheres, most literature concerns colorectal cancer patients[1,2,5], while literature for ^{90}Y glass microspheres concerns mostly hepatocellular carcinoma patients.[13] To put this in perspective: in 2012, 68% of interviewed European centers exclusively used ^{90}Y resin microspheres and only 25% of centers used both ^{90}Y resin and glass microspheres.[14] Since ^{166}Ho microspheres obtained CE-marking in 2015, there will soon be three commercially available types of microspheres. In contrast to ^{90}Y, ^{166}Ho microspheres can be used as a scout dose to predict the distribution of the treatment dose, for example to estimate the lung dose or the intrahepatic distribution. If, in the future, the use of a scout dose becomes indispensable for radioembolization, ^{166}Ho microspheres might be preferred over ^{90}Y microspheres.

At this moment, the established, most important differences between the types of microspheres are the amount of embolization and the lung shunt estimation. Differences in, for example, density, matrix material, aimed absorbed dose, mean

beta particle energy, dose-rate and half-life have not led to meaningful differences in clinical practice yet. This may change in the future because research into these specifications is increasing.[15,16] These characteristics do influence the manufacturing processes and explain why, for example, ^{90}Y glass microspheres have a longer shelf life (with more flexibility in specific activity), or which nuclear reactors are designated for production based on neutron flux and/or logistic reasons.[17]

The first important difference is the amount of embolization, which differs between microspheres because of the specific activity. The amount of energy released, is greater per ^{90}Y glass sphere compared to a ^{90}Y resin sphere or ^{166}Ho microsphere (around 2,500 instead of 50 or 300 Bq/sphere). Radioembolization with ^{90}Y glass microspheres requires infusion of only around 4 million spheres, instead of 50 or 33 million respectively (Table 1). Stasis of blood flow is seldom seen during infusion of ^{90}Y glass microspheres, while this is much more common for ^{90}Y resin microspheres (20-28%), even after the recent switch in carrier fluid (11% using glucose 5% water instead of sterile water).[18,19] In the HEPAR 2 trial, the mean percentage of administered ^{166}Ho microspheres was comparable to ^{90}Y resin microspheres (91.4 ±10.2% vs. 99.6±11.0%).[18] Stasis increases the risk of reflux, extrahepatic deposition of microspheres, and gastrointestinal ulceration or pancreatitis.[20] Indeed, the risk of ulceration has been reported to be lower for ^{90}Y glass microspheres.[21] This is especially relevant for segmental treatments, during which a high number of microspheres is injected in a limited target volume to reach high target doses.[22] An anti-reflux catheter might mitigate the risks by decreasing the downstream pressure and preventing reflux.[23]

The second important difference is that the estimation of the lung shunt after treatment is difficult using ^{90}Y microspheres, while it can be accurately performed with SPECT/CT after administration of ^{166}Ho microspheres. Some patients have a high arteriovenous shunt in their liver tumors which can cause the microspheres to deposit in the lungs after treatment, where they potentially induce radiation pneumonitis.[24] Screening is classically performed by injection of ^{99m}Tc-MAA, but no correlation with the amount of lung shunt after treatment has ever been shown (except by Jha et al, which is refuted in Chapter 1).[25] Elschot et al. showed that a scout dose of ^{166}Ho microspheres is superior in estimating the lung dose.[26] However, the lung doses they found were very low (median 0.02 Gy; range, 0 – 0.7 Gy). In the HEPAR 2 trial, no lung shunt was seen after treatment (maximum 0.8%). We

hypothesize that a lung shunt can only lead to radiation pneumonitis when the arteriovenous shunt is large enough for microspheres to cross, at which time the lung shunt estimation of ^{99m}Tc-MAA is already very large (>>20%). This explains why Elschot et al. saw no high lung doses; no patient with a sufficient arteriovenous shunt was included. It also invalidates ^{99m}Tc-MAA for screening and underlines the importance of using the same type of microspheres as a scout and treatment dose, as is the case for ^{166}Ho microspheres. A high lung shunt is the most common motivation to reduce the treatment activity. This needlessly reduces the efficacy of radioembolization, as is suggested in an article by Ward et al. in which 47% of patients with a reduction responded to ^{90}Y resin radioembolization in contrast to 94% of patients without a dose reduction.[27]

Besides these two differences, which are evident today, other differences between the microspheres are being investigated. The most relevant possible differences include adverse events after treatment, radiobiological effect, and imaging capabilities. Research into the differences between adverse events is still scarce. Unpublished data from Thorlund et al. indicate that ^{90}Y glass microspheres induce less fatigue, abdominal pain and nausea than ^{90}Y resin microspheres.[21] In practice, differences between microspheres are evident; patients treated with ^{90}Y resin microspheres or ^{166}Ho microspheres can experience abdominal pain and nausea in the angiography suite, while patients treated with ^{90}Y glass microspheres often experience this when discharged. In the case of ^{90}Y resin microspheres or ^{166}Ho microspheres, this pain, earlier ascribed to hypoxia, often disappears the same night and can be explained by the increased embolization. Patients treated with any of the three microspheres seem to experience abdominal pain, nausea and fatigue to some extent when at home.

Another difference is the radiobiological effect, caused by differences in specific activity. ^{90}Y glass microspheres are assumed to disperse the radiation dose more heterogeneously. This may explain why a higher radioactivity (around 4 GBq) is given compared with ^{90}Y resin microspheres (around 2.5 GBq): on average, a more heterogeneous distribution decreases the damage done to liver tissue.[28] In contrast, ^{90}Y resin microspheres or ^{166}Ho microspheres are assumed to have a more homogeneous distribution, through the increase in number, and are thus more toxic to normal liver tissue.[29] Accordingly, a more homogeneous distribution may require less absorbed dose to tumors to be equally effective as a heterogeneous

distribution. Bourgeois et al. presented an abstract in which they showed that a low number of ^{90}Y glass microspheres can result in microscopic dose differences in a simulation study.[16] These findings currently do not influence patient care (e.g., in the form of individualized dosimetric planning before radioembolization). In the future, for example, patients with a high uptake in a single tumor could be given less embolic ^{90}Y glass microspheres to increase the tumor absorbed dose, while patients with low uptake in multiple tumors could be treated with more embolic microspheres such as ^{90}Y resin or ^{166}Ho microspheres to cover the tumors as much as possible. Lewandowski et al. used so-called extended shelf-life ^{90}Y glass microspheres (12 days) to increase the number of microspheres; the half-life of ^{90}Y of approximately 3 days implies that a 16-fold (2^4) increase in the number of microspheres is theoretically possible.[30]

Other differences include the different imaging modalities used for ^{90}Y and ^{166}Ho; ^{90}Y can be imaged using Bremsstrahlung SPECT and PET, ^{166}Ho using SPECT and MR imaging. ^{90}Y cannot be used for imaging of a scout dose, which, on the contrary, is possible with SPECT imaging of ^{166}Ho.[31] Therefore, imaging of ^{90}Y is never performed as a scout dose and is limited to detection of extrahepatic deposition after treatment. If a treatment consists of multiple infusions of ^{90}Y microspheres, imaging in between takes an impractical amount of time but is feasible, as shown by Bourgeois et al., who performed two injections with ^{90}Y-PET imaging in between.[32] MR imaging of Ho can offer real-time imaging in addition to a higher resolution, as well as imaging of non-radioactive microspheres.[33,34]

How can ^{166}Ho radioembolization be improved?

The most pressing improvements are in efficacy and safety. Because efficacy is dependent on the absorbed dose, increasing the dose should increase efficacy (but will also increase toxicity). The maximum absorbed dose to the liver that was found to be safe in the HEPAR 1 trial (60 Gy) was based on only 15 patients.[8] Until the response rate is 100%, efficacy can theoretically be increased by increasing the absorbed dose. At some point, the rate of toxicity becomes unacceptable, and the balance of efficacy and toxicity must be assessed. At 60 Gy, there is a response, as is shown in the HEPAR 2, while toxicity is limited; all major toxicities were transient, except for one case of REILD (incidence of 1%). It is unknown whether an increase in absorbed dose would increase: the incidence of the post radioembolization syndrome, the extent of the post radioembolization syndrome, or the incidence of

REILD. Because only 1 patient developed REILD, it should be possible to increase the dose in order to increase the efficacy.

Rather than increasing the aimed absorbed dose in the whole population, a scout dose of ^{166}Ho microspheres can improve patient selection through individualized treatment. If the distribution of a scout dose accurately predicts the distribution of the treatment dose, efficacy and toxicity can be predicted based on the estimated dose to tumors and healthy liver parenchyma. In essence, the dose can be expressed as a ratio of uptake between the tumor and healthy liver: 1 indicates a similar uptake in tumor and healthy liver, while, for example, 2 indicates that twice the amount of radiation is deposited in tumor compared with the healthy liver. Smits et al. found that the median ratio of uptake in the tumor of the 15 HEPAR 1 patients was 1.5 (range, 0.9 – 2.8). Patients with a higher ratio can be given more radiation without harmful effects to healthy liver parenchyma (and the risk of REILD). Alternatively, patients with a ratio smaller than 1 possibly do not benefit from treatment and could be spared the toxicity. Also, this can be tailored per artery as Kao et al. have suggested.[35] However, Smits et al. found that in only 40% (6/15) of patients, all tumors had a ratio higher than 1. Treatment will be limited by toxicity in the other 60%. Still, if radioembolization becomes tailored to individual patients, it would probably increase the efficacy that is already present, and decrease toxicity for patients who experience little efficacy, which would result in benefit for all patients.

One way to individualize treatment is to calculate the increase in absorbed dose by simultaneously assessing the amount of radiation the healthy liver and tumors receive.[36] In the HEPAR Plus trial, patients with neuroendocrine tumors receive peptide receptor radionuclide therapy followed by ^{166}Ho radioembolization (ClinicalTrials.gov, NCT02067988). The administration of ^{166}Ho microspheres is followed by a simultaneous acquisition of the distribution of ^{166}Ho microspheres and ^{99m}Tc-labelled sulfur colloid. The distribution of ^{166}Ho microspheres provides information about the distribution of the absorbed dose, while the ^{99m}Tc-labelled sulfur colloid provides a delineation between healthy liver parenchyma and tumors.[36] Accurately quantifying both isotopes is challenging, but enables the calculation of the optimal activity which needs to be administered to achieve maximum efficacy and safety. For ^{166}Ho microspheres, the same can be achieved in MR imaging by quantification of holmium and administration of gadoxetate disodium to delineate the healthy liver parenchyma.

How can radioembolization be improved in general?

One way, for which there has been a lot of attention in recent literature, is to change the way the administered activity is calculated. There are currently three methods.[28] The first corresponds to a 'one size fits all', which is, for example, still the case for a scout dose of ^{166}Ho microspheres (always 250 MBq). The second tailors the administered activity to every patient, like the body surface area method that is used for ^{90}Y resin microspheres. In non-oncological patients, the body surface area is related to liver size, so the amount of activity is calculated based on the body surface area. The third method includes the amount of liver tissue (as measured using, e.g., CT) and the ratio of uptake of the tumor(s) and healthy liver, assessed by a scout dose. In this method, three compartments are identified, each with a specific aimed absorbed dose: the lungs, the healthy liver, and the tumor(s). The administered activity is maximized with constraints applied to each of the compartments (e.g., 30 Gy for the lungs). There are two implicit assumptions. First, the scout dose distribution should accurately predict the treatment dose distribution, which might not be the case for ^{99m}Tc-MAA and ^{90}Y.[37] Second, the *mean* absorbed dose over the compartment should predict efficacy and safety.[28] Similar to ^{166}Ho microspheres, the resulting individualization of treatment is expected to increase efficacy for patients who already showed response, while decreasing toxicity for patients who showed little response.

Fortunately, multiple other variables can also be controlled, such as: the injection position(s), the type of catheter used, concomitant medication, the number of microspheres, the time in which radiation is deposited (the dose rate), the number of repeat treatments or dose intensifications after posttreatment imaging. Besides adjusting the treatment itself, the timing and indications provide many new opportunities. In this thesis, radioembolization was only performed in a salvage setting, but radioembolization can also be used: as a first line treatment (concurrent with chemotherapy and/or surgery)[38], to downstage patient for resection, or to perform a radiation segmentectomy.[22]

To illustrate these new indications, radiation segmentectomy can increase response rates by choosing a more distal injection site and increasing the absorbed dose by increasing the administered activity.[22] It could also be an alternative for surgery of a liver segment or lobe. Also, it was shown that the intravascular pressure can improve or decrease tumor targeting.[39] This is currently under

investigation in the SIM trial (ClinicalTrial.gov, NCT02208804), in which patients are treated with a normal catheter in one liver lobe and an antireflux catheter in the other (within-patient randomization). For the primary outcome, the investigators compare the uptake in tumors and normal tissue between the two liver lobes. Along the same line, a review showed that tumor targeting is vastly improved by injection of angiotensin II prior to infusion of microspheres[40], but intra-arterial medication to improve tumor targeting is rarely used. Alternatively, the number of microspheres can be adjusted by letting the radioactive element decay and using more microspheres (to achieve the same dose).[30] This can be used to achieve higher degrees of embolization and thus different radiobiologic effects.[28] Possibly, repeated radioembolization treatments could have the same effect as fractionation radiotherapy, allowing healthy cells to recover while affecting tumor cells that were in a different (protective) cell cycle during the prior treatments. In conclusion, there are far more treatment strategies that can be implemented than just a single injection with a single dose.

How can the role of radiology for cancer treatment be improved?

The role of radiologists in cancer treatment is underutilized, mostly because of a lack of publicity. Radioembolization serves as a suitable illustration. In the past years, the UMC Utrecht has had several appearances in Dutch national media, all followed by increased patient referrals. Several participants never considered radiology (i.e., interventional radiology and nuclear medicine) to be able to treat them. More surprisingly, their oncologists never mentioned the treatments radiology had to offer. One cause might be that, as a medical specialty, radiology is only available by referral. While a surgeon can diagnose and treat a patient without any referral, a radiologist is dependent on the referrals from other medical specialists. This disassociation between diagnosis and treatment prevents overtreatment, but has currently led to a situation of *under*treatment. This is manifest in the small number of patients who are referred for radioembolization, even though it is currently mentioned in the evidence based guidelines for colorectal cancer.[7]

Solutions are readily available and not difficult to implement. One solution would be to promote radiological treatments in multidisciplinary tumor boards. In these boards, the radiologist can inform other specialists about the treatments that are possible for each patients. Cancer treatments already depend heavily on imaging for diagnosis, selection and treatment evaluation, so the referring specialist

can be informed about treatment options in addition to the imaging outcome. For radioembolization, this might no longer be relevant, but it is paramount for the development of future radiologic techniques such as high intensity focus ultrasound.

As radiology and nuclear medicine grow towards each other, training for both specialties has been joint since 2015 and the staff of both specialties has been integrated in the UMC Utrecht. These developments question the boundaries of a medical specialty. Classically, boundaries have been formed by technique (surgery, radiology) or disease (oncology, cardiologists). However, as radiologists (including nuclear medicine physicians) have started treating patients, they have crossed these boundaries. For radioembolization, more and more radiobiological knowledge stems from radiation oncology.[28] At the same time, radiation oncology uses image-guidance to improve treatment outcomes. From a patient's perspective, disease-based subdivisions are more helpful. The new training for radiologists is centered on anatomical substrates instead of techniques. Instead of 3 physicians, a single 'image-guided treatment physician' could inform both patients and other specialists about possible treatments for liver metastasis: ablation (radiology), radioembolization (nuclear medicine) or stereotactic radiation treatment (radiotherapy). The treatment can subsequently be performed by superspecialists, as is the case for radiology today.

In conclusion, radioembolization has evolved from single infusion of ceramic spheres loaded with ^{90}Y (in the 1960s) to an individualized treatment with ^{166}Ho microspheres. The results of several large randomized trials will appear in the coming years. Generally, image guided treatments will become more prominent and will further transform radiology from a diagnostic service to a comprehensive specialty.

References

1. Gray B, Hazel GV, Hope M, Burton M, Moroz P, Anderson J, et al. Randomised trial of SIR-Spheres® plus chemotherapy vs. chemotherapy alone for treating patients with liver metastases from primary large bowel cancer. Ann Oncol. 2001;12(12):1711–20.
2. Van Hazel G, Blackwell A, Anderson J, Price D, Moroz P, Bower G, et al. Randomised phase 2 trial of SIR-Spheres plus fluorouracil/leucovorin chemotherapy versus fluorouracil/leucovorin chemotherapy alone in advanced colorectal cancer. J Surg Oncol. 2004;88(2):78–85.
3. Gibbs P, Heinemann V, Sharma NK, Findlay MPN, Ricke J, Gebski V, et al. SIRFLOX: Randomized phase III trial comparing first-line mFOLFOX6 {+/-} bevacizumab (bev) versus mFOLFOX6 + selective internal radiation therapy (SIRT) {+/-} bev in patients (pts) with metastatic colorectal cancer (mCRC). ASCO Meet Abstr. 2015;33(15_suppl):3502.
4. Rosenbaum CENM, Verkooijen HM, Lam MGEH, Smits MLJ, Koopman M, van Seeters T, et al. Radioembolization for treatment of salvage patients with colorectal cancer liver metastases: a systematic review. J Nucl Med. 2013;54(11):1890–5.
5. Hendlisz A, Eynde MV den, Peeters M, Maleux G, Lambert B, Vannoote J, et al. Phase III Trial Comparing Protracted Intravenous Fluorouracil Infusion Alone or With Yttrium-90 Resin Microspheres Radioembolization for Liver-Limited Metastatic Colorectal Cancer Refractory to Standard Chemotherapy. J Clin Oncol. 2010;28(23):3687–94.
6. Seidensticker R, Denecke T, Kraus P, Seidensticker M, Mohnike K, Fahlke J, et al. Matched-Pair Comparison of Radioembolization Plus Best Supportive Care Versus Best Supportive Care Alone for Chemotherapy Refractory Liver-Dominant Colorectal Metastases. Cardiovasc Intervent Radiol. 2011;35(5):1066–73.
7. Van Cutsem E, Cervantes A, Nordlinger B, Arnold D, ESMO Guidelines Working Group. Metastatic colorectal cancer: ESMO Clinical Practice Guidelines for diagnosis, treatment and follow-up. Ann Oncol. 2014;25 Suppl 3:iii1–9.
8. Smits ML, Nijsen JF, van den Bosch MA, Lam MG, Vente MA, Mali WP, et al. Holmium-166 radioembolisation in patients with unresectable, chemorefractory liver metastases (HEPAR trial): a phase 1, dose-escalation study. Lancet Oncol. 2012;13(10):1025-34.
9. Kaji AH, Lewis RJ. Noninferiority trials: Is a new treatment almost as effective as another? JAMA. 2015;313(23):2371–2.
10. Peterson JL, Vallow LA, Johnson DW, Heckman MG, Diehl NN, Smith AA, et al. Complications after 90Y microsphere radioembolization for unresectable hepatic tumors: An evaluation of 112 patients. Brachytherapy. 2013;12(6):573–9.
11. Leung DA, Goin JE, Sickles C, Raskay BJ, Soulen MC. Determinants of postembolization syndrome after hepatic chemoembolization. J Vasc Interv Radiol. 2001;12(3):321–6.
12. Sangro B, Gil-Alzugaray B, Rodriguez J, Sola I, Martinez-Cuesta A, Viudez A, et al. Liver disease induced by radioembolization of liver tumors: description and possible risk factors. Cancer. 2008;112(7):1538–46.
13. Salem R, Lewandowski RJ, Kulik L, Wang E, Riaz A, Ryu RK, et al. Radioembolization results in longer time-to-progression and reduced toxicity compared with chemoembolization in patients with hepatocellular carcinoma. Gastroenterology. 2011;140(2):497–507.e2.
14. Powerski MJ, Scheurig-Münkler C, Banzer J, Schnapauff D, Hamm B, Gebauer B, et al. Clinical practice in radioembolization of hepatic malignancies: a survey among interventional centers in Europe. Eur J Radiol. 2012;81(7):e804–11.
15. Ahuja C., Chadha M., Critchfield J.J., Kharoti Y., Kaufman J.A., Farsad K., et al. Comparison of resin versus glass microsphere radioembolization for neuroendocrine hepatic metastasis: Clinical and imaging response. J Vasc Interv Radiol. 2014;25(5):817.e26.
16. Bourgeois A.C., Bradley Y.C., McElmurray J., Pasciak A. Does the number of infused microspheres impact tumor dose in radioembolization? An analysis of resin versus glass Yttrium-90 microspheres. J Vasc Interv Radiol. 2015;26(2):S111.
17. Vente M a D, Nijsen JFW, de Roos R, van Steenbergen MJ, Kaaijk CNJ, Koster-Ammerlaan MJJ, et al. Neutron activation of holmium poly(L-lactic acid) microspheres for hepatic arterial radioembolization: a validation study. Biomed Microdevices. 2009;11(4):763–72.

18. Ahmadzadehfar H, Meyer C, Pieper CC, Bundschuh R, Muckle M, Gärtner F, et al. Evaluation of the delivered activity of yttrium-90 resin microspheres using sterile water and 5 % glucose during administration. EJNMMI Res. 2015;5(1):54.

19. Piana PM, Bar V, Doyle L, Anne R, Sato T, Eschelman DJ, et al. Early arterial stasis during resin-based yttrium-90 radioembolization: incidence and preliminary outcomes. HPB. 2014;16(4):336–41.

20. Lam MGEH, Banerjee S, Louie JD, Abdelmaksoud MHK, Iagaru AH, Ennen RE, et al. Root cause analysis of gastroduodenal ulceration after yttrium-90 radioembolization. Cardiovasc Intervent Radiol. 2013;36(6):1536–47.

21. Thorlund K., Balijepalli C., Ebrahim S., Sinclair P., Fowers K., Rychcik J.L., et al. Safety of Y90 glass and resin microspheres for the treatment of hepatocellular carcinoma: A systematic review. J Vasc Interv Radiol. 2015;26(2):S109.

22. Riaz A, Gates VL, Atassi B, Lewandowski RJ, Mulcahy MF, Ryu RK, et al. Radiation Segmentectomy: A Novel Approach to Increase Safety and Efficacy of Radioembolization. Int J Radiat Oncol. 2011;79(1):163–71.

23. Fischman AM, Ward TJ, Patel RS, Arepally A, Kim E, Nowakowski FS, et al. Prospective, Randomized Study of Coil Embolization versus Surefire Infusion System during Yttrium-90 Radioembolization with Resin Microspheres. J Vasc Interv Radiol. 2014;25(11):1709–16.

24. Gaba RC, Zivin SP, Dikopf MS, Parvinian A, Casadaban LC, Lu Y, et al. Characteristics of primary and secondary hepatic malignancies associated with hepatopulmonary shunting. Radiology. 2014;271(2):602–12.

25. Jha AK a, Zade A a, Rangarajan V, Purandare N, Shah S a, Agrawal A, et al. Comparative analysis of hepatopulmonary shunt obtained from pretherapy 99mTc MAA scintigraphy and post-therapy 90Y Bremsstrahlung imaging in 90Y microsphere therapy. Nucl Med Commun. 2012;33(5):486–90.

26. Elschot M, Nijsen JFW, Lam MGEH, Smits MLJ, Prince JF, Viergever M a, et al. (99m)Tc-MAA overestimates the absorbed dose to the lungs in radioembolization: a quantitative evaluation in patients treated with (166)Ho-microspheres. Eur J Nucl Med Mol Imaging. 2014;41(10):1965–75.

27. Ward TJ, Tamrazi A, Lam MGEH, Louie JD, Kao PN, Shah RP, et al. Management of High Hepatopulmonary Shunting in Patients Undergoing Hepatic Radioembolization. J Vasc Interv Radiol. 2015;26(12):1751-60.

28. Cremonesi M, Chiesa C, Strigari L, Ferrari M, Botta F, Guerriero F, et al. Radioembolization of hepatic lesions from a radiobiology and dosimetric perspective. Front Oncol. 2014;4:210.

29. Salem R, Thurston KG. Radioembolization with 90Yttrium microspheres: a state-of-the-art brachytherapy treatment for primary and secondary liver malignancies. Part 1: Technical and methodologic considerations. J Vasc Interv Radiol. 2006;17(8):1251–78.

30. Lewandowski RJ, Minocha J, Memon K, Riaz A, Gates VL, Ryu RK, et al. Sustained safety and efficacy of extended-shelf-life (90)Y glass microspheres: long-term follow-up in a 134-patient cohort. Eur J Nucl Med Mol Imaging. 2014 ;41(3):486-93.

31. Elschot M. Quantitative nuclear imaging for dosimetry in radioembolization. PhD [dissertation]. Utrecht University; 2013.

32. Bourgeois AC, Chang TT, Bradley YC, Acuff SN, Pasciak AS. Intraprocedural yttrium-90 positron emission tomography/CT for treatment optimization of yttrium-90 radioembolization. J Vasc Interv Radiol. 2014;25(2):271–5.

33. van de Maat GH, Seevinck PR, Elschot M, Smits MLJ, de Leeuw H, van Het Schip AD, et al. MRI-based biodistribution assessment of holmium-166 poly(L-lactic acid) microspheres after radioembolisation. Eur Radiol. 2013;3(23):827–35.

34. Nijsen JFW, Seppenwoolde J-H, Havenith T, Bos C, Bakker CJG, van het Schip AD. Liver tumors: MR imaging of radioactive holmium microspheres–phantom and rabbit study. Radiology. 2004;231(2):491–9.

35. Kao YH, Tan AEH, Burgmans MC, Irani FG, Khoo LS, Lo RHG, et al. Image-Guided Personalized Predictive Dosimetry by Artery-Specific SPECT/CT Partition Modeling for Safe and Effective 90Y Radioembolization. J Nucl Med. 2012;53(4):559–66.

36. Lam MGEH, Goris ML, Iagaru AH, Mittra ES, Louie JD, Sze DY. Prognostic Utility of 90Y Radioembolization Dosimetry Based on Fusion 99mTc-Macroaggregated Albumin-99mTc-Sulfur Colloid SPECT. J Nucl Med. 2013;54(12):2055–61.

37. Wondergem M, Smits MLJ, Elschot M, de Jong HWAM, Verkooijen HM, van den Bosch MAAJ, et al. 99mTc-macroaggregated albumin poorly predicts the intrahepatic distribution of 90Y resin microspheres in hepatic radioembolization. J Nucl Med. 2013;54(8):1294–301.

38. Braat AJAT, Huijbregts JE, Molenaar IQ, Borel Rinkes IHM, van den Bosch MAAJ, Lam MGEH. Hepatic radioembolization as a bridge to liver surgery. Front Oncol. 2014;4:199.

39. Pasciak AS, McElmurray JH, Bourgeois AC, Heidel RE, Bradley YC. The impact of an antireflux catheter on target volume particulate distribution in liver-directed embolotherapy: a pilot study. J Vasc Interv Radiol. 2015;26(5):660–9.

40. van den Hoven AF, Smits MLJ, Rosenbaum CENM, Verkooijen HM, van den Bosch M a. a. J, Lam MGEH. The Effect of Intra-Arterial Angiotensin II on the Hepatic Tumor to Non-Tumor Blood Flow Ratio for Radioembolization: A Systematic Review. Morishita R, editor. PLoS ONE. 2014;9(1):e86394.

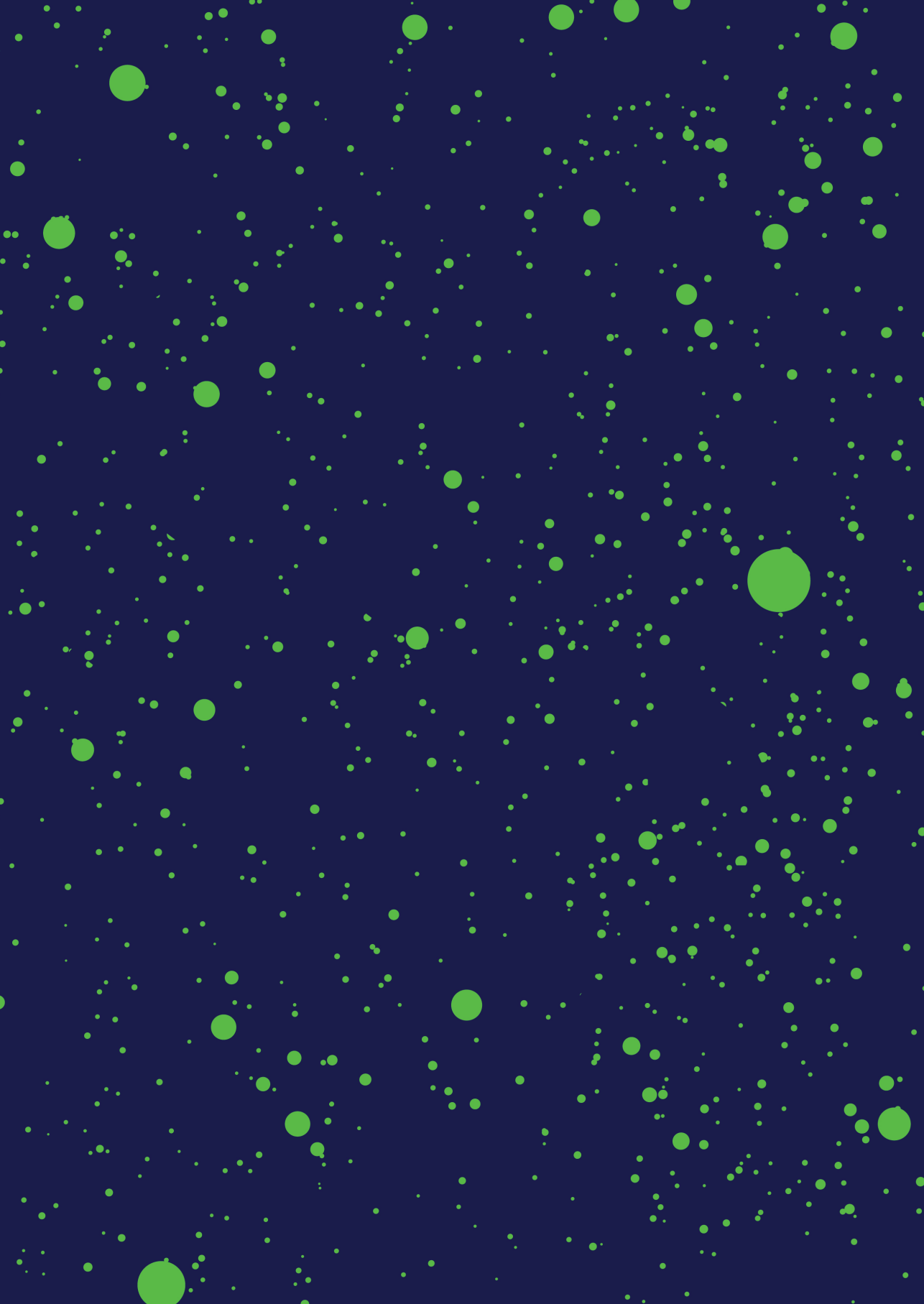

CHAPTER 9

Summary

This thesis describes the application of holmium-166 (^{166}Ho) microspheres for radioembolization of hepatic malignancies. The outline of this thesis followed the typical clinical workflow of a radioembolization treatment. First, a scout dose of technetium-99m macroaggregated albumin (^{99m}Tc-MAA) is injected and analyzed for any of two contraindications for treatment: deposition of microspheres in the lungs (Chapter 2, 3) or in extrahepatic tissue (Chapter 4, 5). If found safe, the treatment ensues and is evaluated after 3 months (Chapter 6). After treatment, patients are given temporary contact restrictions because of the possible radiation risk to others (Chapter 7).

Key Points

- A scout dose of ^{99m}Tc-MAA does not accurately predict the lung shunt after ^{90}Y microsphere injection
- The lung shunt of ^{99m}Tc-MAA is overestimated on planar scintigraphy and is more accurately quantified on SPECT/CT
- A small catheter adjustment can alter preferential blood flow to decrease the absorbed dose to the gallbladder
- ^{99m}Tc-MAA can safely be replaced by a scout dose of ^{166}Ho microspheres
- Radioembolization using ^{166}Ho microspheres showed efficacy and is safe in salvage patients with liver metastases
- Contact restrictions are necessary in only a minority of patients

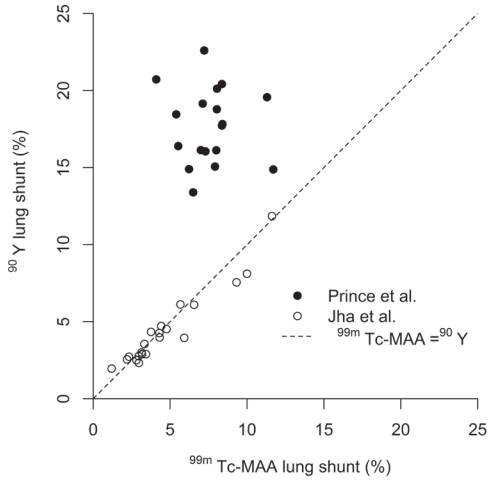

Figure 1 *Jha et al. showed a strong correlation which could not be replicated*

Chapter 2 describes the attempt to reproduce a study that validated the use of ^{99m}Tc-MAA for the prediction of the lung shunt after radioembolization. Jha et al. showed an excellent correlation between lung shunts after a scout dose with ^{99m}Tc-MAA and a treatment with yttrium-90 (^{90}Y) (Pearson's r = 0.96).[1] However, replication with 20 of our patients was unsuccessful: no correlation was found (Figure 1). A scout dose of ^{99m}Tc-MAA did not predict the lung shunt after ^{90}Y microsphere injection.

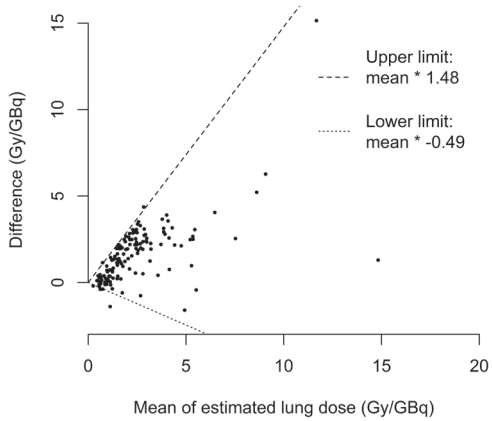

Figure 2 *Overestimation of planar scintigraphy is shown by plotting the mean lung dose versus the difference (planar scintigraphy – SPECT/CT)*

Chapter 3 showed that planar scintigraphy and SPECT/CT differ in their estimation of the number of microspheres that shunt to the lungs. After a scout dose injection of ^{99m}Tc-MAA, the predicted shunt to the lungs is estimated using either planar scintigraphy, which uses a gamma camera in two fixed positions (front and back) to detect the gamma rays from ^{99m}Tc-MAA, or a SPECT, which is made by revolving the gamma camera around the patient in 120 angles to enable a 3D reconstruction. Treatment with radioembolization is not advocated if the predicted absorbed dose to the lungs exceeds 30 Gy. Planar scintigraphy overestimated the lung shunt compared with SPECT/CT (Figure 2). The upper boundary of 30 Gy on planar scintigraphy corresponded to a much lower threshold of only 15 Gy on SPECT/CT. The scientific foundation for using 30 Gy as a threshold based on planar scintigraphy is slim, while as many as 40% of patients have their treatment activity reduced to stay below this threshold.[2] Because no radiation pneumonitis was observed in our cohort, the threshold is probably too low and should be revised using more accurate quantification techniques (i.e., SPECT). This is important because efficacy is expected to rise correspondingly.

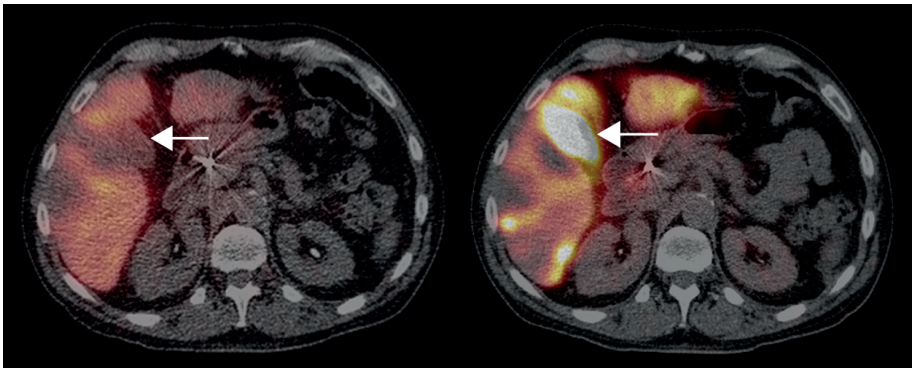

Figure 3 *High uptake in the gallbladder (A, white arrow) corrected after catheter adjustment (B)*

In Chapter 4, a clinical case is presented in which a large uptake of microspheres in the gallbladder was seen after a scout dose injection of ^{99m}Tc-MAA. After slightly changing the catheter position, the preferential blood flow changed and the predicted absorbed dose to the gallbladder decreased by 93%, reducing the risk of cholecystitis (Figure 3). Based on a literature review, a treatment algorithm was presented; if possible, adjusting the catheter position is an easy remedy, otherwise, embolization may be considered.

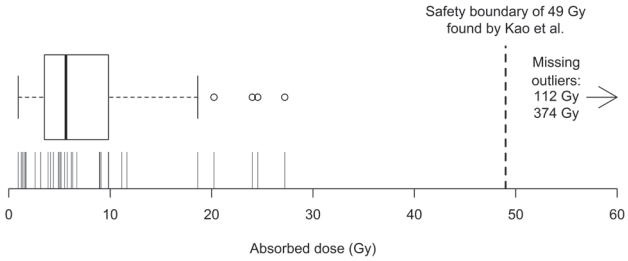

Figure 4 *Distribution of extrahepatic absorbed doses of ^{99m}Tc-MAA translated to a 250 MBq ^{166}Ho scout dose.*

In Chapter 5, the safety of replacing ^{99m}Tc-MAA as a scout dose by ^{166}Ho microspheres was assessed. ^{99m}Tc is used as a diagnostic isotope only. In contrast, ^{166}Ho can be used as a therapeutic isotope too. In other words, a scout dose of ^{166}Ho microspheres could do exactly the damage it was given to prevent. In the phase 1 and 2 clinical studies on ^{166}Ho radioembolization, ^{99m}Tc-MAA always preceded radioembolization with ^{166}Ho microspheres (and its scout dose). After these initial studies, either ^{99m}Tc-MAA or ^{166}Ho microspheres had to be chosen as a scout dose to reduce patient burden and redundancy. To analyze the safety of a scout dose of ^{166}Ho microspheres, all prior extrahepatic depositions of ^{99m}Tc-MAA were analyzed to determine the absorbed dose in the theoretical case that a scout dose of ^{166}Ho microspheres (250 MBq) had been injected instead of ^{99m}Tc-MAA. A safety threshold was estimated from reports by Kao et al.[3,4] Our analysis showed that, in the majority of cases, administration of ^{166}Ho microspheres would have been safe. In two cases, a large extrahepatic deposition was seen which might not have been safe in case ^{166}Ho would have been injected (Figure 4). However, it can be expected that the incidence (and severity) of extrahepatic depositions will decrease because of C-arm CT imaging and novel anti-reflux catheters. The risk was ultimately deemed low enough to initiate new trials without ^{99m}Tc-MAA injection (the SIM trial and HEPAR PLUS trial). In these trials, ^{166}Ho microspheres serve as both a scout and treatment dose.

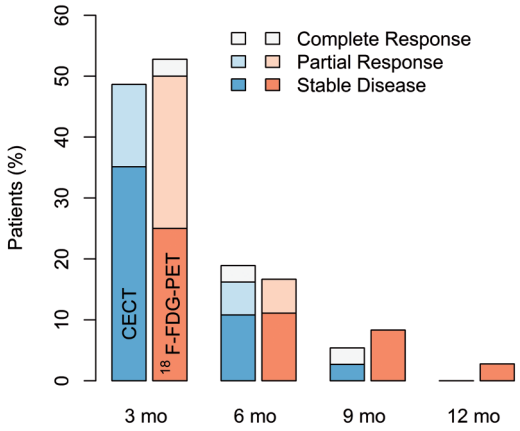

Figure 5 *Response to ^{166}Ho radioembolization on contrast enhanced CT (RECIST, blue hue) and ^{18}F-FDG-PET (PERCIST, red hue). Shaded bars indicate complete response, partial response, or stable disease. CT images were scored by 3 raters. No progressive disease indicates no consensus and none of the raters scored progressive disease. CECT = contrast enhanced CT*

In Chapter 6, the primary results of the HEPAR 2 trial are described. ^{166}Ho radioembolization was performed in 38 patients to assess its efficacy and safety. After a first-in-man study (the HEPAR trial) identified a safe ^{166}Ho absorbed dose (60 Gy to the liver), the efficacy of that dose was investigated. The HEPAR 2 trial confirmed the hypothesis that ^{166}Ho microspheres were effective in treating liver metastases. In 49% of all patients, tumors in the liver did not show progression for 3 months after treatment. In patients with colorectal cancer, 45% showed no progression. Furthermore, most of the adverse events were transient and were related to the so-called post radioembolization syndrome which consists of abdominal pain, nausea, vomiting, fever and fatigue. Impact on the quality of life was also transient; it decreased from a median of 83 (scale, 0-100) to 42 after 1 week, but recovered to 67 after 6 weeks. Both SPECT/CT and MRI were used to quantify the amount of infused ^{166}Ho activity after treatment. Using SPECT/CT, a mean of 105.1±6.3% of all ^{166}Ho activity was recovered in the liver.

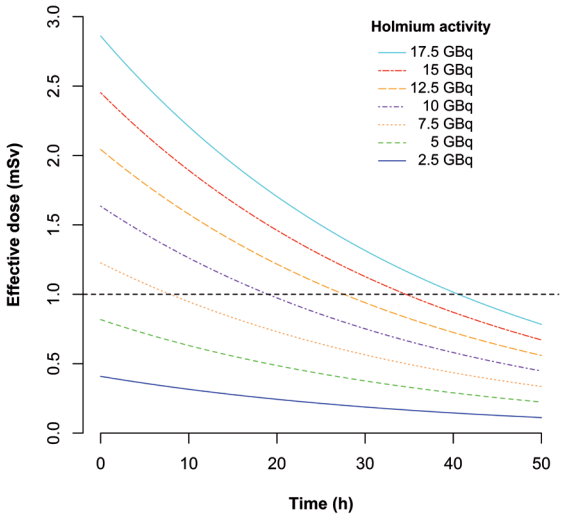

Figure 6 *Effective doses for bystanders coming from patients treated with different activities of ^{166}Ho. If patients are released after 24 hours, a treatment up to 11 GBq does not require contact restrictions.*

In Chapter 7, the safety of patients' radiation emissions was analyzed. Patients emit radiation after implantation of ^{166}Ho microspheres. In the HEPAR 2 trial, patients were requested to abide restrictions for 2 days after discharge. These restrictions can impact patient's quality of life, because the interaction with relatives had to be limited; for example, patients had to sleep in a different room for 2 days. For treatments with a radioactivity up to 11 GBq, these restrictions were shown to be unnecessary because the radiation emissions are sufficiently attenuated by the patient's body.

References

1. Jha AK a, Zade A a, Rangarajan V, Purandare N, Shah S a, Agrawal A, et al. Comparative analysis of hepatopulmonary shunt obtained from pretherapy 99mTc MAA scintigraphy and post-therapy 90Y Bremsstrahlung imaging in 90Y microsphere therapy. Nucl Med Commun. 2012;33(5):486–90.
2. Gaba RC, Zivin SP, Dikopf MS, Parvinian A, Casadaban LC, Lu Y, et al. Characteristics of primary and secondary hepatic malignancies associated with hepatopulmonary shunting. Radiology. 2014;271(2):602–12.
3. Kao Y-H, Steinberg JD, Tay Y-S, Lim GK, Yan J, Townsend DW, et al. Post-radioembolization yttrium-90 PET/CT - part 1: diagnostic reporting. EJNMMI Res. 2013;3(1):56.
4. Kao Y-H, Steinberg JD, Tay Y-S, Lim GK, Yan J, Townsend DW, et al. Post-radioembolization yttrium-90 PET/CT - part 2: dose-response and tumor predictive dosimetry for resin microspheres. EJNMMI Res. 2013;3(1):57.

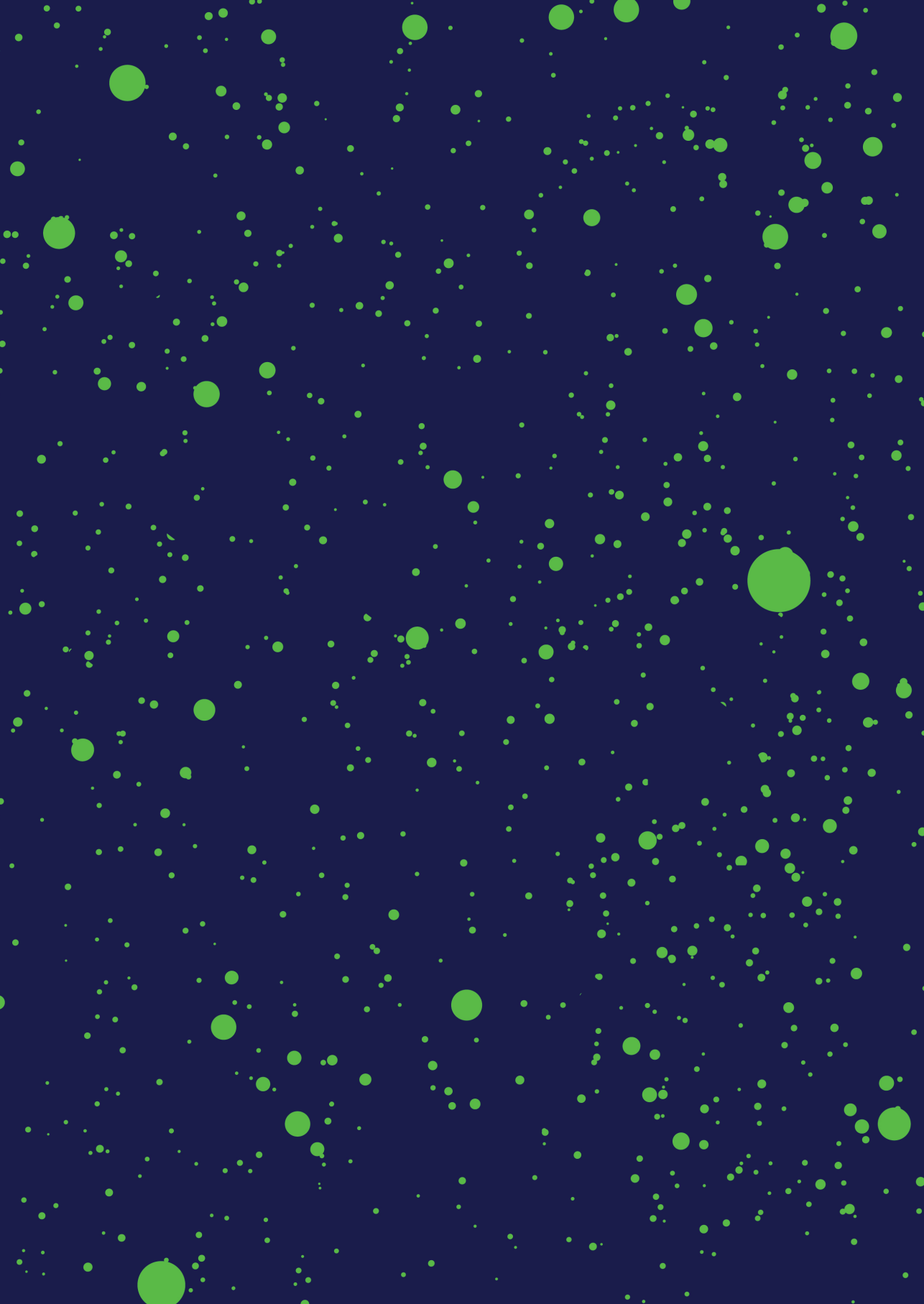

CHAPTER 9

Nederlandse samenvatting

Dit proefschrift beschrijft de toepassing van microsferen geladen met holmium-166 (^{166}Ho) voor radioembolisatie van levertumoren. De indeling volgt de klinische workflow van een radioembolisatie behandeling. Eerst wordt een proefdosis met technetium-99m albumine macro-aggregaten (^{99m}Tc-MAA) geïnjecteerd. Deze wordt gecontroleerd op twee contra-indicaties: aanwezigheid van microsferen in de longen (Hoofdstuk 2, 3) of buiten de lever (Hoofdstuk 4, 5). Vervolgens wordt de behandeling gegeven waarbij na 3 maanden wordt gekeken of er respons is opgetreden (Hoofdstuk 6). Na de behandeling krijgen de patiënten leefregels mee om de stralingsdosis aan anderen te beperken (Hoofdstuk 7).

Belangrijkste punten

- Een proefdosis ^{99m}Tc-MAA voorspelt niet nauwkeurig de long shunt na injectie van ^{90}Y microsferen
- De long shunt van ^{99m}Tc-MAA wordt overschat op planaire scintigrafie en is beter te kwantificeren op SPECT/CT
- Een kleine aanpassing aan de katheterpositie kan de preferentiële bloedstroom veranderen en de geabsorbeerde dosis op de galblaas verminderen
- ^{99m}Tc-MAA kan veilig worden vervangen door een proefdosis met ^{166}Ho microsferen
- Radioembolisatie met ^{166}Ho microsferen bleek werkzaam en veilig in uitbehandelde patiënten met levermetastasen
- Leefregels zijn slechts nodig in een minderheid van de patiënten

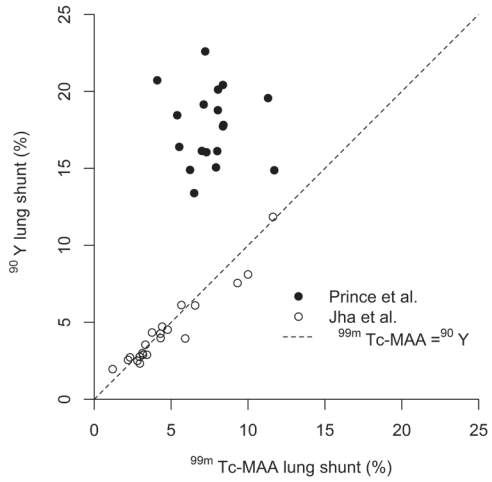

Figuur 1 *Jha et al. toonden een sterke correlatie die niet te repliceren was*

Hoofdstuk 2 beschrijft de poging een studie te repliceren die het gebruik rechtvaardigt van ^{99m}Tc-MAA om de long shunt te voorspellen. Jha et al. lieten een uitstekende correlatie zien tussen de long shunt na een proefdosis met ^{99m}Tc-MAA en na behandeling met yttrium-90 (^{90}Y) (Pearson's r = 0.96).[1] Replicatie met 20 van onze patiënten was niet succesvol: er werd geen correlatie gevonden (Figuur 1). Een proefdosis ^{99m}Tc-MAA voorspelde de long shunt na behandeling met ^{90}Y microsferen niet.

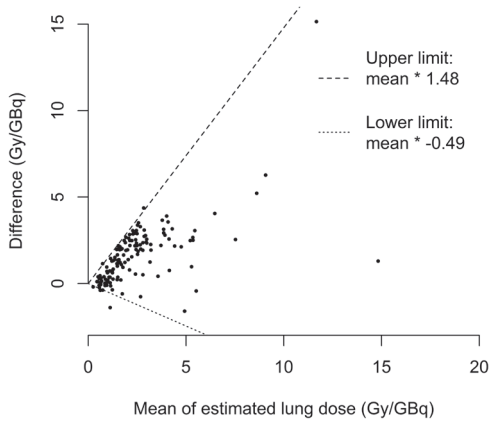

Figuur 2 *Overschatting van de long shunt door planaire scintigrafie, getoond door de gemiddelde dosis op de long dosis te plotten tegen het verschil (planaire scintigrafie – SPECT/CT)*

In Hoofdstuk 3 werd getoond dat planaire scintigrafie en SPECT/CT verschillen in hun schatting van de hoeveelheid microsferen die naar de longen shunten. Na een proefdosis ^{99m}Tc-MAA wordt de long shunt geschat met planaire scintigrafie, waarbij een gammacamera in twee posities (voor- en achterwaarts) de gamma fotonen van ^{99m}Tc-MAA detecteert, of met SPECT, waarbij de gammacamera ronddraait om een 3D reconstructie mogelijk te maken. Als de voorspelde longdosis boven de 30 Gy uitkomt is de behandeling niet aanbevolen. Planaire scintigrafie overschatte de long shunt in vergelijking met SPECT/CT (Figuur 2). De grens van 30 Gy, welke gebruikt wordt bij planaire scintigrafie, kwam overeen met een veel lagere grens van 15 Gy bij SPECT/CT. Het bewijs voor de grens van 30 Gy bij planaire scintigrafie is dun, terwijl de radioactiviteit van de behandeling wel wordt gereduceerd bij tot 40% van de patiënten vanwege een hoge long shunt.[2] Omdat wij in ons cohort geen complicaties van een hoge long shunt zagen (radiatie pneumonitis), denken we dat de grens te laag is en gereviseerd moet worden met een betere kwantificatie techniek (i.e., SPECT). Dit is van belang omdat de werkzaamheid van de behandeling hiermee kan stijgen.

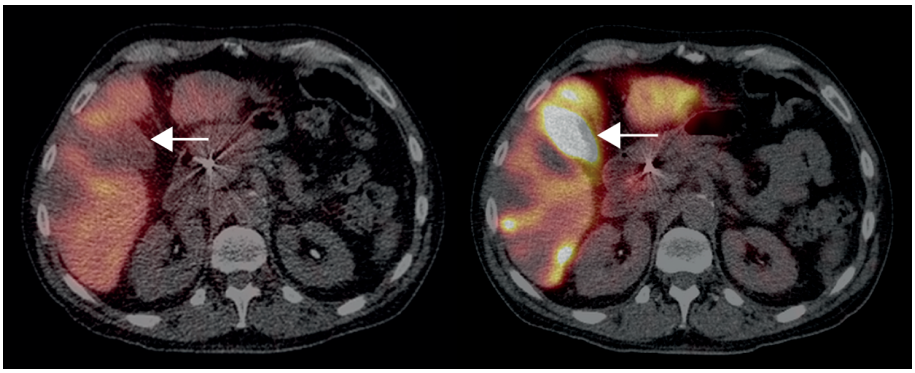

Figuur 3 *Hoge opname in de galblaas (A, witte pijl), gecorrigeerd na aanpassing van de katheterpositie (B)*

In Hoofdstuk 4 werd een case besproken waarin een grote opname van microsferen in de galblaas te zien was na injectie van de proefdosis met ^{99m}Tc-MAA. Nadat de katheterpositie gering aangepast werd veranderde de preferentiële bloedstroom en verminderde de voorspelde dosis op de galblaas met 93%, wat het risico op cholecystitis verkleinde (Figuur 3). Op basis van een literatuuronderzoek werd een behandelalgoritme voorgesteld; indien mogelijk, is het makkelijk om de katheterpositie te veranderen, anders kan embolisatie van de slagader van de galblaas overwogen worden.

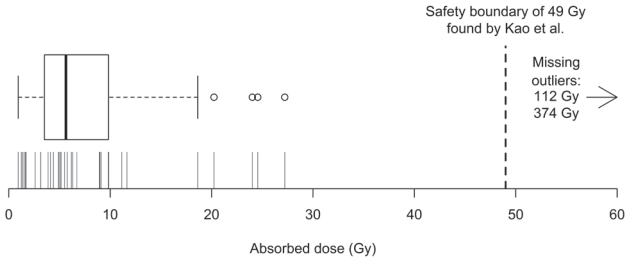

Figuur 4 *Verdeling van extrahepatische dosissen na een proefdosis van ^{166}Ho (250 MBq), geëxtrapoleerd uit data van proefdosissen met ^{99m}Tc-MAA.*

In Hoofdstuk 5 werd de veiligheid onderzocht van het vervangen van een proefdosis van ^{99m}Tc-MAA met een proefdosis ^{166}Ho microsferen. ^{99m}Tc wordt enkel gebruikt als diagnostisch isotoop. ^{166}Ho kan, in tegenstelling, ook worden gebruikt als therapeutisch isotoop. In andere woorden, een proefdosis ^{166}Ho microsferen kan juist die schade toebrengen, die het als proefdosis zou moeten voorkomen. In de fase 1 en 2 studies naar radioembolisatie met ^{166}Ho microsferen werd ^{99m}Tc-MAA altijd gegeven voorafgaand aan ^{166}Ho microsferen (en de proefdosis daarmee). Na deze studies moest gekozen worden tussen een proefdosis met ^{99m}Tc-MAA of ^{166}Ho microsferen om patiënten zo min mogelijk te belasten. Om de veiligheid van een proefdosis met ^{166}Ho microsferen te beoordelen, werden alle voorgaande proefdosissen van ^{99m}Tc-MAA geanalyseerd om vast te stellen wat de dosis op extrahepatisch weefsel zou zijn geweest als niet ^{99m}Tc-MAA, maar een proefdosis ^{166}Ho microsferen (250 MBq) was geïnjecteerd. Een veilige grens werd geschat op basis van eerder werk door Kao et al.[3,4] Onze analyse toonde dat toediening van een proefdosis ^{166}Ho microsferen veilig zou zijn geweest in de meerderheid van gevallen. In twee gevallen werd een grote opname buiten de lever gezien, welke misschien niet veilig zou zijn bij toediening van een proefdosis van ^{166}Ho microsferen. Er kan verwacht worden dat het voorkomen (en de ernst) van extahepatische opnames zal afnemen vanwege recent geïntroduceerde beeldvorming met C-arm CT en het gebruik van nieuwe anti-reflux katheters. Het risico werd uiteindelijk laag genoeg geschat om nieuwe studies zonder proefdosis van ^{99m}Tc-MAA te starten (de SIM trial en de HEPAR PLUS trial). In deze studies zullen ^{166}Ho microsferen zowel als proefdosis en als behandeling gegeven worden.

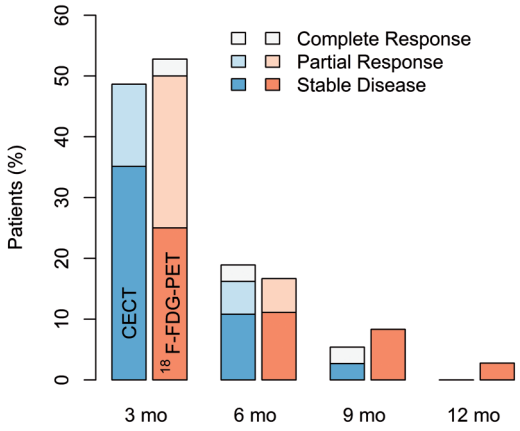

Figuur 5 *Werkzaamheid van radioembolisatie met ^{166}Ho microsferen op contrast CT (RECIST, blauw) en ^{18}F-FDG-PET (PERCIST, rood). Arcering toont complete respons, partiele respons, of stabiele ziekte. CT-beelden werden door 3 raters gescoord. CECT = contrast CT*

In Hoofdstuk 6 werden de primaire resultaten van de HEPAR 2 trial gepresenteerd. Radioembolisatie met ^{166}Ho microsferen werd in 38 patiënten verricht om de werkzaamheid en veiligheid te toetsen. Nadat de eerste studie op mensen (de HEPAR trial) 60 Gy als veilig dosis identificeerde, werd de werkzaamheid van die dosis onderzocht. De HEPAR 2 bevestigde de hypothese dat ^{166}Ho microsferen werkzaam waren in het behandelen van levermetastasen. Tumoren in de lever lieten geen progressie zien in de lever in 49% van de patiënten. Voor patiënten met colorectaal carcinoom was dit in 45% van de patiënten het geval. Verder waren de meeste bijwerkingen tijdelijk en onderdeel van het post radioembolisatie syndroom, wat bestaat uit buikpijn, misselijkheid, braken, koorts en moeheid. De kwaliteit van leven was ook tijdelijk aangedaan; die verminderde van een mediaan van 83 (schaal, 0-100) tot 42 na 1 week, maar herstelde tot 67 na 6 weken. Zowel SPECT/CT als MRI werden gebruikt om de hoeveelheid ^{166}Ho in de lever na behandeling te kwantificeren. Met SPECT/CT werd gemiddeld 105.1±6.3% van al het toegediende ^{166}Ho gemeten.

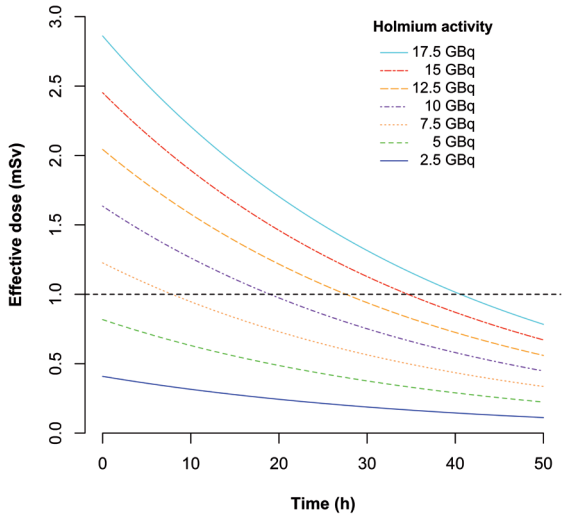

Figuur 6 *Effectieve dosis op naasten afkomstig van patiënten behandeld met verschillende activiteiten ^{166}Ho. Als patiënten worden ontslagen na 24 uur, hoeven leefregels pas ingesteld te worden vanaf 11 GBq.*

In Hoofdstuk 7 werd de veiligheid van de straling die uit patiënten komt onderzocht. Patiënten zenden straling uit na implantatie van ^{166}Ho microsferen. In de HEPAR 2 kregen patiënten leefregels mee voor de 2 dagen na ontslag uit het ziekenhuis. Deze regels verminderden de kwaliteit van leven, omdat de omgang met naasten wordt beperkt; zo moeten patiënten bijvoorbeeld 2 dagen in een andere kamer slapen. Er werd aangetoond dat leefregels pas ingesteld hoeven worden bij behandelingen met een radioactiviteit boven 11 GBq, omdat de straling anders genoeg afgeschermd worden door het eigen lichaam van patiënten.

References

1. Jha AK a, Zade A a, Rangarajan V, Purandare N, Shah S a, Agrawal A, et al. Comparative analysis of hepatopulmonary shunt obtained from pretherapy 99mTc MAA scintigraphy and post-therapy 90Y Bremsstrahlung imaging in 90Y microsphere therapy. Nucl Med Commun. 2012;33(5):486–90.
2. Gaba RC, Zivin SP, Dikopf MS, Parvinian A, Casadaban LC, Lu Y, et al. Characteristics of primary and secondary hepatic malignancies associated with hepatopulmonary shunting. Radiology. 2014;271(2):602–12.
3. Kao Y-H, Steinberg JD, Tay Y-S, Lim GK, Yan J, Townsend DW, et al. Post-radioembolization yttrium-90 PET/CT - part 1: diagnostic reporting. EJNMMI Res. 2013;3(1):56.
4. Kao Y-H, Steinberg JD, Tay Y-S, Lim GK, Yan J, Townsend DW, et al. Post-radioembolization yttrium-90 PET/CT - part 2: dose-response and tumor predictive dosimetry for resin microspheres. EJNMMI Res. 2013;3(1):57.

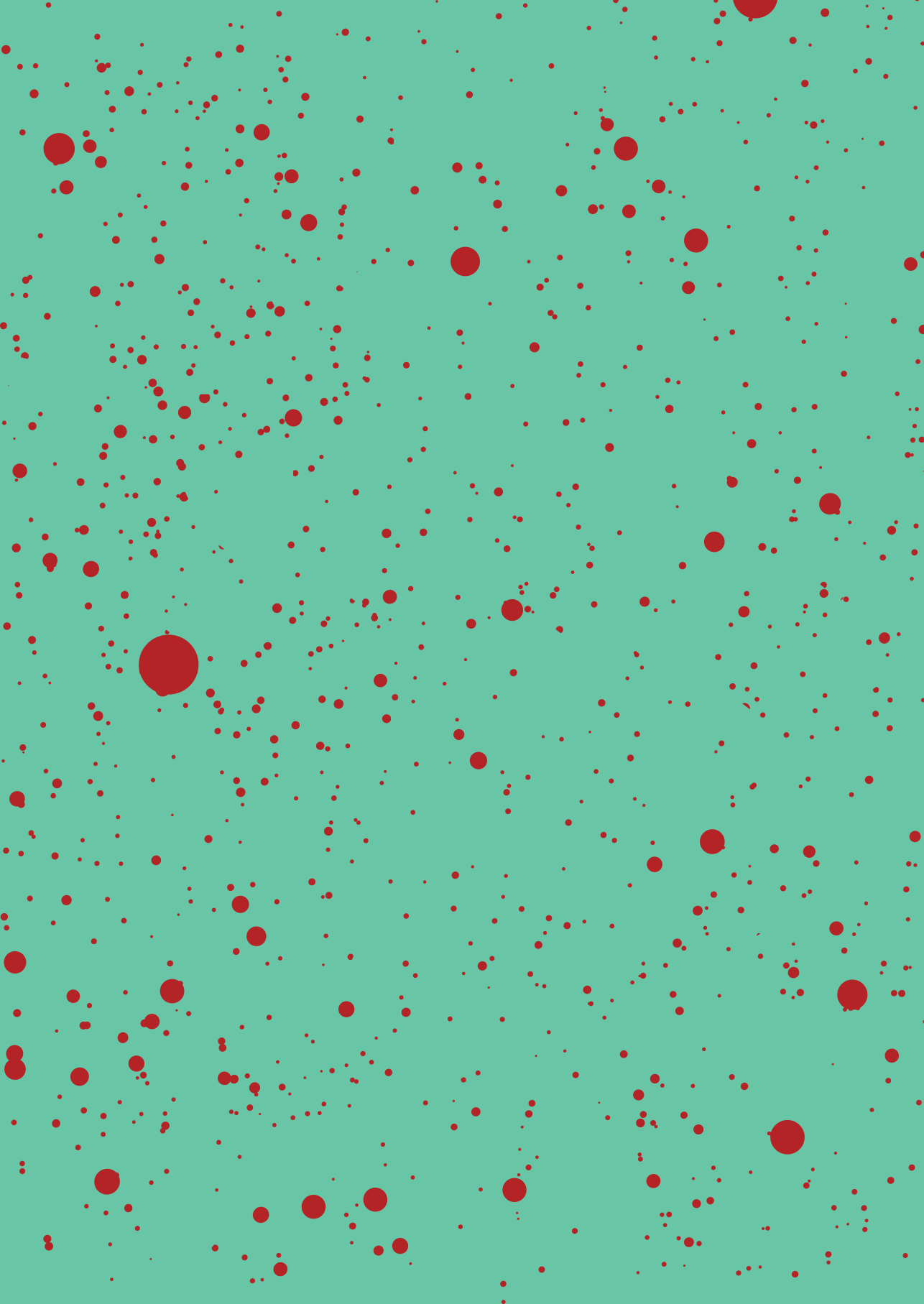

CHAPTER 10

Acknowledgements (Dankwoord)
-
Biography
-
List of Publications

Acknowledgements (Dankwoord)

Graag wil ik alle proefpersonen en ook hun familie bedanken voor het vertrouwen in ons team. In de laatste periode van hun leven namen zij deel aan wetenschappelijk onderzoek. Dit proefschrift is er dankzij en voor hun.

Dit proefschrift was onmogelijk tot stand gekomen zonder de hulp van onderstaande personen. Ik prijs me dan ook gelukkig dat ik met hun heb mogen samenwerken.

Prof. dr. van den Bosch, Maurice. Je plukte mij in januari 2011 letterlijk van de gang en gaf me de mogelijkheid extracurriculair onderzoek te doen met Maarten Smits. Dit leidde uiteindelijk tot het overnemen van de HEPAR 2 studie en dit proefschrift. Jouw stijl van leidinggeven paste goed bij mijn idee van een promotietraject. Door me op juiste momenten los te laten kon ik veel ervaring opbouwen en groeien, maar als ik je nodig had, reageerde je ongekend doelmatig en efficiënt. Bedankt voor het vertrouwen dat je me hebt gegeven.

Dr. Lam, Marnix. Ik kon ik me geen betere copromotor wensen. Onze kamers grenzen aan elkaar en bij ieder bezoek klinkt na een tijdje een schaterlach door de muren. Volgens mij eindigden onze gesprekken ook altijd met een (slechte) grap. Het spijt me dat ik 'kopje koffie, glazenwasser?' niet kende, dat zal je steeds vaker meemaken denk ik. Iedereen zal het herkennen als ik je bedank voor je laagdrempelige overleg, voorwaartse blik en leuke tijd.

Foppen, Wouter, bedankt dat je mijn paranimf wilt zijn, voor je kennis van koffie en lekker eten, en je hardlooptips. Als ik kijk naar hoe gestructureerd en goed jij je promotie hebt aangepakt, kan mijn verdediging niet meer stuk met jou naast me.

Dr. Smits, Maarten. Volgens mij heb ik deze promotie vooral aan jou te danken. Het enthousiasme voor interventieradiologie straalt van je af, en de HEPAR 1 en 2 vormen een mooie afspiegeling daarvan. Bedankt dat je me destijds een running start gegeven hebt en dank voor de mooie tijd (o.a. bij congressen).

Andy, **Andor**, ik ken niemand die zo gedreven kan werken als jij. Toen we bij elkaar op de kamer kwamen was ik even bang dat het saai zou worden. Niets bleek

minder waar. Je humor breekt dwars door je ijzeren discipline heen. Mijn promotie is dankzij jou verrijkt met discussies over de gouden standaard, papers van 'experts', filmpjes van dansende robots en een bezoek aan de NY Yankees.

Collega's van het trialbureau, in het bijzonder **Tjitske**. Toen je tijdelijk afwezig was besefte ik pas hoeveel jij voor de HEPAR 2 deed, erg bedankt voor alles wat je gedaan hebt en de rustige, perfecte manier waarop het altijd geregeld was. **Anneke**, we maakten het je met inplannen af en toe niet makkelijk maar ik heb het erg gewaardeerd dat jij het toch altijd weet te regelen. **Cees**, bedankt voor de database, je updates daarvan om 7:00 blijven me verbazen. **Lenny**, bedankt voor de lessen op gebied van methodologie, epidemiologie, en reizen. **Saskia** en **Shanta**, bedankt voor jullie audit en andere ondersteuning.

Leden van het Holmium team, bedankt voor jullie steun. **Bernard**, voor je gedrevenheid, de onnavolgbare ideeën en dat ik op de polikliniek mee kon kijken. **Frank**, voor je tomeloze enthousiasme. **Gerard**, voor de kritische noot die altijd op ontspannen toon gegeven werd. **Remmert** (en eerder ook **Fred**), voor het altijd met oplossingen komen. **Gerrit**, voor ondersteuning bij het MRI-gedeelte van de HEPAR 2 (zo ook **Peter**). **Jan**, voor de samenwerking in het slot van mijn promotie.

Radiologen en nucleair geneeskundigen van het UMC Utrecht, bedankt dat jullie altijd even tijd konden maken voor een vraag, die achteraf vaak moeilijker bleek dan verwacht. **Rutger**, **Jan**, **Pieter-Jan** en **Evert-Jan**, jullie ging altijd ontspannen om met mijn protocollen, maar wisten me tegelijk enthousiast te maken voor de kliniek, bedankt. **Manon**, bedankt voor het delen van je radiologische kennis. **Frank**, voor het scoren. **Collega's van de angiokamer**, ik voelde me door jullie telkens deel van het angioteam, dank daarvoor. **Henny**, **Monique**, **Bart**, **Julia**, **Maarten**, **Rowena**, **Christina**, de HEPAR-patiënten waren bij jullie in goede handen. **Arthur**, bedankt voor de discussies over radioembolisatie, je nuchtere blik en je gulle lach. **NUG-medewerkers**, bedankt voor het intekenen en de flexibiliteit die er altijd op jullie afdeling schijnt te heersen (vooral bij **John** en **Roel**). **Verpleegkundigen van de stralingsunit**, dank voor jullie hulp bij metingen voor en de coördinatie van de HEPAR 2 trial.

Het stafsecretariaat, **Annet** en **Marja**, dank voor jullie hulp op allerlei gebieden (van handtekeningen van de prof tot hulp bij het navigeren tussen alle afdelingen).

CBOI: **Barentsz**, **Charly**, **Lorjé**, **Merel**, **Suus**, bedankt dat ik na mijn introtijd in de kweekvijver toch deel kon uitmaken van het mooie CBOI. **Floor**, bedankt voor de tijd in de kweekvijver en later in Q-gebouw, waar we gelukkig dezelfde muzieksmaak hadden. **Herwie**, dank voor de coördinatie van verwijzingen en voor je onuitputtelijke bron van spreekwoordelijke meesterwerken, toch blijft je quote van Martin Bril me het meest bij 'Je mist meer dan je meemaakt. Helemaal niet erg'. **G**, dank voor de overheerlijke brownies.

Alex, **Alexandra** en **Björn, Anouk, Anouk, Antoinette, Danny, Hanke, Jan-Willem, Jennifer, Joris, Laura, Marleen**, **Martin**, **Max**, **Pushpa**, **Richard**, **Sofie**, **Tom**, dank voor de leuke tijd.

Do, bedankt voor Brabantse gezelligheid, knap hoe jij zoveel gedaan krijgt en ook nog regelt nu in Stanford te zitten, doei! **Braber**, jouw energie is een inspiratie voor je omgeving, zo ook voor mij. **Ali**, dank voor je tips, vooral vlak voor de eindstreep. **Morsal**, bedankt voor het delen je assertiviteit en energie. **Lennart**, dank voor je droge humor. **Annemarie**, **Anouk**, **Esther**, **Marjolein**, **Remko**, **Robbert** en **Wieke**, dank voor de loensj-en. **Bastiaan**, **Rob**, **Mattijs**, geniale mannen, dank dat jullie het geduld hadden om me de fijne kneepjes van de SPECT/CT en reconstructies bij te brengen. **Gijsbert**, bedankt dat je met een paar toetsaanslagen zoveel voor elkaar hebt gekregen voor Hoofdstuk 5. **57000: The Special Ones**, dank voor de hulp bij verdwenen bestanden, kapotte fietsen, en in het bijzonder **Gert** die mijn vakantiefoto's met een soldeertang van een doorgebrande harde schijf redde! **Chris**, **Roy**, **Karin** en **Jan**, bedankt voor jullie hulp bij multimedia, m.n. posters en de radioembolisatie website.

Aanstaande collega's: **Akke**, **Alicia**, **Anadeijda**, **Charlotte** en **Coco**, bedankt voor al jullie inzet. Het was/is prettig samenwerken.

Leden van de beoordelingscommissie, **prof. dr. Kranenburg**, **prof. dr. Borel Rinkes**, **prof. dr. Reekers**, **prof. dr. van Vulpen**, en **prof. dr. Witteveen**, ik ben jullie dankbaar dat jullie de tijd hebben genomen mijn proefschrift te beoordelen.

Vrienden van mijn jaarclub, fijn dat ik na een dag statistiek in de chaos die clubeten heet mocht verkeren. Dat we nog drie keer per maand eten toont hoe mooi het is. **Daan**, al spreken we vaak last minute af, ik hecht er veel waarde aan.

Heeren van het **Jonge Heeren Gezelschap**, bedankt voor alle avonden en activiteiten in deze, volgens Bob, 'tweede studententijd'.

Familie Gerkens, bedankt voor jullie interesse, sommigen als collega, anderen als familie. **Familie Prince**, da ge bedankt zijt da witte!

Lieveke en **Jeroen**, bedankt voor de collegiale interesse maar vooral het bourgondisch leven uit Voerendaal. **Benjamin**, **Noortje** en **Friso** voor de gezelligheid. **Coen**, **Sarah**, **Matthijs** en **Lisanne** voor de etentjes. Ik voel me opgenomen in een grote, hechte familie.

Fons, **Freddy**, jullie onvoorwaardelijke trots geeft me ontzettend veel kracht. Ik ben zo blij dat we deze mijlpaal samen kunnen vieren. Geniet ervan!

Puck en **Bart**, leuk dat we nu zo dicht bij elkaar wonen. Fijn dat ik zo'n zus heb die collega is, en mijn paranimf wil zijn. Ik ben trots op je!

Lieveke, lief, ondanks je eerste reactie toen ik eens zei dat ik een drukke dag had ('oh, waren de nietjes op?') waren de afgelopen jaren met jou onvergetelijk. Jij zorgt ervoor dat ik met beide benen op de grond sta en tegelijk met mijn hoofd in de wolken ben. Bedankt dat je bent wie je bent en je leven met mij wilt delen, ik wil niets liever

Biography

Jip Frederik Prince was born in 's-Hertogenbosch on the 24th of March, 1989. After graduating from Gymnasium Beekvliet (Sint Michielsgestel, the Netherlands) he went to the Simon Langton Grammar School for Boys (Canterbury, United Kingdom), where he obtained A-level qualifications. He attended Utrecht University and obtained his medical degree, supplemented with a minor in Economics. In March 2013, he started his PhD with the subject of radioembolization with holmium microspheres under the supervision of prof. dr. Maurice van den Bosch and dr. Marnix Lam. He also started with a postgraduate Master of Clinical Epidemiology. From June 2016, he will be a resident in Radiology at the Meander MC under supervision of dr. H.J. Baarslag.

List of Publications

Is there a correlation between planar scintigraphy after ^{99m}Tc-MAA and 90Y administration?
Prince JF, van Diepen R, van Rooij R, Lam MG.
Nucl Med Commun. 2016;37(2):218-9

Use of C-Arm Cone Beam CT During Hepatic Radioembolization: Protocol Optimization for Extrahepatic Shunting and Parenchymal Enhancement.
van den Hoven AF, Prince JF, de Keizer B, Vonken EJ, Bruijnen RC, Verkooijen HM, Lam MG, van den Bosch MA.
Cardiovasc Intervent Radiol. 2016;39(1):64-73

^{90}Y Hepatic Radioembolization: An Update on Current Practice and Recent Developments.
Braat AJ, Smits ML, Braat MN, van den Hoven AF, Prince JF, de Jong HW, van den Bosch MA, Lam MG.
J Nucl Med. 2015;56(7):1079-87

Safety of a Scout Dose Preceding Hepatic Radioembolization with 166Ho Microspheres.
Prince JF, van Rooij R, Bol GH, de Jong HW, van den Bosch MA, Lam MG.
J Nucl Med. 2015;56(6):817-23

Radiation-induced cholecystitis after hepatic radioembolization: do we need to take precautionary measures?
Prince JF, van den Hoven AF, van den Bosch MA, Elschot M, de Jong HW, Lam MG.
J Vasc Interv Radiol. 2014;25(11):1717-23

Radiation emission from patients treated with holmium-166 radioembolization.
Prince JF, Smits ML, Krijger GC, Zonnenberg BA, van den Bosch MA, Nijsen JF, Lam MG.
J Vasc Interv Radiol. 2014;25(12):1956-1963.e1

Hepatic radioembolization as a true single-session treatment.
van den Hoven AF, Prince JF, van den Bosch MA, Lam MG.
J Vasc Interv Radiol. 2014;25(7):1143-4

(^{99}m)Tc-MAA overestimates the absorbed dose to the lungs in radioembolization: a quantitative evaluation in patients treated with ^{166}Ho-microspheres.
Elschot M, Nijsen JF, Lam MG, Smits ML, Prince JF, Viergever MA, van den Bosch MA, Zonnenberg BA, de Jong HW.
Eur J Nucl Med Mol Imaging. 2014;41(10):1965-75

Posttreatment PET-CT-confirmed intrahepatic radioembolization performed without coil embolization, by using the antireflux Surefire Infusion System.
van den Hoven AF, Prince JF, Samim M, Arepally A, Zonnenberg BA, Lam MG, van den Bosch MA.
Cardiovasc Intervent Radiol. 2014;37(2):523-8

Endovascular treatment of internal iliac artery stenosis in patients with buttock claudication.
Prince JF, Smits ML, van Herwaarden JA, Arntz MJ, Vonken EJ, van den Bosch MA, de Borst GJ.
PLoS One. 2013;8(8):e73331

Intra-arterial radioembolization of breast cancer liver metastases: a structured review.
Smits ML, Prince JF, Rosenbaum CE, van den Hoven AF, Nijsen JF, Zonnenberg BA, Seinstra BA, Lam MG, van den Bosch MA.
Eur J Pharmacol. 2013;709(1-3):37-42